N° d'ordre : 389

T H E S E

présentée à

L'UNIVERSITE DES SCIENCES ET TECHNIQUES DE LILLE

pour obtenir le grade de

DOCTEUR ES SCIENCES PHYSIQUES

par

MARC DE BACKER

SPECTRES D'ABSORPTION DE L'ELECTRON SOLVATE ET INTERACTIONS ELECTRON-ION EN SOLUTION

Membres du Jury MM. les Professeurs :

M. DELHAYE	Président
P. GOUDMAND	Rapporteurs
P. LENGLART	
G. LEPOUTRE	
J. JOUSSOT-DUBIEN	Examinateurs
M. MAGAT	
R. CATTERALL	

Soutenue le 16 septembre 1977

NIVERSITE DES SCIENCES
T TECHNIQUES DE LILLE

08.03.1977

DOYENS HONORAIRES de l'Ancienne Faculté des Sciences

MM. R. DEFRETIN, H. LEFEBVRE, M. PARREAU.

PROFESSEURS HONORAIRES des Anciennes Facultés de Droit et Sciences Economiques, des Sciences et des Lettres

M. ARNOULT, Mme BEAUJEU, MM. BROCHARD, CHAPPELON, CHAUDRON, CORDONNIER, CORSIN, DECUYPER DEHEUVELS, DEHORS, DION, FAUVEL, FLEURY, P. GERMAIN, GLACET, HEIM DE BALSAC, HOCQUETTE KAMPE DE FERIET, KOUGANOFF, LAMOTTE, LASSERRE, LELONG, Mme LELONG, MM. LHOMME, LIEBAERT, MARTINOT-LAGARDE, MAZET, MICHEL, PEREZ, ROIG, ROSEAU, ROUELLE, SAVARO, WATERLOT, WIEMAN, ZAMANSKI.

PRESIDENTS HONORAIRES DE L'UNIVERSITE DES SCIENCES ET TECHNIQUES DE LILLE

MM. R. DEFRETIN, M. PARREAU.

PRESIDENT DE L'UNIVERSITE DES SCIENCES ET TECHNIQUES DE LILLE

M. M. MIGEON.

PROFESSEURS TITULAIRES

M.	BACCHUS Pierre	Astronomie
M.	BEAUFILS Jean-Pierre	Chimie Physique
M.	BECART Maurice	Physique Atomique et Moléculaire
M.	BILLARD Jean	Physique du Solide
M.	BIAYS Pierre	Géographie
M.	BONNEMAN Pierre	Chimie Appliquée
M.	BONNOT Ernest	Biologie Végétale
M.	BONTE Antoine	Géologie Appliqué
M.	BOUGHON Pierre	Algèbre
M.	BOURIQUET Robert	Biologie Végétale
M.	CELET Paul	Géologie Générale
M.	COEURE Gérard	Analyse
M.	CONSTANT Eugène	Electronique
M.	DEBOURSE Jean-Pierre	Gestion des Entreprises
M.	DELATTRE Charles	Géologie Générale
M.	DELHAYE Michel	Chimie Physique
M.	DERCOURT Jean	Géologie Générale
M.	DURCHON Maurice	Biologie Expérimentale
M.	FAURE Robert	Mécanique
M.	FOURET René	Physique du Solide
M.	GABILLARD Robert	Electronique
M.	GONTIER Gérard	Mécanique
M.	GRANELLE Jean-Jacques	Sciences Economiques
M.	GRUSON Laurent	Algèbre
M.	GUILLAUME Jean	Microbiologie
M.	HEUBEL Joseph	Chimie Minérale
M.	LABLACHE-COMBIER Alain	Chimie Organique
M.	LACOSTE Louis	Biologie Végétale
M.	LANSRAUX Guy	Physique Atomique et Moléculaire
M.	LAVEINE Jean-Pierre	Paléontologie
M.	LEBRUN André	Electronique
M.	LEHMANN Daniel	Géométrie

Mme	LENOBLE Jacqueline	Physique Atomique et Moléculaire
M.	LINDER Robert	Biologie et Physiologie Végétales
M.	LOMBARD Jacques	Sociologie
M.	LOUCHEUX Claude	Chimie Physique
M.	LUCQUIN Michel	Chimie Physique
M.	MAILLET Pierre	Sciences Economiques
M.	MONTARIOL Frédéric	Chimie Appliquée
M.	MONTREUIL Jean	Biochimie
M.	PARREAU Michel	Analyse
M.	POUZET Pierre	Analyse numérique
M.	PROUVOST Jean	Minéralogie
M.	SALMER Georges	Electronique
M.	SCHILTZ René	Physique Atomique et Moléculaire
Mme	SCHWARTZ Marie-Hélène	Géométrie
M.	SEGUIER Guy	Electrotechnique
M.	TILLIEU Jacques	Physique Théorique
M.	TRIDOT Gabriel	Chimie Appliquée
M.	VIDAL Pierre	Automatique
M.	VIVIER Emile	Biologie Cellulaire
M.	WERTHEIMER Raymond	Physique Atomique et Moléculaire
M.	ZEYTOUNIAN Radyadour	Mécanique

PROFESSEURS SANS CHAIRE

M.	BELLET Jean	Physique Atomique et Moléculaire
M.	BKOUCHE Rudolphe	Algèbre
M.	BODARD Marcel	Biologie Végétale
M.	BOILLET Pierre	Physique Atomique et Moléculaire
M.	BOILLY Bénoni	Biologie Animale
M.	BRIDOUX Michel	Chimie Physique
M.	CAPURON Alfred	Biologie Animale
M.	CORTOIS Jean	Physique Nucléaire et Corpusculaire
Mme	DACHARRY Monique	Géographie
M.	DEPREZ Gilbert	Physique Théorique
M.	DEVRAINNE Pierre	Chimie Minérale
Mme	EVRARD Micheline	Chimie Appliquée
M.	GOSSELIN Gabriel	Sociologie
M.	GOUDMAND Pierre	Chimie Physique
M.	GUILBAULT Pierre	Physiologie Animale
M.	HERMAN Maurice	Physique Spatiale
Mme	LEHMANN Josiane	Analyse
M.	LENTACKER Firmin	Géographie
M.	LEROY Jean-Marie	Chimie Appliquée
M.	LOUAGE Francis	Electronique
M.	MAIZIERES Christian	Automatique
Mlle	MARQUET Simone	Probabilités
M.	MIGEON Michel	Chimie Physique
M.	MONTEL Marc	Physique du Solide
M.	MONTUELLE Bernard	Biologie Appliquée
M.	NICOLE Jacques	Chimie Appliquée
M.	PAQUET Jacques	Géologie Générale
M.	RACZY Ladislas	Electronique
M.	ROUSSEAU Jean-Paul	Physiologie Animale
M.	SLIWA Henri	Chimie Organique
M.	WATERLOT Michel	Géologie Générale

MAITRES DE CONFERENCES (Et Chargés d'Enseignement)

M.	ADAM Michel	Sciences Economiques
M.	ANTOINE Philippe	Analyse
M.	BART André	Biologie Animale
Mme	BATTIAU Yvonne	Géographie

.../...

M.	BEGUIN Paul	Mécanique
M.	BONNELLE Jean-Pierre	Chimie
M.	BOSCQ Denis	Probabilités
M.	BREZINSKI Claude	Analyse Numérique
M.	BRUYELLE Pierre	Géographie
M.	CARREZ Christian	Informatique
M.	COQUERY Jean-Marie	Psycho-Physiologie
M.	CORDONNIER Vincent	Informatique
M.	COUTURIER Daniel	Chimie Organique
M.	CRAMPON Norbert	Géologie
M.	CROSNIER Yves	Electronique
M.	DEBRABANT Pierre	Géologie Appliquée
M.	DEGAUQUE Pierre	Electronique
M.	DELORME Pierre	Physiologie Animale
M.	DE PARIS Jean-Claude	Mathématiques
M.	DHAINAUT André	Biologie Animale
M.	DELAUNAY Jean-Claude	Sciences Economiques
M.	DERIEUX Jean-Claude	Microbiologie
M.	DOUKHAN Jean-Claude	Physique du Solide
M.	DUBOIS Henri	Physique
M.	DUEE Gérard	Géologie
M.	DYMENT Arthur	Mécanique
M.	ESCAIG Bertrand	Physique du Solide
M.	FAKIR Sabah	Algèbre
M.	FLAMME Jean-Marie	Technologie de Construction
M.	FOCT Jacques	Génie Mécanique
M.	FONTAINE Hubert	Physique
M.	FONTAINE Jacques	Electronique
M.	FOURNET Bernard	Biochimie
M.	GAMBLIN André	Géographie
M.	GERVAIS Michel	Gestion des Entreprises
M.	GOBLOT Rémi	Algèbre
M.	HECTOR Joseph	Géométrie
M.	JACOB Gérard	Informatique
M.	JOURNEL Gérard	Physique Atomique et Moléculaire
M.	KREMBEL Jean	Biochimie
M.	LAURENT François	Automatique
Mle	LEGRAND Denise	Algèbre
Mle	LEGRAND Solange	Algèbre
M.	LEROY Yves	Electronique
M.	LHENAFF René	Géographie
M.	LOCQUENEUX Robert	Physique théorique
M.	MACKE Bruno	Physique
M.	MAHIEU Jean-Marie	Physique Atomique et Moléculaire
M.	MESSELYN Jean	Physique Atomique et Moléculaire
M.	MIGNOT Fulbert	Analyse Numérique
M.	N'GUYEN VAN CHI Régine	Géographie
M.	NOTELET Francis	Electrotechnique
M.	NUSSEMBAUM Maurice	Sciences Economiques
M.	PARSY Fernand	Mécanique
M.	PAUPARDIN Colette	Biologie Physiologie Végétales
M.	PECQUE Marcel	Chimie Physique
M.	PERROT Pierre	Chimie Appliquée
M.	PERTUZON Emile	Physiologie Animale
M.	PETIT Francis	Chimie Organique
M.	PONSOLLE Louis	Chimie Physique
M.	POVY Lucien	Automatique
M.	RICHARD Alain	Biologie
M.	ROGALSKI Marc	Analyse
M.	ROY Jean-Claude	Psycho-Physiologie
M.	SIMON Michel	Sociologie
M.	SOMME Jean	Géographie

.../...

Mlle SPIK Geneviève	Biochimie
M. STANKIEWICZ François	Sciences Economiques
M. STERBOUL François	Informatique
M. TAILLEZ Roger	Biologie
M. THERY Pierre	Electronique
M. TOP Gérard	Sciences Economiques
M. TOULOTTE Jean-Marc	Automatique
M. TREANTON Jean-René	Sociologie
M. VANDORPE Bernard	Chimie Minérale
M. VILLETTE Michel	Mécanique
M. WALLART Francis	Chimie
M. WERNER Georges	Informatique
Mme ZIN-JUSTIN Nicole	Algèbre

Ce travail a été réalisé dans le laboratoire du Professeur G. Lepoutre à Lille, et dans celui du Professeur J. L. Dye à Michigan State University (U. S. A.). Leurs conseils et encouragements ont rendu ce travail possible; qu'ils trouvent ici l'expression de ma reconnaissance.

Je tiens à remercier Monsieur le Professeur M. Delhaye de l'Université des Sciences et Techniques de Lille pour l'utilisation de son équipement de spectroscopie Raman ainsi que le Professeur L. Dorfman d'Ohio State University (USA) pour l'utilisation de son installation de radiolyse pulsée.

Monsieur le Professeur P. Goudmand et Monsieur P. Lenglart ont bien voulu accepter le travail de rapporteurs de cette thèse, je leur exprime ma profonde gratitude.

Je remercie Messieurs les Professeurs Joussot-Dubien de l'Université de Bordeaux, Magat de l'Université de Paris Sud et Catterall de l'Université de Salford (Angleterre) d'avoir accepté d'être membres du Jury.

Ce travail n'aurait pas été possible sans la collaboration des collègues qui figurent comme co-auteurs des publications. En particulier l'aide apportée par Messieurs J. N. Decarpigny et M. Lannoo de l'équipe de Physique des Solides a permis le développement des calculs théoriques.

SOMMAIRE

LISTE DES FIGURES

LISTE DES TABLES

Liste des Publications servant de base à la thèse de

Mr Marc De Backer

"Spectres d'absorption de l'électron solvaté et interactions électron - ion en solution"

-:-:-:-:-:-:-

1. Pulse Radiolysis Studies XVIII
   Spectrum of the solvated electron in the systems ethylenediamine water and ammonia-water
   J. Chem. Phys., 1970, 52, 6251-8

2. Solvated electron spectra. Study of the absorption curves by a method of moments
   J. Phys. Chem. 1977, 81, 159-61

3. Raman spectra of dilute metal-ammonia solutions dans Electrons in Fluids, J. Jortner et N.R. Kestner Editeurs, Springer-Verlag, Berlin, 1973, 161-6

4. Metal ethylenediamine solutions. Extinction coefficients and equilibria
   J. Phys. Chem. 1971, 75, 3092-6

5. Pulse radiolysis study of the kinetics of formation of Na^- in ethylenediamine by the reaction of solvated electrons with sodium ions
   J. Phys. Chem., 1972, 76, 839-46

6. Solubilization of alkali metals in tetrahydrofuran and diethyl ether by use of a cyclic polyether
   J. Am. Chem. Soc., 1970, 92, 5226-8

7. Alkali metal solutions. Effect of two cyclic polyethers an solubility and spectra
   Ber. Bunsenges. Phys. Chem. 1971, 75, 659-62

I. INTRODUCTION

Dans ce travail nous présentons les résultats obtenus au cours d'une étude des spectres d'absorption de l'électron solvaté dans divers milieux ainsi qu'une étude des interactions électron - ion alcalin en solution.

L'étude expérimentale a d'abord porté sur l'obtention des spectres de l'électron solvaté produit par radiolyse pulsée dans les mélanges eau-ammoniac et eau-éthylenediamine. Leur variation en fonction de la composition du solvant a été étudiée. Nous avons parallèlement étudié les spectres de solutions de métaux alcalins dans l'éthylène-diamine. Le spectre d'absorption de ces solutions montre l'existence de plusieurs espèces. L'une d'entre elles est l'électron solvaté et son spectre est identique à celui obtenu par radiolyse pulsée, l'autre est dépendante du métal. L'électron solvaté est en équilibre avec l'espèce dépendant du métal. La cinétique de la réaction entre l'électron solvaté et l'ion sodium a été étudiée dans l'éthylenediamine par radiolyse pulsée.

Ce travail est divisé en deux parties. La première traite du spectre de l'électron solvaté et de l'interprétation des variations spectrales en fonction de la composition du mélange. Un nouveau modèle est proposé. La seconde partie présente les résultats obtenus dans les solutions métal-éthylenediamine sur les interactions électron - ion alcalin.

I. 1. Première partie.

L'interprétation des spectres de l'électron solvaté a fait l'objet de nombreuses publications. Un certain nombre d'entre elles donnent de bons résultats pour la position du maximum, mais échouent complètement pour représenter la forme de la courbe d'absorption.

Nous présentons une méthode empirique d'analyse du spectre d'absorption utilisant les moments expérimentaux. Les moments théoriques peuvent être évalués à partir de l'hamiltonien du système et de la fonction d'onde de l'état fondamental. La comparaison entre les quantités expérimentales et théoriques permet de connaître les divers paramètres introduits dans le modèle microscopique de la solution.

Cette méthode de calcul est testée dans le cas de solutions de métaux dans l'ammoniac liquide. Elle sert ensuite à interpréter les variations du spectre de l'électron solvaté dans les mélanges eau-ammoniac et eau-éthylenediamine. Dans le cadre d'une étude des modèles de solutions, nous avons réalisé des spectres Raman de solutions métal-ammoniac afin de varifier une théorie qui prévoyait qu'un mode de vibration de la cavité serait actif en Raman dans la région 50 - 200 cm^{-1}.

I. 2. Deuxième partie.

Les spectres d'absorption des métaux alcalins dans les amines sont différents de ceux qu'on observe dans l'ammoniac. Pour les expliquer, les espèces M^+, M, M^- et e^- sont postulées. Nous avons étudié le spectre de Na^- qui est l'espèce prépondérante dans les solutions de sodium dans l'éthylenediamine et nous avons déterminé son coefficient d'extinction. Pour les autres espèces nous avons mis en évidence l'existence d'équilibres. La cinétique de la réaction Na^+ et e^- a été étudiée par radiolyse pulsée.

L'utilisation de complexants de cations du type ethers macrocycliques permet de déplacer les équilibres en solution et ouvre une nouvelle catégorie de solvants dans lesquels des métaux peuvent être dissous.

II. ETUDE DES SPECTRES DE L'ELECTRON SOLVATE DANS LES MELANGES EAU-AMMONIAC ET EAU-ETHYLENEDIAMINE.

Dans un nombre restreint de solvantsla dissolution de métaux alcalins conduit à la formation d'électrons solvatés. Les solutions de métaux alcalins dans l'ammoniac et les amines ont été les plus étudiées.

La radiolyse pulsée permet de générer des électrons solvatés dans presque tous les solvants. On obtient un spectre d'absorption identique à celui des solutions de métaux dans les mêmes solvants.

II. 1. Obtention des spectres.

Dans la publication 1, nous avons mesuré le spectre d'absorption de l'électron solvaté produit par radiolyse pulsée dans les mélanges eau - ammoniac et eau - éthylenediamine.

Nous avons étudié la variation de la position du maximum d'absorption et de la largeur du pic en fonction de la composition des mélanges. Nous avons noté que, dans tous les cas, une seule espèce absorbante était responsable du spectre. Les essais de décomposition du spectre en une somme de pics dus à diverses espèces n'ont pas donné de résultats significatifs.

L'obtention des spectres se faisant point par point, de nombreuses données de cinétique de réaction de l'électron avec divers substrats ont été obtenues en particulier celle de $e^- + NH_4^+$.

Dans la publication 1, nous décrivons les techniques expérimentales mises en jeu et la méthode d'exploitation des mesures. Nous présentons les résultats obtenus et les discutons.

PUBLICATION 1

PULSE RADIOLYSIS STUDIES. XVIII. SPECTRUM OF THE SOLVATED ELECTRON IN THE SYSTEMS ETHYLENEDIAMINE-WATER AND AMMONIA-WATER.

Reprinted from THE JOURNAL OF CHEMICAL PHYSICS, Vol. 52, No. 12, 6251-6258, 15 June 1970
Printed in U. S. A.

Pulse Radiolysis Studies. XVIII. Spectrum of the Solvated Electron in the Systems Ethylenediamine–Water and Ammonia–Water*

JAMES L. DYE AND MARC G. DEBACKER
Department of Chemistry, Michigan State University, East Lansing, Michigan 48823
AND
LEON M. DORFMAN
Department of Chemistry, The Ohio State University, Columbus, Ohio 43210
(Received 16 February 1970)

The pulse radiolysis technique with fast infrared detection was used to determine the optical absorption spectrum of the solvated electron in the systems ethylenediamine–water and ammonia–water. These spectra, determined over the entire concentration range, show the following: In ammonia and in ethylenedamine, the bands at 1550 and 1350 nm, respectively, have the same shape and position as those attributed to the solvated electron in alkali metal solutions. In each of the two-component systems a single band is seen with the peak position intermediate to those in the pure solvents. For ethylenediamine–water mixtures, the band shape (normalized) and half-width (energy scale) are invariant with composition, while for ammonia–water mixtures the ratio of the peak position to the half-width is invariant. These observations suggest a delocalized electron with optical characteristics determined by the aggregate properties of the solvent. Models which require that the optical properties be strongly influenced by solvation with a small number of solvent molecules are not in accord with these observations. Kinetic data indicate that the decay of the solvated electron in ammonia and in ethylenediamine is a complex process. The rate constant for the reaction of the solvated electron in ammonia with ammonium ion was found to be at least four orders of magnitude lower than the diffusion-controlled limit.

INTRODUCTION

Information about the optical absorption spectrum of the solvated electron derives principally from two sources. These are the continuing investigations of alkali metal solutions in ammonia[1–3] and in various amines[4–6] in which the solvated electron is relatively stable, and the pulse radiolysis[7,8] studies of the solvated electron[9] in water[10,11] and in various organic liquids[12–16] in which it is unstable. Some four years ago a beginning[9] was made at unifying the data from these two sources, as there are some special features in the alkali metal–amine systems which are unique to the metal. Pulse radiolysis experiments have been reported for liquid ammonia,[17,18] and there have been some disputed observations in ethylenediamine,[19,20] and some partial spectra in other amines.[21] There have been only a limited number of investigations of the electron in two-component solvent systems[21,22] in which it has been shown that one does not observe separate absorption band maxima, and that the absorption band is, to this extent, dependent upon the aggregate properties of the solvent.

This investigation of the spectrum of the solvated electron in the systems ethylenediamine–water and ammonia–water is directed at both objectives, namely, the unification of the experimental observations of the two methods and the determination of whether there is any selective solvent behavior in electron solvation in these two-component systems. In the course of this work many observations have also been made of the kinetics, from which it is possible to estimate rate constants for some of the elementary reactions of the solvated electron in ammonia and in ethylenediamine.

EXPERIMENTAL

The general methods of pulse radiolysis[7,8,23] and the particular experimental arrangement used in this laboratory[24] have been described in detail and need be outlined here only briefly. Two new techniques will be described in somewhat greater detail. These are the extension of our detection capability into the infrared, a feature essential to the present investigation, and the use of a new sample handling technique which has proved very effective for multicomponent chemical systems.

Pulse Irradiation

A Varian V-7715A linear accelerator was used as the electron source with 3–4-MeV electrons, generally at a pulse current of about 350 mA. The pulse width was varied from 0.1 to 1.2 μsec. Precise dosimetry was not explicitly needed for interpretation of the present work, but it was known[25] from measurements with a modified Fricke dosimeter that a 0.1-μsec pulse delivers a dose of about 6×10^{16} eV/g.

Optical Detection

The transient optical absorption was observed with two separate photodetectors. An RCA 7102 photomultiplier was used for the visible region up to about 1.0 μ. Most of the measurements, up to 1.6 μ (the limitation of the grating available at that time) were made with a liquid-nitrogen-cooled indium antimonide detector, type A10X, obtained from American Electronic Laboratories, Inc. (Barnes Engineering, Inc.). The rise time, using operational amplifier feedback techniques to minimize RC time constant effects, was

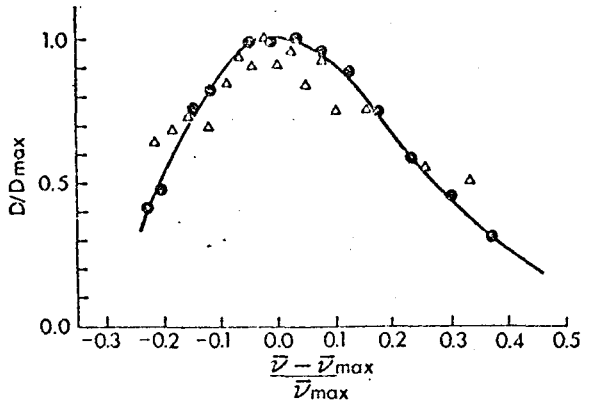

FIG. 1. Effect of pulsing the xenon lamp and using reference detection on absorbance reproducibility. △, Without lamp pulsing, single beam; $X_{H_2O}=0.496$; ●, with lamp pulsing and reference photomultiplier; $X_{H_2O}=0.367$.

found to be less than 0.2 μsec. The linearity was tested by superimposing a chopped light signal from a gallium arsenide emitter at about 0.9 μ, upon a steady light signal. Varying the steady light signal over the output range of the amplifier, no deviation from linearity was observed within a detection sensitivity of 1%. The indium antimonide detector could be used down to 0.6 μ. The 7102 detector was used principally as a reference wavelength monitor with a split optical beam in point-by-point spectral scanning.

The light source used was a 500-W Osram xenon lamp, type XBO 450 W. For effective use of the indium antimonide detector it was found desirable to pulse this lamp to obtain higher output. In the high-intensity pulsed mode a current pulse of 150 A is added to the normal continuous current of 20 A. The resulting increase in intensity is about 25–40 times that of the steady operation, depending on the wavelength. The duration of the light flash is several milliseconds, with a usable constant intensity portion of about 0.15 msec synchronized with the electron pulse. Scale expansions up to tenfold showed no appreciable time variation of intensity during the flash.

Although satisfactory split-beam measurements could be made up to 1.0 μ using two monochromators and photomultipliers, the response of the solid-state infrared detector was too low to permit split-beam operation without pulsing the lamp. In addition, the large solvent absorption in the infrared made reliable measurements difficult. The improvement in spectral characteristics which resulted from pulsing the lamp and employing a reference beam may be seen in Fig. 1, which compares the spectra obtained in these two ways.

Bausch and Lomb grating monochromators, Type 33-86-25, $f/3.5$, were used with the light beam split by a partially reflecting mirror. The grating for the infrared to 1.6 μ had a dispersion of 25 nm/mm. Since the exit slit was generally set at less than 1.2 mm, the bandwidth of the light monitored was less than 30 nm. Although this band width would be unsuitable for the study of narrow lines, it was satisfactory for the study of the broad absorption band of the solvated electron.

Reaction Cells

These cells were of the standard type, previously described,[24] made of high-purity silica. For work in the infrared, thin cells with an optical path of 3.0 mm were used to reduce absorption of the monitoring light by the solvent.

The cells were connected to a sample handling device in which samples of materials to be added were contained in sealed, evacuated, thin-walled glass bulbs which could be successively broken *in situ* to change the composition of the system as predetermined. This sample system is shown in Fig. 2.

The bulbs were evacuated either after the addition of a solid or before distillation of volatile compounds into them. The stem of the thin-walled bulb was inserted into a drawn-out piece of Pyrex tubing which was attached, along with four or five others, to a manifold. To form a vacuum-tight seal, heat-shrinkable tubing of either polyvinyl chloride (available from any electronic supply house) or Teflon (Flo-Tite Tubing, Pope Scientific, Inc., Menomonee Falls, Wisc.) was collapsed with a heat gun. After the bulbs had been sealed off under vacuum, the plastic tubing could be easily cut off with a razor blade, thus allowing the stems to be weighed. For very small amounts of nonvolatile compounds, solutions containing the compound at a known concentration could be introduced into the bulb with a hypodermic syringe. After weighing the bulb to determine the amount of solution added and attaching it to the vacuum line, the solvent could be removed by distillation.

This technique has been very useful since all solute additions are made to the *same* sample of solvent. When care is used in cleaning and handling of the bulbs, no problems of contamination occur and empty bulbs

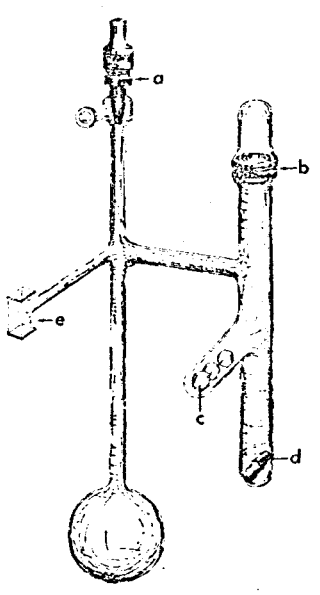

FIG. 2. Sample cells with breakable ampoules for the addition of solute. (a) Delmar–Urry valve; (b) Fischer-Porter 15-mm "Solv-Seal" joint; (c) breakable ampoules; (d) Teflon-covered magnet; (e) optical cell.

can be broken with no change in the decay kinetics of the electron in the solvent.

The cells were cleaned first with an $HF-HNO_3$-detergent cleaner[26] and then with boiling *aqua regia*. This was followed by at least 10 rinses with hot triply distilled water. The cells were kept full of triply distilled water until just before use. They were dried, when necessary, by evacuation.

Cryostat

For the investigation of the ammonia–water system it was necessary to use either reduced temperatures or to resort to pressurized systems for solutions which were high in ammonia content. Temperature was regulated by means of a simple thermostatic box, which has been described,[27] in which the control was obtained by a flow of cooled nitrogen gas. In the intermediate concentration region, runs were carried out at both room temperature and −15°C to permit the determination of an appropriate temperature coefficient for the low-temperature spectral data.

Materials

Water was triply distilled, with the first two distillations from acidic dichromate and alkaline permanganate solutions, respectively. The third distillation was carried out in a quartz still. Ammonia was condensed onto potassium, and the resultant blue solution was allowed to stand for several days before the final distillation into the radiolysis cell. For solutions of low ammonia content, reagent grade aqueous ammonia was used. Ethylenediamine was freeze purified,[26] allowed to form a blue solution with Na–K alloy, and finally distilled from the blue solution *in vacuo*. All solutions which were not prepared directly on the high-vacuum line were thoroughly degassed before use by repeated freeze–pump–thaw cycles. A greaseless high-vacuum system containing an oil diffusion pump was used in all preparations. Solution concentrations were determined by one of several methods. For low concentrations of ammonia in water, *p*H titrations were used. For higher concentrations and for some of the ethylenediamine runs the cell was weighed before and after each addition. Finally, for some of the ethylenediamine runs, weighed amounts of water contained in sidearms equipped with break seals were added to a weighed amount of ethylenediamine. Weighed amounts of reagent grade ammonium bromide in fragile glass ampoules could be added to the ammonia as desired. Anhydrous ethanol could also be added in this way. In order to eliminate reducible impurities from the ammonia and the ethylenediamine and to make the final solutions basic, enough potassium in glass capillaries could be added to make the solutions from 10^{-3} to $10^{-2}M$ in base if desired.

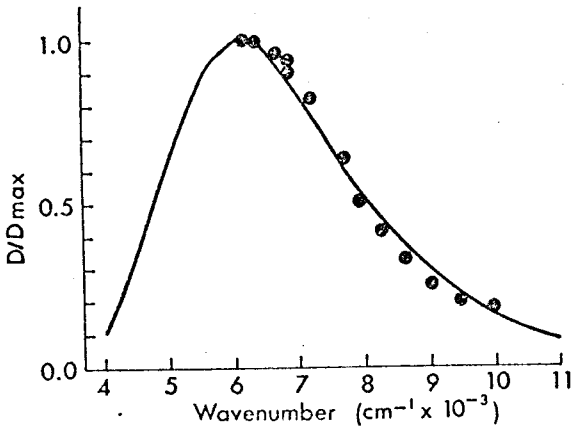

FIG. 3. Absorption spectrum of the solvated electron in liquid ammonia at −15°C. —, Potassium solutions (Ref. 2, corrected for temperature difference); ●, pulse radiolysis.

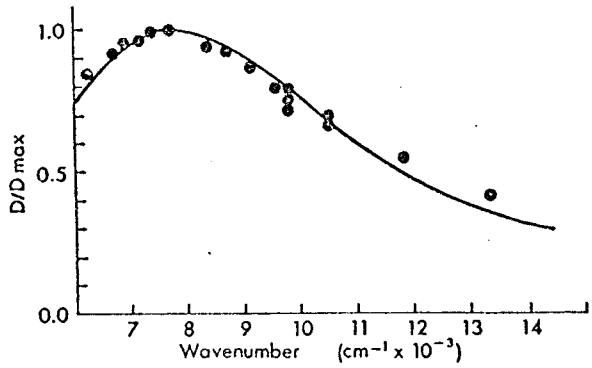

FIG. 4. Absorption spectrum of the solvated electron in ethylenediamine at room temperature. —, Cesium solution (Ref. 5); ●, pulse radiolysis.

RESULTS AND DISCUSSION

This paper deals primarily with the optical absorption spectrum of the solvated electron in the systems ethylenediamine–water and ammonia–water. Nevertheless, since the spectral data are obtained photometrically by point mapping, these observations include an abundance of rate data from which some general statements may be made about the nature of the decay of the absorption band of the solvated electron in ammonia and in ethylenediamine.

Solvated Electron Spectra

Solvated electron absorption spectra were measured up to 1600 nm for pure ammonia and for 16 solutions containing ammonia and water. They were also measured for pure ethylenediamine and for 11 mixtures of it with water. As shown in Figs. 3 and 4, the agreement between the results obtained by pulsing pure ammonia and pure ethylenediamine and those obtained by using metal solutions[1,5] is excellent. This agreement provides confirmatory evidence that the solvated electron produced by radiolysis is the same as that formed in metal solutions in ammonia and amines.

The spectra obtained for the mixtures with water

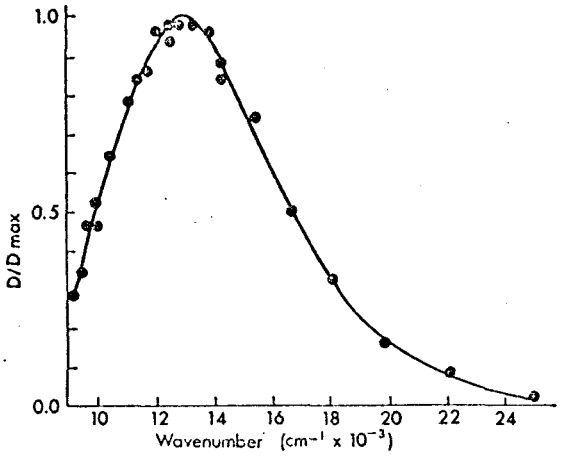

FIG. 5. Least-squares fit of the absorption spectrum (X_{H_2O} = 0.862) to a combined Gaussian–Lorentzian function for the ammonia–water system. —, Least-squares curve; ●, observed values.

were generally well defined when the pulsed lamp was used together with a reference photomultiplier. The spectra shown in Figs. 3–5 are representative of the precision obtained in this way. All of the spectra obtained for ethylenediamine–water mixtures and all but five of the spectra for ammonia–water mixtures used a reference photomultiplier. In order to obtain reliable linewidth information, the spectra were measured over as wide a range of wavelengths as possible.

A method of treating the data was sought which would permit error estimates to be made for both peak positions and half-widths. The procedure finally chosen involved fitting the data with a shape function by using a damped nonlinear least-squares program[23] which provided estimates of the standard deviations of the parameters. Since the absorption spectra on an energy basis are highly asymmetric with pronounced high-energy "tails," the high-energy half of the band was fitted with a Lorentzian shape function while a Gaussian shape function was used for the low-energy half. The two functions were constrained to have their maxima at the same energy, but their half-widths were independently variable. This procedure yielded excellent representations of the spectra. Figure 5 shows a typical spectrum and the least-squares curve which resulted from this fitting procedure.

TABLE I. Solvated electron absorption band position and half-width for ammonia–water mixtures.[a]

Mole fraction water	Peak position	Width at half-height	Peak position ÷ half-width
0.0	6 300	3100	2.03
0.144	6 350±210	3410±710	1.86
0.213	6 970±700	3700±200	1.88
0.358	7 180±90	4470±360	1.61
0.367	7 470±40	3710±60	2.01
0.421	7 650±110	4000±160	1.91
0.421	7 620±140	4200±200	1.81
0.489	8 234±70	4935±100	1.67
0.496	8 300±270	5550±424	1.50
0.533	8 900±120	5800±400	1.53
0.594	9 570±240	6520±440	1.48
0.594	9 570±50	5850±100	1.64
0.717	11 090±100	6580±215	1.69
0.752	11 820±80	7230±133	1.64
0.759	12 170±250	6530±600	1.86
0.841	12 950±70	6780±80	1.91
0.862	12 900±80	7120±170	1.81
0.929	13 370±110	6930±135	1.93
0.949	13 470±100	7100±200	1.90
1.000	13 640±70	7210±105	1.89

[a] Uncertainties given are standard deviations obtained from a least-squares fit of the data (see text). Units are cm⁻¹ in all cases.

TABLE II. Solvated electron absorption band position and half-width for ethylenediamine–water mixtures.[a]

Mole fraction water	Peak position	Width at half-height
0.0	7 360±145	7070±533
0.263	8 860±140	7930±360
0.424	9 340±210	7050±330
0.424	9 390±200	7260±350
0.524	10 160±250	6600±360
0.537	10 170±70	7210±100
0.603	11 000±100	7000±135
0.655	11 400±100	6916±150
0.702	12 460±150	6730±150
0.757	13 020±170	6815±180
0.820	13 840±230	7140±220
0.863	13 700±160	7000±190
1.000	13 640±70	7200±100

[a] Uncertainties given are standard deviations obtained from a least-squares fit of the data (see text). Units are cm⁻¹ in all cases.

The results for ammonia-water mixtures are given in Table I and shown in Fig. 6, and those for ethylenediamine–water mixtures are given in Table II and Fig. 7. The error limits shown represent linear estimates of the standard deviations resulting from the fit of the individual spectra. In some cases, the spectra obtained immediately after the pulse and after the initial fast decay ($t > 10$ μsec) were both measured. Within experimental error they are identical.

Interpretation of the Spectra

In this work, as in previous studies[21,22] in other systems, the peak positions and half-widths are intermediate to those in the pure solvents. Clearly, the results rule out the possibility that the optical properties in the two-component solvents result from the superposition of bands arising from two species characteristic of the individual solvents. Although the solvated electron is generally considered to be de-

localized over a number of solvent molecules, there are models which consider stronger interaction with one,[29] two,[30] or four[31] solvent molecules than with the others.

If the factors which influence the peak position, linewidth, and extinction coefficient were determined mainly by solvation to a small number of species, one would expect a superposition to broaden the line. In order to determine the extent of the broadening which would result, spectra were calculated for mixtures of ammonia and water on the basis of a simple substitution model. While any correct model would have to permit selective solvation and perhaps allow for a change in the solvation number, the qualitative conclusions of the present simple model as they pertain to linewidths would apply to any substitution model.

The assumptions used to calculate the spectra are the following:

(1) The number of solvent molecules involved in a "strong" interaction with the electron is the same for ammonia, water, and mixtures. Therefore, for a total solvation number n there would be $(n+1)$ molecular species present in a mixture.

(2) The peak positions and half-widths (in wavenumbers) and the molar extinction coefficients for the intermediate species, $[(S_1)_m(S_2)_{n-m}]^-$, are linear functions of m. S_1 and S_2 represent ammonia and water.

(3) The fraction of solvated electrons present in a given species is given by the simple probability expression[32]

$$P_m = (X_1)^m(X_2)^{n-m}[n!/m!(n-m)!],$$

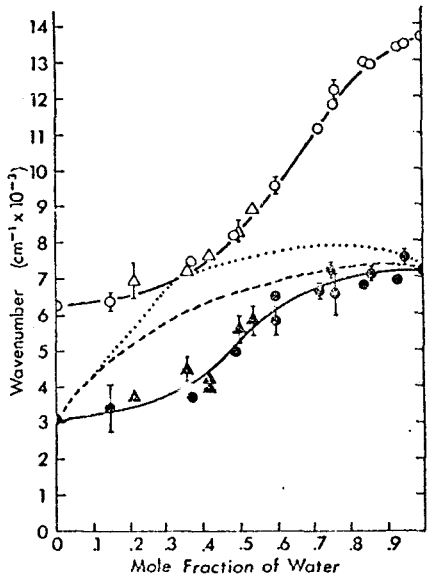

FIG. 6. Variation with composition of the peak position (upper curve, open symbols) and half-width (lower curve, solid symbols) of the solvated electron spectrum in ammonia–water mixtures. Triangles represent single-beam measurements obtained without lamp pulsing. When no error bars are shown, the standard deviation is less than the size of the symbol. ···, Half-width calculated for a solvation number of 3; ---, half-width calculated for a solvation number of 5.

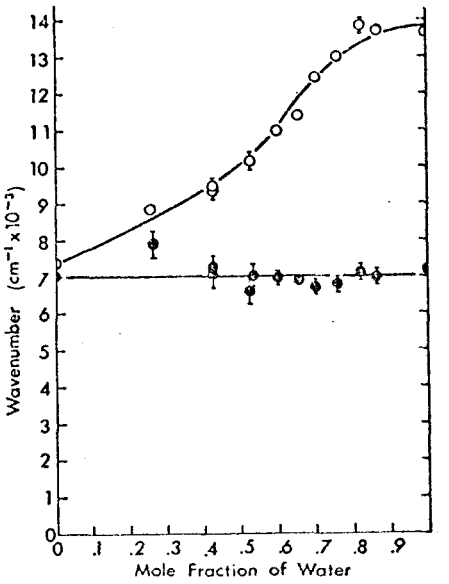

FIG. 7. Variation with composition of the peak position (upper curve, open circles) and half-width (lower curve, solid circles) of the solvated electron in ethylenediamine–water mixtures. All measurements employed a reference detector. When no error bars are shown the standard deviation is less than the size of the symbol.

in which X_1 and X_2 are the mole fractions of components 1 and 2 in the mixture.

The composite spectra were calculated as a function of mole fraction for various values of n. As expected, when n became very large, the predicted peak position and half-width approached linear functions of mole fraction. However, for small values of n, the model predicted large positive deviations from linearity. Indeed, for $n=2$ and 3, this model predicts the appearance of well-defined shoulders at intermediate concentrations. The predicted variations of half-width with mole fraction for $n=3$ and 5 are shown in Fig. 6.

It is clear that a simple substitution model based upon a small solvation number for the solvated electron is not sustained by the present results. This conclusion is reinforced by the results for ethylenediamine–water mixtures. In this case, although the position of the peak shifts some 6000 cm^{-1} the half-width does not change perceptibly with water content.

These results are in agreement with models for the solvated electron which consider the electron to be delocalized so that the electron can sample the average environment of the mixture, in accord with theories which treat the medium as a continuous dielectric.[33] Alternatively, of course, the factors which determine the transition energy and local fluctuations of the transition energy could be smooth functions of composition not necessarily related to specific interactions of the electron with solvent molecules.

Decay Kinetics in Ammonia and in Ethylenediamine

The observation by Compton *et al.*[17] that an initial rapid decay of the transient absorbance in pulse-

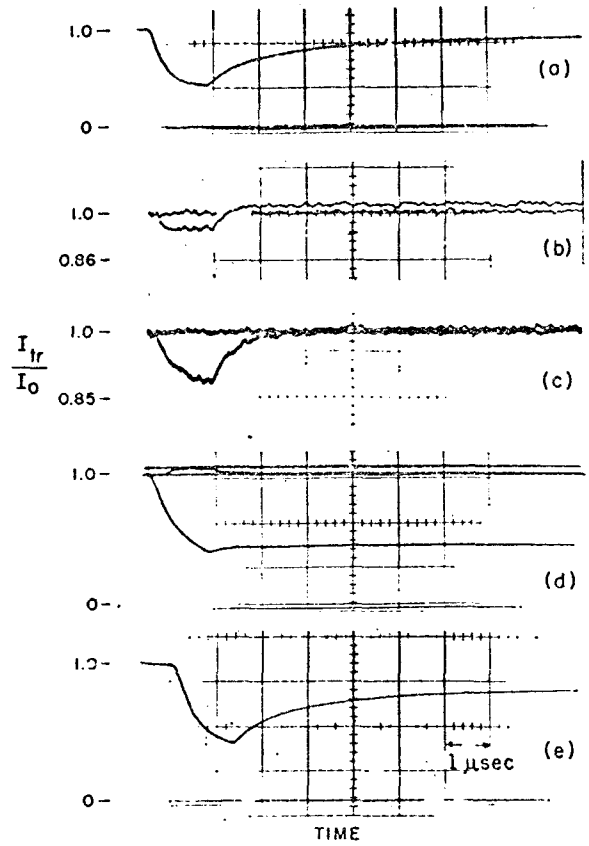

FIG. 8. Pulse radiolysis of ammonia under various conditions. Rate curves were observed at a wavelength of 1000 nm. (a) Pure anhydrous ammonia; (b) dilute blue solution of K in NH_3 ($\lesssim 10^{-4}M$); (c) solution of KNH_2 in ammonia ($\simeq 10^{-3}M$); (d) solution of KNH_2 and ethanol ($\simeq 1.4\times 10^{-2}M$) in ammonia; (e) solution (d) with water added to give $X_{H_2O}=0.144$.

radiolyzed pure liquid ammonia is followed by a very slow decay was confirmed in this work. Although no systematic study of the temperature dependence of the decay was made in the present work, it is in qualitative agreement with their observation[17] that the relative fraction of the total decay which occurs at the fast rate increases with increasing temperature. At the temperature of most of this work (−15 to −25°C) the absorbance remaining after the fast decay amounted to only 5%–10% of the initial absorbance. The fast decay was essentially complete in 10 μsec, and the decay of the residual absorbance was at least three orders of magnitude slower. The same general behavior was observed for pure ethylenediamine.

Judging from the relative absorbances corrected for the optical path length, the solvated electron concentrations produced by the pulse in this work were some 20 times those studied by Compton *et al.* Although they reported that both the fast and the slow decay were first order in the absorbance, in the present work the fast decay (first 3 μsec) was found to be second order in the absorbance. This decay is shown in Figs. 8(a) and 9 which are representative of a large number of traces made under different conditions. The addition of ethanol (to give concentrations as high as $10^{-2}M$) had no apparent effect upon the decay rate.

Compton *et al.*[17] and Cleaver, Collinson, and Dainton[34] noted that the radiolysis of metal solutions in ammonia caused an increase in light transmittance. This behavior was confirmed in the present work for both ammonia and ethylenediamine solutions of potassium. Figure 8(b) shows the trace obtained when a pale blue solution ($\lesssim 10^{-4}M$) of potassium in ammonia was pulsed. Dilute blue solutions ($\lesssim 5\times 10^{-4}M$ in potassium) in either ammonia or ethylenediamine could be completely bleached by repeated 1.0-μsec pulses. This required from 5 to 25 pulses depending upon concentration. Presumably the bleaching produces amide or ethylenediamide ions. After the buildup of a high enough base concentration ($\gtrsim 10^{-3}M$) the pulsing of blue solutions in ethylenediamine resulted in the growth of the absorbance rather than its decay.

Solutions of potassium amide in ammonia, produced either by repeated pulsing of potassium solutions or by allowing a potassium solution to decompose (amide concentration $\gtrsim 10^{-3}M$) showed the following behavior upon radiolysis: The formation of the solvated electron absorbance during the pulse was followed by a fast decay ($t_{1/2}<0.5$ μsec), at least four or five times faster than the decay in neutral anhydrous ammonia [see Fig. 8(c)]. The addition of ethanol (10^{-3} to $10^{-2}M$) resulted in the complete elimination of this rapid decay [Fig. 8(d)]. The residual absorbance lasted for times as long as several seconds. With basic ethylenediamine (formed by the decomposition or pulsing of potassium solutions) the solvated electron band required seconds to disappear even in the absence of ethanol. In the case of basic ethylenediamine, the absorbance showed a

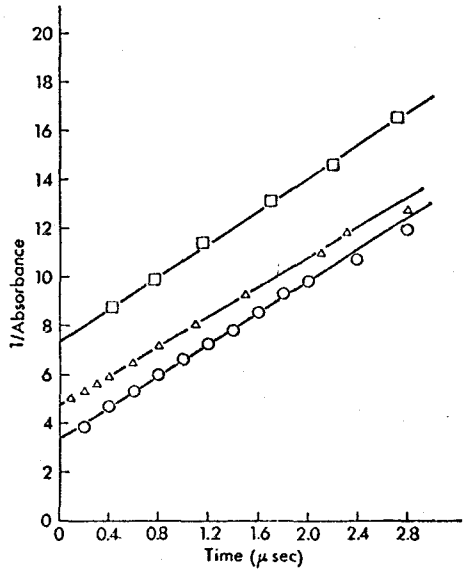

FIG. 9. Initial electron decay in ammonia under various conditions, observed at 1000 nm. ○, Pure anhydrous NH_3, $t=-35$°C; ◁, 0.06M NH_4Br in NH_3 at −25°C; □, NH_3–H_2O mixture at −35°C; $X_{H_2O}=0.213$.

first-order growth ($t_{1/2}$=3–8 μsec) after the end of the pulse.

The addition of water to either basic ammonia or to basic ethylenediamine to yield mole fractions of water up to 0.5 resulted in a partial decay of the solvated electron absorbance at a rate comparable to that in the pure neutral solvent [Figs. 8(e) and 9] followed by a decay at least three orders of magnitude slower, whose rate increased with increasing water concentration. As shown in Fig. 9, the initial decay rate in ammonia containing added ammonium bromide (as high as 0.06M) is nearly the same as that in pure ammonia.

The reaction of the solvated electron with ammonium ions in liquid ammonia is very slow indeed. This was confirmed by examining the decay of the residual absorbance of the solvated electron in the presence of known concentrations of ammonium bromide at −25°C. This decay was first order in the absorbance. Less than 10% of the initial absorbance of the solvated electron remained after the initial fast decay, so that it was necessary to amplify the signals tenfold in order to follow the reaction with NH_4^+. In order to obtain reproducible results, it was also necessary to preirradiate the solutions with eight to ten 1.0-μsec pulses before recording the decay kinetics. At ammonium ion concentrations below $10^{-2}M$, the apparent rate constant for the reaction of $e_{NH_3}^-$ with NH_4^+, assuming first-order behavior for each component decreased with increasing concentration of NH_4Br, suggesting that the properties of the preirradiated solution affected the decay rate. With $2.0\times10^{-2}M$ NH_4Br, apparent rate constants of 4.4, 3.4, and $3.8\times10^{4}M^{-1}\cdot$sec^{-1} were obtained, while $6.0\times10^{-2}M$ NH_4Br yielded values of 3.5, 3.2, and $3.8\times10^{4}M^{-1}\cdot$sec^{-1} for the reaction. Since this calculation neglects the effect of ion pairing and of ionic strength on the rate constant, it does not necessarily represent the rate of reaction of isolated solvated electrons and ammonium ions in pure ammonia. An approximate upper limit for the direct reaction rate at −25°C may be obtained by assuming that the ion pair $NH_4^+\cdot Br^-$ does not react and by correcting for the kinetic salt effect. This correction uses conductance data[35] to determine the concentration of free ions and the ionic strength, and gives an upper limit of $6\pm2\times10^{5}M^{-1}\cdot$sec^{-1} for the rate constant of the direct reaction of $e_{NH_3}^-$ with NH_4^+ in NH_3. The low value for this rate constant is somewhat comparable, taking into account the temperature difference, to the analogous reaction of e_{aq}^- with NH_4^+ in water[36] ($k\cong1.3\times10^{6}$) and of e_{solv}^- with RNH_2^+ in ethylenediamine.[26] The value is orders of magnitude lower than the value of $3\times10^{9}M^{-1}\cdot$sec^{-1} cited by Shubin *et al.*,[37] whose subsequent comments in their paper indicate that they were aware that reaction with NH_4^+ was not the rate-limiting reaction under their conditions.

The results obtained in this study may be summarized as follows: In neutral or acidic ammonia (made acidic with either NH_4^+ or H_2O) the ammoniated electron reacts rapidly with an oxidizing species (such as the NH_2 radical) which is not scavenged by ethanol. Since the initial concentration of the oxidizing species is not known, and since NH_2 is also presumed to disappear by another reaction, the rate constant for the reaction of the solvated electron with NH_2 cannot be calculated. However, assuming nearly equal initial concentrations and using the extinction coefficient for metal–ammonia solutions[1,2] gives a second-order rate constant greater than $10^{10}M^{-1}\cdot$sec^{-1}. In addition to its reaction with $e_{NH_3}^-$, the oxidizing species presumably disappears by another reaction (possibly $2NH_2\rightarrow N_2H_4$). Therefore, a residual concentration of the ammoniated electron is produced which depends upon the relative yields and reaction rates. Since dilute solutions of potassium in ammonia are bleached by pulsing, the total yield of oxidizing species with which $e_{NH_3}^-$ can react rapidly is probably greater than the yield of $e_{NH_3}^-$.

In basic solutions, another radical (possibly NH^-) is produced, which is effectively scavenged by ethanol (in ethylenediamine, the solvent appears to act as a scavenger for the corresponding species). In the absence of a scavenger, the solvated electron absorbance in basic ammonia disappears completely and rapidly after the pulse ($t_{1/2}$<0.5 sec).

ACKNOWLEDGMENTS

We are indebted to Mr. John Richter for construction of the electronic instrumentation required for the fast infrared detector and pulsed xenon lamp and for maintaining the linac.

* This work was supported by the U.S. Atomic Energy Commission and was done while J. L. D. was a visiting scientist on sabbatical leave at The Ohio State University.

[1] R. C. Douthit and J. L. Dye, J. Am. Chem. Soc. 82, 4472 (1960).
[2] M. Gold and W. L. Jolly, Inorg. Chem. 1, 818 (1962).
[3] R. K. Quinn and J. J. Lagowski, J. Phys. Chem. 73, 2326 (1969).
[4] H. Blades and J. W. Hodgins, Can. J. Chem. 33, 411 (1955).
[5] R. R. Dewald and J. L. Dye, J. Phys. Chem. 68, 121 (1964).
[6] M. Ottolenghi, K. Bar-Eli, and H. Linschitz, J. Chem. Phys. 43, 206 (1965).
[7] L. M. Dorfman and M. S. Matheson, Progr. Reaction Kinetics 3, 237 (1965).
[8] M. S. Matheson and L. M. Dorfman, *Pulse Radiolysis* (M.I.T. Press, Cambridge, Mass., 1969).
[9] R. F. Gould (Ed.), Advan. Chem. Ser. 50 (1965).
[10] E. J. Hart and J. W. Boag, J. Am. Chem. Soc. 84, 4090 (1962).
[11] J. W. Boag and E. J. Hart, Nature 197, 45 (1963).
[12] I. A. Taub, M. C. Sauer, Jr., and L. M. Dorfman, Discussions Faraday. Soc. 36, 206 (1963).
[13] I. A. Taub, D. A. Harter, M. C. Sauer, Jr., and L. M. Dorfman, J. Chem. Phys. 41, 979 (1964).
[14] L. M. Dorfman, in Ref. 9, p. 36.
[15] G. E. Adams, J. H. Baxendale, and J. W. Boag, Proc. Chem. Soc. 1963, 241.
[16] J. H. Baxendale, E. M. Fielden, and J. P. Keene, Science 148, 637 (1965).
[17] D. M. J. Compton, J. F. Bryant, R. A. Cesena, and B. L. Gehman, in *Pulse Radiolysis* (Academic, New York, 1965), p. 43.
[18] B. Ward, Advan. Chem. Ser. 81, 601 (1968).
[19] M. Anbar and E. J. Hart, J. Phys. Chem. 69, 1244 (1965).
[20] L. R. Dalton, J. L. Dye, E. M. Fielden, and E. J. Hart J. Phys. Chem. 70, 3358 (1966).

[21] S. Arai and M. C. Sauer, J. Chem. Phys. 44, 2297 (1966).
[22] J. H. Baxendale and M. A. J. Rodgers, J. Phys. Chem. 72, 3849 (1968).
[23] M. S. Matheson and L. M. Dorfman, J. Chem. Phys. 32, 1870 (1960).
[24] W. D. Felix, B. L. Gall, and L. M. Dorfman, J. Phys. Chem. 71, 384 (1967).
[25] R. Wander, P. Neta, and L. M. Dorfman, J. Phys. Chem. 72, 2946 (1968).
[26] L. H. Feldman, R. R. Dewald, and J. L. Dye, in Ref. 9, p. 163.
[27] S. Arai, E. L. Tremba, J. R. Brandon, and L. M. Dorfman, Can. J. Chem. 45, 1119 (1967).
[28] V. A. Nicely and J. L. Dye (unpublished).
[29] S. Golden, C. Guttman, and T. R. Tuttle, Jr., J. Chem. Phys. 44, 3791 (1966).
[30] L. Raff and H. A. Pohl, in Ref. 9, p. 173.
[31] M. Natori and T. Watanabe, J. Phys. Soc. Japan 21, 1573 (1966).
[32] W. Feller, *Introduction to Probability Theory and its Applications* (Wiley, New York, 1950), p. 168.
[33] See for example, J. Jortner, S. A. Rice, and E. G. Wilson, in *Metal-Ammonia Solutions*, edited by G. Lepoutre and M. J. Sienko (Benjamin, New York, 1964), p. 22, and references therein.
[34] D. Cleaver, E. Collinson, and F. S. Dainton, Trans. Faraday Soc. 56, 1640 (1960).
[35] E. C. Franklin and C. A. Kraus, J. Am. Chem. Soc. 27, 191 (1905).
[36] M. Anbar and P. Neta, Intern. J. Radiation Isotopes 18, 493 (1967).
[37] V. N. Shubin, V. A. Zhigunov, G. I. Khaikin, L. P. Beruchashvili, and P. I. Dolin, Advan. Chem. Ser. 81, 95 (1968).

II. 2. Interprétation des résultats.

La variation de la position du maximum du spectre d'absorption en fonction de la composition des mélanges (en fraction molaire) ne peut pas être décrite d'une façon simple. Nous avons montré qu'une combinaison linéaire de diverses espèces absorbantes ne pouvait pas rendre compte de cette variation.

Aucun des nombreux modèles et traitements théoriques de l'électron solvaté ne permet de traiter le cas de mélanges de solvants.

Nous avons développé une méthode empirique d'analyse des spectres.

II. 2. 1. Analyse des spectres par une méthode de moments. (Publication 2)

a) Définition

Les moments d'une courbe de distribution $y = f(x)$ sont définis par la relation suivante

$$M_n = \int_{-\infty}^{+\infty} x^n f(x)\, dx$$

où n indique l'ordre de ce moment.

b) Sens physique des moments

Le moment d'ordre zéro est égal à la surface comprise sous la courbe de distribution, le moment d'ordre 1 donne la valeur moyenne de l'abscisse x.

Le sens physique des moments d'ordre supérieur peut se déterminer en utilisant un changement d'origine. Le moment d'ordre 2 centré sur la valeur moyenne est la variance ou pour une courbe gaussienne la largeur à mi-hauteur. De même les moments d'ordre supérieur sont reliés à l'asymétrie de la courbe et à la déviation de la courbe à une distribution normale.

c) Calcul de moments théoriques

Il a été démontré que les moments de la courbe de dispersion de la partie imaginaire de la constante diélectrique ε_2 (E) pouvaient être calculés d'une façon simple en termes de la fonction d'onde de l'état fondamental et de commutateurs de l'hamiltonien (Publication 2, équations 1 et 3).

d) Relation entre ε_2 (E) et le spectre d'absorption dans le cas de l'électron solvaté.

La partie imaginaire de la constante diélectrique est liée au coefficient d'extinction de l'électron solvaté par la formule

$$\alpha(E) = \frac{2\pi E \varepsilon_2(E)}{h c n (E)}$$

où n (E) est l'indice de réfraction, c la vitesse de la lumière, ε_2 (E) la constante diélectrique imaginaire, ε (E) l'absorptivité de la solution et E l'énergie de la radiation incidente. Nous avons déduit des mesures expérimentales de réflectance de Koehler (réf. 14, publication 2), que pour des solutions diluées d'électrons solvatés, l'indice de réfraction était constant dans la région d'intérêt. Un simple examen de la formule ci-dessus permet de voir que le moment d'ordre n de la courbe d'absorption dit moment expérimental μ_n $\quad \mu_n = \int \alpha(E)\, E^n \, dE$ correspond au moment d'ordre n + 1 de ε_2 (E)

e) Calcul des moments expérimentaux

Pour décrire la forme des spectres de l'électron solvaté, une forme mathématique rendant compte de l'asymétrie de la courbe devait être choisie. Nous avons utilisé la courbe gaussienne asymétrique de Fraser et Suzuki pour laquelle Rusch et Lelieur ont démontré que les moments sont définis. (1)

f) Méthode de calcul des paramètres d'un modèle.

Le modèle utilisé dans la publication 2 est celui du puits de potentiel sphérique de profondeur V_w et de rayon a . Nous avons évalué les premiers moments de la courbe de dispersion de la partie imaginaire de la constante diélectrique : M_0 , M_1 , M_2 , M_3 . Pour la suite du calcul, les moments sont normés de telle sorte que $m_n = \frac{M_n}{M_0}$

Les expressions de m_1 , m_2 , m_3 sont données dans les équations 10 a, b, c .

Les moments expérimentaux sont calculés à partir de la formule mathématique ajustée à la courbe expérimentale. Pour pouvoir comparer les valeurs obtenues aux expressions théoriques, il faut calculer les moments d'ordre - 1, 0, 1, 2 . Les valeurs normées de ces moments sont

$$\overline{\mu}_n = \frac{\mu_n}{\mu_{-1}}$$

Pour évaluer les divers paramètres introduits dans les expressions théoriques, il suffit de résoudre le système d'équations :

$$\overline{\mu}_n = m_{n+1}$$

Deux moments suffisent pour obtenir deux équations indépendantes qui permettent de calculer V_w et a .

A l'aide de ces valeurs, on recalcule m_3 et on le compare à la valeur expérimentale $\overline{\mu}_2$ pour avoir une indication de la qualité du calcul.

g) Résultats.

Nous avons appliqué cette méthode aux spectres de l'électron solvaté dans l'ammoniac liquide à -65°C.

Nous avons utilisé les spectres publiés sous forme tabulée dans la littérature.

Les résultats que nous avons obtenus pour diverses concentrations sont cohérents. Nous obtenons une profondeur du puits de 1.84 ± 0.02 eV et un rayon de 4.07 ± 0.05 A°.

Dans tous les cas la valeur de m_3 calculée à l'aide de ces données est légèrement supérieure à la valeur expérimentale mais du même ordre de grandeur, ceci montre que le modèle est valable pour représenter les spectres d'absorption de l'électron solvaté dans l'ammoniac liquide.

On peut voir d'après les valeurs de la profondeur et du rayon du puits, qu'un seul état lié existe dans ce puits et que les transitions doivent être du type état lié $\longrightarrow$ continuum.

PUBLICATION 2

SOLVATED ELECTRON SPECTRA. STUDY OF THE ABSORPTION CURVES BY A METHOD OF MOMENTS.

Solvated Electron Spectra. Study of the Absorption Curves by a Method of Moments

Marc G. Debacker,*

Laboratoire des Métaux alcalins dans NH_3 liquide,[1] 59046 Lille Cedex, France

J. N. Decarpigny, and M. Lannoo

Laboratoire de Physique des Solides[1] I.S.E.N., 59046 Lille Cedex, France *(Received March 22, 1976)*

The optical spectrum of the solvated electron in liquid ammonia is analyzed by a method of moments. A general formalism to compute the theoretical moments is presented. These moments are function of only the ground state wave function. The moments of the experimental curves are obtained by using a fit to a skewed Gaussian. A comparison of theory and experiment is presented using a spherical well model. The parameters of the well thus obtained are $V_w = 1.85$ eV and $a = 4.1$ Å and only one bound state is allowed.

I. Introduction

The optical absorption spectrum of solvated electrons in liquid ammonia consists of a broad asymmetric band centered in the near-infrared and tailing in the visible.[2] The nature of this absorption band has been extensively studied and various approaches such as the cavity model,[3] the semicontinuum model,[4,5] or ab initio calculations[7,8] have been used. In most of these works, one starts from a given theoretical model and directly calculates the quantities of interest, namely, the position of the absorption peak, which are then compared to the experimental results. Nevertheless, some workers have attempted to reproduce the shape of the spectrum. Delahay[9] has decomposed the spectrum into several bands arising from bound–bound and bound–continuum transitions, but this does not fit the solvated electron absorption band in ammonia. More recently, Mazzacurati et al.[10] have used an exact expression of the absorbance for the case of a particle in a spherical box. Their results are in good agreement with experiment but the method cannot be extended to more realistic model potentials.

In this paper, a general method to derive, from the experimental spectrum, the characteristic parameters of a given model potential featuring the solvated electron potential is presented. From this, it is then possible to discuss the nature of the allowed optical transitions and, for instance, the number of bound states in the case of a spherical box. For this purpose a method of moments is used. The theoretical expressions for the moments of the absorption curve can be determined from the ground state wave function in terms of the parameters of the model potential. By equating these expressions to the experimental values of the lowest order moments, a set of equations allowing the determination of the parameters is then obtained. Moreover, when the number of calculated moments is greater than the number of parameters, a critical test of the validity of the model potential can be done.

In section II, a formalism is developed showing that one only requires the knowledge of the ground state wave function, without any assumptions concerning the transitions. In section III, the computation of the experimental moments is described and in section IV a simple application to the case of an electron in a spherical box is given. Then, in section V, numerical results are discussed and possible improvements are described.

II. General Formalism

The contribution of a solvated electron to the imaginary part of the dielectric constant is given by[11]

$$\epsilon_2(E) = 4\pi^2 \Sigma \langle g|\zeta|e\rangle\langle e|\zeta|g\rangle \delta\,[E - (E_e - E_g)] \qquad (1)$$

where atomic units are used. $|e\rangle$ represents the wavefunction of one of the excited states, and E_e the energy associated to this state; $|g\rangle$ the wave function of the ground state, and E_g the ground state energy; ζ is the component of the electron position along a given direction. In this expression, it is implied that the ground state is nondegenerate. The summation is extended over all the excited states.

The nth order moment of $\epsilon_2(E)$ is defined by

$$M_n = \frac{2}{\pi} \int \epsilon_2(E) E^n \, dE \qquad (2)$$

Using the closure relation, Lannoo and Decarpigny[12] have shown that these moments can be expressed in the form

$$M_n = 8\pi\,[\langle g|\zeta\,[n]\,|g\rangle - \langle g|\zeta|g\rangle\langle g|[n]\,|g\rangle] \qquad (3)$$

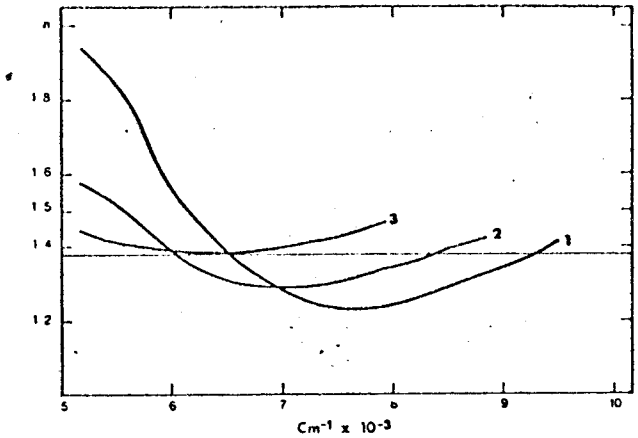

Figure 1. Variation of the refractive index with energy calculated from ref 12: curve 1, 1 MPM; curve 2, 0.5 MPM; curve 3, 0.1 MPM. The horizontal line indicates the refractive index of the pure solvent.[13]

where $[n]$ is the commutator of order n:

$$[n] = [H, [H, \ldots [H,\xi] \ldots] \tag{4}$$

and H is the electron Hamiltonian.

This expression shows that it is possible to evaluate the moments knowing only the Hamiltonian and the exact wave function of the ground state. Equation 3 takes into account all the transitions to all excited states: bound-bound transitions as well as bound-continuum transitions.

In the following sections, the moments needed for computation are normalized to unit M_0. They are referred to as m_n where

$$m_n = M_n/M_0 \tag{5}$$

III. Experimental Moments

The absorptivity α of the solution is related to the imaginary part of the dielectric constant by

$$\alpha(E) = \frac{2\pi E \epsilon_2(E)}{hcn(E)} \tag{6}$$

where $n(E)$ is the refractive index and c the velocity of light. In order to obtain $\epsilon_2(E)$ from the absorption curve, one has to know the values of $n(E)$ for each wavelength.

The work of Koehler[14] on the reflectance spectra of metal-ammonia solutions gives some values of the real and imaginary parts of the dielectric constant as a function of the energy. From these data, the variation of the refractive index with energy can can be calculated. These values are plotted in Figure 1 for the three concentrations used by Koehler: 1, 0.5, and 0.1 MPM at about −50 °C. The variation of $n(E)$ as a function of energy becomes smaller as the concentration is decreased.

Since the concentrations used in studies of the spectrum of solvated electrons are factor of 100 smaller than 0.1 MPM, we can consider that the refractive index is a constant equal to the refractive index of pure ammonia.[15] Thus, it follows from (6) that the moment of order n of $\epsilon_2(E)$ is related to the $(n - 1)$th order moment of the absorption curve.

To calculate the moments, the optical spectrum was fitted with a skewed-Gaussian equation[16]

$$\alpha(E) = \alpha_{max} \exp\left[-\ln 2\left[\ln\left(1 + \frac{2b(E - E_{max})}{\Delta E}\right)\frac{1}{b}\right]^2\right] \tag{7}$$

TABLE I: Experimental Results for $NaNH_3$ Solutions at −65 °C

No.	Concn, M	E_{max}, cm⁻¹	ΔE, cm⁻¹	b
1[a]	1.26×10^{-3}	6830 ± 50	3241 ± 80	0.465 ± 0.050
2[a]	1.63×10^{-3}	6815 ± 20	3105 ± 30	0.493 ± 0.020
3[a]	3.89×10^{-3}	6705 ± 30	3180 ± 45	0.532 ± 0.028
4[b]	0	6920 ± 40	3319 ± 55	0.506 ± 0.024
5[c]	1.39×10^{-4}	6950 ± 35	3365 ± 50	0.465 ± 0.022

[a] Taken from ref 16 curves 10, 25, and 28 for nos. 1, 2, and 3, respectively. [b] Reference 17. Data extrapolated to infinite dilution. [c] Reference 17 curve 4.

TABLE II: Experimental Moments (in atomic units)

No.	$\bar{\mu}_0$	$\bar{\mu}_1$	$\bar{\mu}_2$
1	3.368×10^{-2}	1.190×10^{-3}	4.431×10^{-5}
2	3.378×10^{-2}	1.195×10^{-3}	4.449×10^{-5}
3	3.364×10^{-2}	1.191×10^{-3}	4.479×10^{-5}
4	3.450×10^{-2}	1.253×10^{-3}	4.819×10^{-5}
5	3.427×10^{-2}	1.234×10^{-3}	4.694×10^{-5}

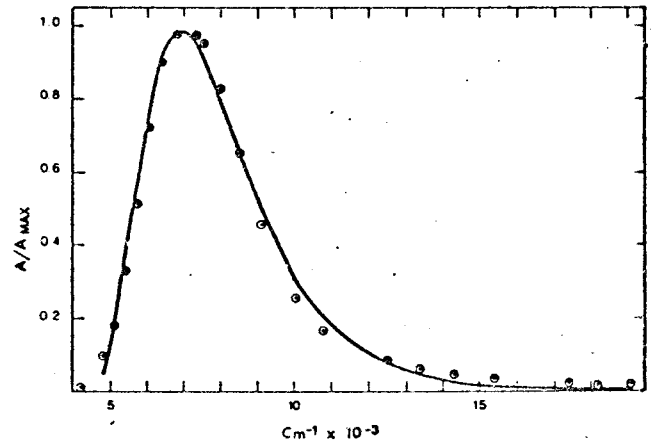

Figure 2. Nonlinear least-squares fit of $NaNH_3$ spectrum at infinite dilution and −65 °C.[17]

where α_{max} is the value of the absorptivity at the maximum E_{max}, b is an asymmetry parameter, and ΔE is related to the half-width w by the relation

$$w = \Delta E \frac{\sinh b}{b} \tag{8}$$

The moments of this curve are defined and can be evaluated in an analytical form.[17] The experimental moments are designed μ_n. It follows from (6) that μ_n corresponds to M_{n+1}. Therefore the experimental moments are normalized in the following way:

$$\bar{\mu}_n = \mu_n/\mu_{-1} \tag{9}$$

so that $\bar{\mu}_n$ corresponds to m_{n+1}.

The experimental data were taken from the literature. The values used were those of Dye and Douthit[18] and of Rubenstein[19] for $NaNH_3$ solutions. For the later,[19] both the experimental data and data extrapolated to infinite dilution were used.

The spectra were fitted to eq 7 by using a nonlinear weighted least-squares program.[20] The parameter used for the fit were α_{max}, E_{max}, ΔE, and b. The weights were calculated using the standard deviation given in Rubenstein's thesis.

The values of the parameters with their standard error are given in Table I. A typical fit is shown in Figure 2.

The moments were calculated by numerical integration of eq 7. The normalized values are given in Table II.

TABLE III: Final Results

No.	m_3	V_0, eV	a, Å	E, eV
1	5.448×10^{-5}	1.83	4.11	−0.70
2	5.470×10^{-5}	1.84	4.14	−0.72
3	5.489×10^{-5}	1.82	4.05	−0.67
4	5.913×10^{-5}	1.87	4.01	−0.69
5	5.769×10^{-5}	1.86	4.05	−0.70

IV. Application of the Theory to a Simple Potential Well

The evaluation of the theoretical moments necessitates the choice of a model Hamiltonian for which the ground state wave function must be determined.

The cavity model has been widely used, and we have chosen to apply our method to one of the simplest cases: the particle in a spherical box of radius a and of depth V_w. For this model the 1s wave function of the ground state is known. The number of excited states is given by the size of the potential well.

The values of the moments are (in atomic units)

$$m_1 = \frac{3}{2}\frac{K^2}{T}\left(Ka - \frac{\sin 2Ka}{2} + \frac{K}{\chi}\sin^2 Ka\right) \quad (10a)$$

$$m_2 = K^5 a/T \quad (10b)$$

$$m_3 = \frac{2K^3\chi}{T} V_0\left(1 + \frac{1}{\chi a}\right)\sin^2 Ka \quad (10c)$$

where

$$T = \frac{(Ka)^3}{3} - \frac{\sin 2Ka}{2}\left[(Ka)^2 - \frac{1}{2}\right] - \frac{Ka\cos 2Ka}{2} + \frac{K^3}{\chi^3}\sin^2 Ka\left[(\chi a)^2 + \chi a + \frac{1}{2}\right] \quad (11)$$

with

$$K = \sqrt{2(E + V_w)};\ \chi = \sqrt{-2E};\ -\chi = K \operatorname{cotg} Ka \quad (11b)$$

and E is the energy of the ground state.

The two unknowns are V_w and a. They can be obtained by solving the two equations

$$\bar{\mu}_0 = m_1$$

$$\bar{\mu}_1 = m_2$$

The values of V_w and a are obtained with a program solving simultaneous nonlinear equations.[20] These values were used to recalculate m_3. The results are shown on Table III.

V. Discussion

The values obtained for V_w and a, satisfying the Landau condition,[21] indicate that, in the framework of the spherical box model, there is only one bound state in the well. Therefore the optical band is due to transitions to the continuum. This confirms the results obtained by Mazzacurati et al.[10] who have fitted the optical spectrum with the complete expression for the absorbancy first derived in this case by Breit and Condon.[22]

The values of m_3 recalculated from V_w and a are of the right order of magnitude, being systematically 20% higher than the experimental values. Since m_3 is very sensitive to the magnitude of the ground state wave function at the edge of the well, this discrepancy can be considered as an indication of a slight inadequacy of the model.

The calculated energy $|E|$ can be compared with the threshold on the low energy side. The values we have obtained, though reasonable, are too high. This point can be related to the discrepancy mentioned above with regard to m_3, since, when the well's edge is rounded off, the bound level moves upward.[23]

The energy E cannot be directly compared with the experimental data of photoemission by solvated electron solutions,[24,25] since these values include transitions to the vacuum and not to the delocalized states in the bulk of the solution.

This difference is well pointed out in the model of Copeland, Kestner, and Jortner[3b] in which a constant term V_0 represents the difference between the energy of the quasi-free electron in the medium and that of the electron under vacuum. This difference was described by Magat.[26]

Our calculations based only on the shape of the optical spectrum cannot give the value of V_0. It could be obtained by the difference between the values of the photoemission threshold and that of the threshold to the delocalized states in the bulk of the solutions.

These results obtained in a simple case show that the application of the method of moments to the analysis of the solvated electron spectra can give important informations about the potential well, the electronic ground state, and the type of transitions involved. Its main interest resides in the fact that the calculations are relatively easy and thus can be extended to more realistic potentials where the calculation of the complete absorption spectrum is no longer possible. It is also to be remembered that no particular assumptions concerning the transitions are necessary.

In a further work, we intend to compute the moments using a more realistic potential model, as well as to correlate the characteristic parameters of these potentials for solvated electrons in various media.

References and Notes

(1) Laboratoire associé au CNRS No. 253.
(2) For a general review on this subject see the Proceedings of Colloque Weyl IV, *J. Phys. Chem.*, 79, (26), 2789–3079 (1975).
(3) (a) R. A. Ogg, *Phys. Rev.*, 69, 668 (1946); (b) D. A. Copeland, N. R. Kestner, and J. Jortner, *J. Chem. Phys.*, 53, 1189 (1970).
(4) D. E. O'Reilly, *J. Chem. Phys.*, 41, 3736 (1964).
(5) T. Kajiwara, K. Funabashi, and C. Naleway, *Phys. Rev. A*, 6, 808 (1972).
(6) K. Iguchi, *J. Chem. Phys.*, 48, 1735 (1968).
(7) B. J. Mc Aloon and B. C. Webster, *Theor. Chim. Acta*, 15, 385 (1969).
(8) B. C. Webster and G. Howat, *Radiat. Res. Rev.*, 4, 259 (1972).
(9) R. Lugo and P. Delahay, *J. Chem. Phys.*, 57, 2122 (1972).
(10) V. Mazzacurati and G. Signorelli, *Lett. Nuovo Cimento*, 12, 347 (1975).
(11) J. M. Ziman, "Principles of the Theory of Solids", Cambridge University Press, New York, N.Y., 1969, p 226.
(12) M. Lannoo and J. N. Decarpigny, *J. Phys. (Paris)*, 35, C3-97 (1974); *Phys. Rev. B*, 14, 538 (1976).
(13) "The Optical Properties of Solids", J. Tauc, Ed., Academic Press, New York, N.Y., p 37.
(14) W. H. Koehler and J. J. Lagowski, *J. Phys. Chem.*, 73, 2329 (1969).
(15) A. W. Francis, *J. Chem. Eng. Data*, 5, 534 (1960).
(16) R. D. B. Fraser and E. Suzuki, *Anal. Chem.*, 41, 37 (1969).
(17) P. F. Rusch and J. P. Lelieur, *Anal. Chem.*, 45, 1541 (1973).
(18) R. C. Douthit and J. L. Dye, *J. Am. Chem. Soc.*, 82, 4472 (1960).
(19) G. Rubenstein, Ph.D. Thesis, Brandeis University, 1972.
(20) J. L. Dye and V. A. Nicely, *J. Chem. Ed.*, 48, 443 (1971).
(21) L. D. Landau and E. M. Lifshitz, "Quantum Mechanics", Pergamon Press, New York, N.Y., 1965, p 109.
(22) G. Breit and E. V. Condon, *Phys. Rev.*, 49, 904 (1936).
(23) "Problems in Quantum Mechanics", D. Ter Haar, Ed., Infosearch Ltd., London, p 31.
(24) J. Hasing, *Ann. Phys.*, 37, 509 (1940).
(25) H. Aulich, B. Baron, P. Delahay, and R. Lugo, *J. Chem. Phys.*, 58, 4439 (1973).
(26) M. Magat, *Ber. Bunsenges. Phys. Chem.*, 75, 666 (1971).

II. 2. 2. Applications de la méthode.

Dans cette partie du travail, nous appliquerons la méthode décrite en II. 2. 1. pour interpréter les modifications du spectre de l'électron solvaté causées soit par effet de température, soit par des modifications du solvant.

Ce travail sera publié ultérieurement.

Dans ce qui va suivre nous donnerons pour chaque spectre les valeurs des paramètres obtenus par l'ajustement de la courbe gaussienne asymétrique aux données expérimentales.

L'équation de la courbe est :

$$A(E) = A_{max} \exp\left\{ -\ln 2 \left[\ln \left(1 + \frac{2b\,(E - E_{max})}{\Delta E} \right) \frac{1}{b} \right]^2 \right\}$$

où A_{Max} est la valeur de l'absorbance au maximum E_{Max}, b est un paramètre d'asymétrie et ΔE est relié à la largeur à mi hauteur W par la relation

$$W = \Delta E \; \frac{\operatorname{sh} b}{b}$$

Nous donnerons aussi les valeurs des moments expérimentaux $\overline{\mu}_0$, $\overline{\mu}_1$, $\overline{\mu}_2$, et la valeur du moment théorique m_3 calculée à partir de la profondeur et du rayon du puits de potentiel.

a) Effet de température dans l'ammoniac pur.

Nous avons réalisé cette étude à l'aide des résultats tabulés publiés dans la littérature. Pour assurer la cohérence des calculs, seuls les résultats extrapolés à dilution infinie par Rubenstein (2) ont été utilisés. Cela entraîne que les trois températures étudiées sont : -55, -65 et -75°C.

Nous avons reporté les résultats dans le tableau 1. Nous obtenons une bonne précision sur les paramètres décrivant la courbe.

Dans la seconde partie de la table sont reportés les moments et les paramètres du puits. Comme précédemment (3), il faut noter que le moment m_3 calculé à partir de V_w et de a est légèrement supérieur au moment $\overline{\mu}_2$ expérimental mais du même ordre de grandeur.

TABLE I

ANALYSE DES SPECTRES D'ABSORPTION DE SOLUTIONS DE POTASSIUM DANS L'AMMONIAC EN FONCTION DE LA TEMPERATURE

T °C	E_{max} cm^{-1}	ΔE cm^{-1}	b
-55	6810 ± 30	3400 ± 50	0.43 ± 0.02
-65	6920 ± 40	3320 ± 60	0.51 ± 0.02
-75	7160 ± 40	3400 ± 50	0.48 ± 0.02

MOMENTS ET PARAMETRES DU PUITS

T °C	$\overline{\mu}_0$ $x10^2$	$\overline{\mu}_1$ $x10^3$	$\overline{\mu}_2$ $x10^5$	m_3 $x10^5$	V_w eV	a Å
-55	3.38	1.21	4.63	5.66	1.82	3.97
-65	3.45	1.23	4.82	5.91	1.87	4.01
-75	3.54	1.32	5.17	6.36	1.92	3.99

$\overline{\mu}$: moments expérimentaux. $\overline{\mu}_0$ et $\overline{\mu}_1$ servent à calculer V_w et a

m_3 : moment d'ordre 3 calculé d'après V_w et a à comparer à $\overline{\mu}_2$

UNITES

- Les moments normés sont exprimés en unités atomiques d'énergie (1 u.a. = 27,21 eV ; 1 eV = 8060 cm^{-1})
  Les moments m_1 et $\overline{\mu}_0$ en u.a.
  Les moments m_2 et $\overline{\mu}_1$ en $(u.a.)^2$ etc..

b) Effet de la composition du solvant.

Nous avons réanalysé toutes les données obtenues dans le cas des mélanges eau-ammoniac et eau-éthylènediamine (4).
Nous n'avons tenu compte que des données obtenues, par radiolyse pulsée, dans les mêmes conditions expérimentales, ce qui explique l'absence des points correspondant aux solvants purs.
Nous avons reporté les résultats de l'ajustement de la courbe gaussienne asymétrique aux données expérimentales dans le tableau 2 . On peut voir que les incertitudes sur ces valeurs sont importantes. Ceci tient au fait que les spectres sont obtenus point par point et qu'un nombre restreint de points est disponible pour chaque spectre. De plus la nécessité d'avoir suffisamment de lumière sur le détecteur infrarouge forçait à ouvrir les fentes du monochromateur et donc à diminuer la résolution.
(Voir publication 1 pour les détails expérimentaux).
Pour certaines concentrations les spectres ont été réalisés plusieurs fois ce qui explique que ces points apparaissent plusieurs fois dans les tables. Il faut noter que tous les spectres sont corrigés pour l'effet de température.
Nous avons reporté dans la table 3 les résultats de l'analyse des courbes par la méthode des moments. Bien que ces résultats soient plus imprécis que dans le cas de l'ammoniac, on observe la même différence entre le moment calculé m_3 et le moment expérimental $\overline{\mu}_2$. Cette différence est toujours dans le même sens et de l'ordre de 22%. Cette comparaison montre que le modèle est valable dans toute la gamme de concentrations.
Nous pouvons vérifier la cohérence de nos résultats en observant que les valeurs de V_w et de a tendent vers la même limite lorsque l'on s'approche de l'eau pure. Ceci est mis en évidence sur les figures 1 et 2 .

TABLE 2

MELANGES EAU - NH_3 . SPECTRES EXPERIMENTAUX
VALEURS CORRIGEES à 25°C

$x(H_2O)$	E_{max} cm^{-1}	ΔE cm^{-1}	b
0.144	6310 ± 100	2650 ± 500	0.76 ± 0.38
0.213	6630 ± 120	2790 ± 460	0.86 ± 0.21
0.358	7140 ± 30	4100 ± 225	0.42 ± 0.10
0.367	7380 ± 20	3790 ± 40	0.32 ± 0.02
0.421	7600 ± 90	3890 ± 200	0.45 ± 0.12
0.421	7600 ± 90	3960 ± 240	0.56 ± 0.14
0.489	8400 ± 50	4900 ± 80	0.46 ± 0.04
0.496	8300 ± 200	5400 ± 450	0.28 ± 0.20
0.594	9521 ± 140	6033 ± 480	0.41 ± 0.25
0.594	9760 ± 30	5740 ± 60	0.39 ± 0.03
0.717	10790 ± 70	5740 ± 280	0.68 ± 0.06
0.752	11250 ± 110	6850 ± 340	0.56 ± 0.07
0.759	11600 ± 100	6510 ± 250	0.56 ± 0.06
0.841	12630 ± 130	7230 ± 220	0.40 ± 0.06
0.862	12830 ± 60	7400 ± 110	0.41 ± 0.03
0.930	13400 ± 110	7500 ± 160	0.48 ± 0.04
0.949	13450 ± 125	7580 ± 190	0.48 ± 0.05

TABLE 2 (suite)

MELANGES EAU - ETHYLENEDIAMINE

$x(H_2O)$	E_{max} cm^{-1}	ΔE cm^{-1}	b
0.263	8910 ± 110	7380 ± 380	0.47 ± 0.12
0.263	8710 ± 60	8200 ± 420	0.27 ± 0.09
0.263	8680 ± 150	6660 ± 700	0.53 ± 0.20
0.424	9520 ± 140	6590 ± 270	0.61 ± 0.14
0.424	9600 ± 130	6800 ± 270	0.61 ± 0.13
0.524	10480 ± 190	6560 ± 330	0.55 ± 0.12
0.603	11110 ± 80	7050 ± 130	0.50 ± 0.04
0.655	11630 ± 80	7070 ± 130	0.48 ± 0.04
0.702	12600 ± 110	7200 ± 150	0.44 ± 0.05
0.757	13150 ± 140	7290 ± 180	0.35 ± 0.05
0.820	13980 ± 200	7710 ± 220	0.30 ± 0.07
0.863	14000 ± 160	7520 ± 200	0.34 ± 0.05

TABLE 3

APPLICATION DE LA METHODE DES MOMENTS
MELANGES EAU - AMMONIAC

x (H_2O)	$\overline{\mu}_0$ x10^1	$\overline{\mu}_1$ x10^3	$\overline{\mu}_2$ x10^5	m_3 x10^5	V_w eV	a A
* 0.0					1.49	4.00
0.144	3.35	1.19	4.63	5.60	1.80	3.90
0.213	3.62	1.42	6.26	7.46	1.96	3.59
0.358	3.48	1.29	5.15	6.32	1.87	3.83
0.367	3.50	1.28	4.97	6.13	1.90	4.0
0.421	3.74	1.48	6.20	7.62	2.10	3.64
0.421	3.86	1.59	7.05	8.60	2.00	3.82
0.489	4.15	1.85	8.84	10.8	2.23	3.45
0.496	3.86	1.61	7.24	8.95	2.10	3.50
0.594	4.64	2.32	12.60	15.48	2.50	3.20
0.717	5.70	3.51	23.80	28.82	3.10	2.90
0.752	5.75	3.60	24.53	29.9	3.10	2.85
0.759	5.93	3.78	26.11	31.8	3.20	2.90
0.841	6.14	4.00	27.95	34.3	3.30	2.90
0.862	6.25	4.16	29.60	36.4	3.36	2.90
0.930	6.66	4.70	36.1	44.2	3.60	2.76
0.949	6.68	4.77	36.5	44.8	3.60	2.75
* 1.00					3.65	2.90

* Valeurs extrapolées

TABLE 3 (suite)

MELANGES EAU - ETHYLENEDIAMINE

$x(H_2O)$	$\overline{\mu_0}$ $\times 10^2$	$\overline{\mu_1}$ $\times 10^3$	$\overline{\mu_2}$ $\times 10^4$	m_3 $\times 10^4$	V_w eV	a Å
0.00					2.00	2.90 *
0.263	4.44	2.23	1.29	1.58	2.51	2.92
0.263	3.83	1.74	0.90	1.14	2.30	2.92
0.263	4.42	2.20	1.24	1.51	2.47	3.00
0.424	5.00	2.77	1.74	2.10	2.76	2.88
0.424	5.03	2.83	1.80	2.17	2.79	2.85
0.524	5.35	3.11	1.99	2.42	2.90	2.93
0.603	5.59	3.40	2.25	2.75	3.02	2.88
0.702	6.20	4.10	2.90	3.56	3.33	2.86
0.757	6.29	4.19	2.96	3.64	3.39	2.91
0.820	6.59	4.59	3.38	4.17	3.55	2.86
0.863	6.67	4.70	3.50	4.31	3.60	2.85
1.000					3.65	2.90 *

* Valeurs extrapolées

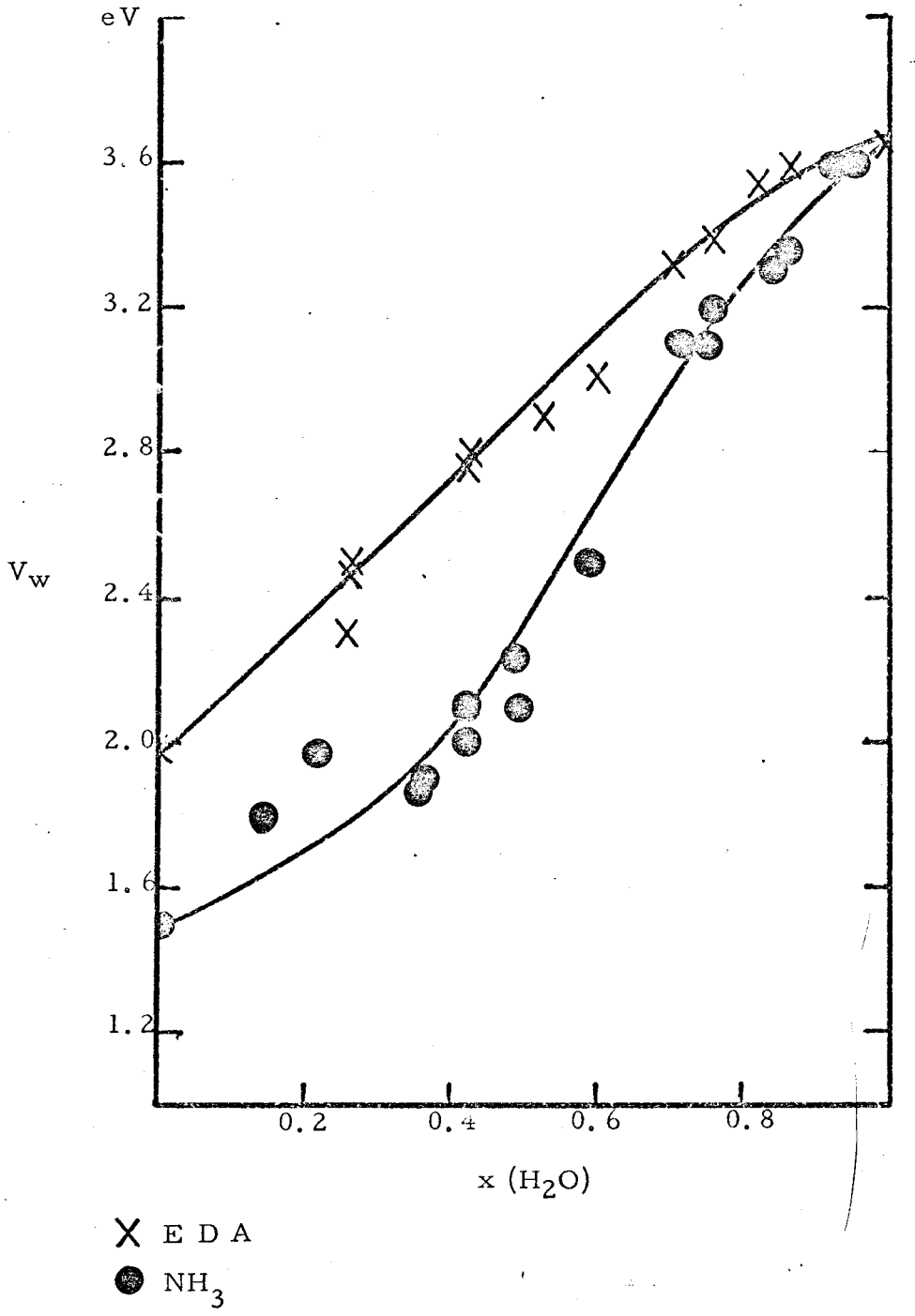

Fig. 1 . Profondeur du puits de potentiel en fonction de la composition du mélange.

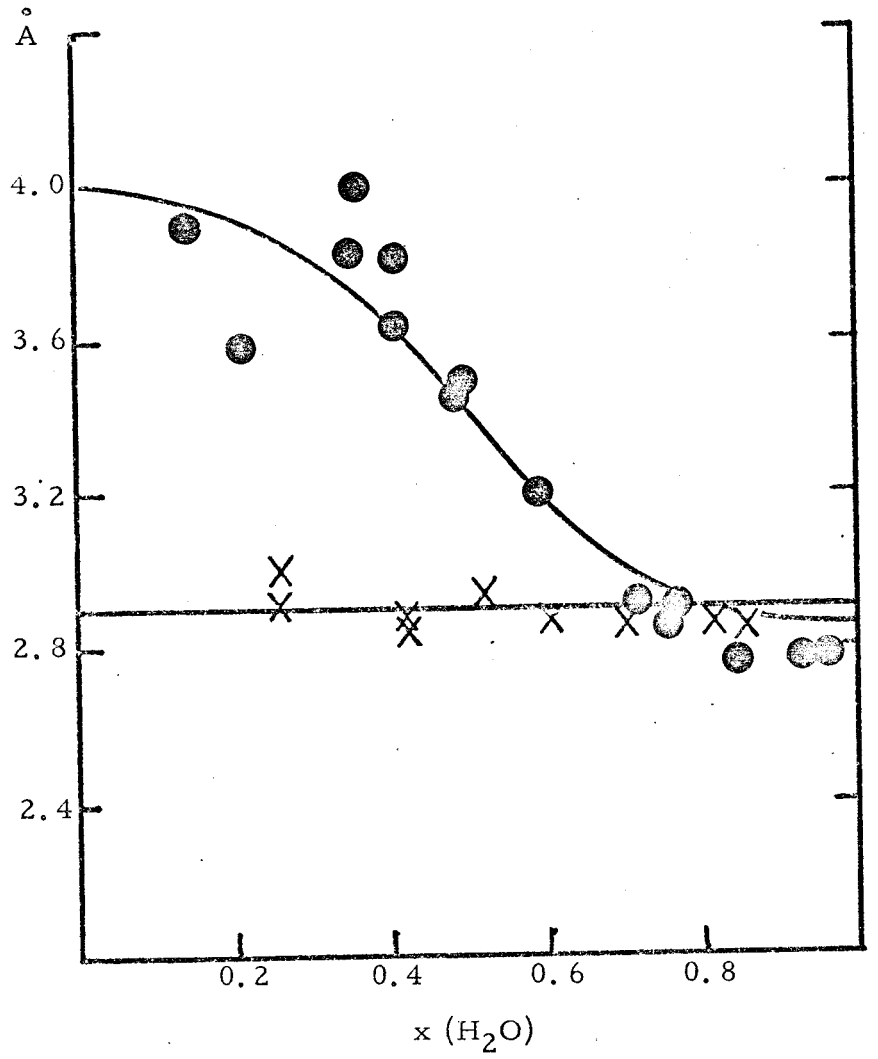

X E D A

● NH_3

Fig. 2 . Rayon de la cavité en fonction de la composition du mélange.

II. 2. 3. Interprétation.

a) Nombre d'états liés dans le puits.

A partir des valeurs de V_w et de a, nous avons calculé l'énergie des états liés possibles dans le puits. Dans le cas du puits de potentiel sphérique la condition d'existence d'états liés est obtenue par la solution d'équations traduisant la continuité de la fonction d'onde et de ses dérivés à la limite du puits. Ces équations sont différentes pour chaque type de fonction d'onde.

Pour une fonction d'onde 1 s, il y aura un état lié ($E < 0$) si l'équation $-\chi a = Ka \cot g\, Ka$ peut être vérifiée pour $V_w < E < 0$

$\chi = \sqrt{-2E}$; $K = \sqrt{2(E+V)}$; a = rayon du puits

Nous avons vérifié qu'il existait un état lié de type 1 s dans tous les cas. Cet état est le plus stable qui puisse exister dans le puits. L'état lié d'énergie supérieure est un état 2 s dont la condition d'existence est donnée par :

$$\frac{K^2}{1 - Ka \cot g\, Ka} = \frac{-\chi^2}{1 + \chi a}$$

Nous avons vérifié que dans tous les cas de puits de potentiel obtenus, il n'existe pas d'état 2 s lié. Il est évident qu'il n'y aura pas non plus d'état lié 2 p ou d'état d'énergie supérieure. Dans le cadre de notre modèle, nous devons considérer que la transition responsable de l'absorption est du type 1 s $\longrightarrow$ continuum. Cette conclusion est renforcée par les travaux d'autres auteurs qui ont utilisé la formule théorique du spectre d'absorption d'une particule placée dans un puits sphérique pour décrire le spectre de l'électron dans l'eau et dans l'ammoniac. (5)

Ces auteurs utilisent un ajustement d'une formule théorique aux valeurs expérimentales et obtiennent de cette façon les valeurs de la profondeur du puits et de son rayon. L'accord plus ou moins bon entre l'absorbance calculée et expérimentale doit donc s'évaluer par la qualité de l'ajustement ce qui est une quantité difficile à mesurer. Notre méthode utilisant les moments de la courbe permet d'évaluer la qualité du modèle en comparant des valeurs numériques de moments expérimentaux et calculés. De plus la méthode des moments procède par intégration ce qui est un bon procédé de lissage des données expérimentales.

Les valeurs de l'énergie du premier niveau sont reportées dans la table 4 . Cette valeur peut être comparée au seuil d'énergie correspondant au début du pic d'absorption. Comme nous l'avons remarqué dans la publication 2, le niveau d'énergie E_T(exp) obtenu d'après la courbe expérimentale extrapolée est situé plus haut que le niveau calculé. Ceci indique que le puits est correct à sa base mais que les bords du puits sont probablement arrondis. Il faut aussi noter que dans aucun des cas la valeur de l'énergie de seuil d'absorption expérimentale E_T ne permet de postuler plusieurs niveaux liés dans le puits. En effet un autre état lié produirait une autre bande d'absorption à une énergie inférieure au seuil d'apparition de la bande d'absorption.

b) Interprétation du déplacement des pics.

Notre analyse nous permet de retirer des spectres d'absorption une quantité de renseignements qui ne seraient pas disponibles par une autre méthode.

Nous pouvons en particulier essayer de trouver des corrélations entre les paramètres du puits et la position du maximum d'absorption.

T A B L E 4

ENERGIE DE SEUIL

Eau - Ammoniac

	x (H_2O)	E (1 s) eV	E_T (exp) eV
*	0.00	0.41	
	0.144	0.60	0.57 ± 0.16
	0.213	0.59	0.62 ± 0.10
	0.358	0.63	0.28 ± 0.19
	0.367	0.72	0.18 ± 0.06
	0.421	0.74	0.41 ± 0.18
	0.421	0.70	0.50 ± 0.15
	0.489	0.73	0.38 ± 0.07
	0.496	0.64	
	0.594	0.77	0.30 ± 0.08
	0.717	0.94	0.81 ± 0.08
	0.752	0.93	0.64 ± 0.15
	0.759	1.01	0.72 ± 0.12
	0.862	1.13	0.47 ± 0.11
	0.930	1.20	0.69 ± 0.11
	0.949	1.20	0.69 ± 0.14
*	1.00	1.39	

* valeurs extrapolées

TABLE 4 (suite)

Eau - Ethylenediamine

	x (H_2O)	E (1s) eV	E_T (exp) eV
*	0.0	0.28	
	0.263	0.59	0.13 ± 0.31
	0.263	0.45	0.80 ± 0.73
	0.263	0.61	0.30 ± 0.39
	0.424	0.72	0.51 ± 0.20
	0.424	0.72	0.50 ± 0.19
	0.524	0.85	0.56 ± 0.22
	0.603	0.90	0.50 ± 0.10
	0.702	1.11	0.55 ± 0.15
	0.757	1.19	0.34 ± 0.23
	0.820	1.27	0.14 ± 0.44
	0.863	1.31	0.36 ± 0.26
*	1.00	1.39	

* valeurs extrapolées

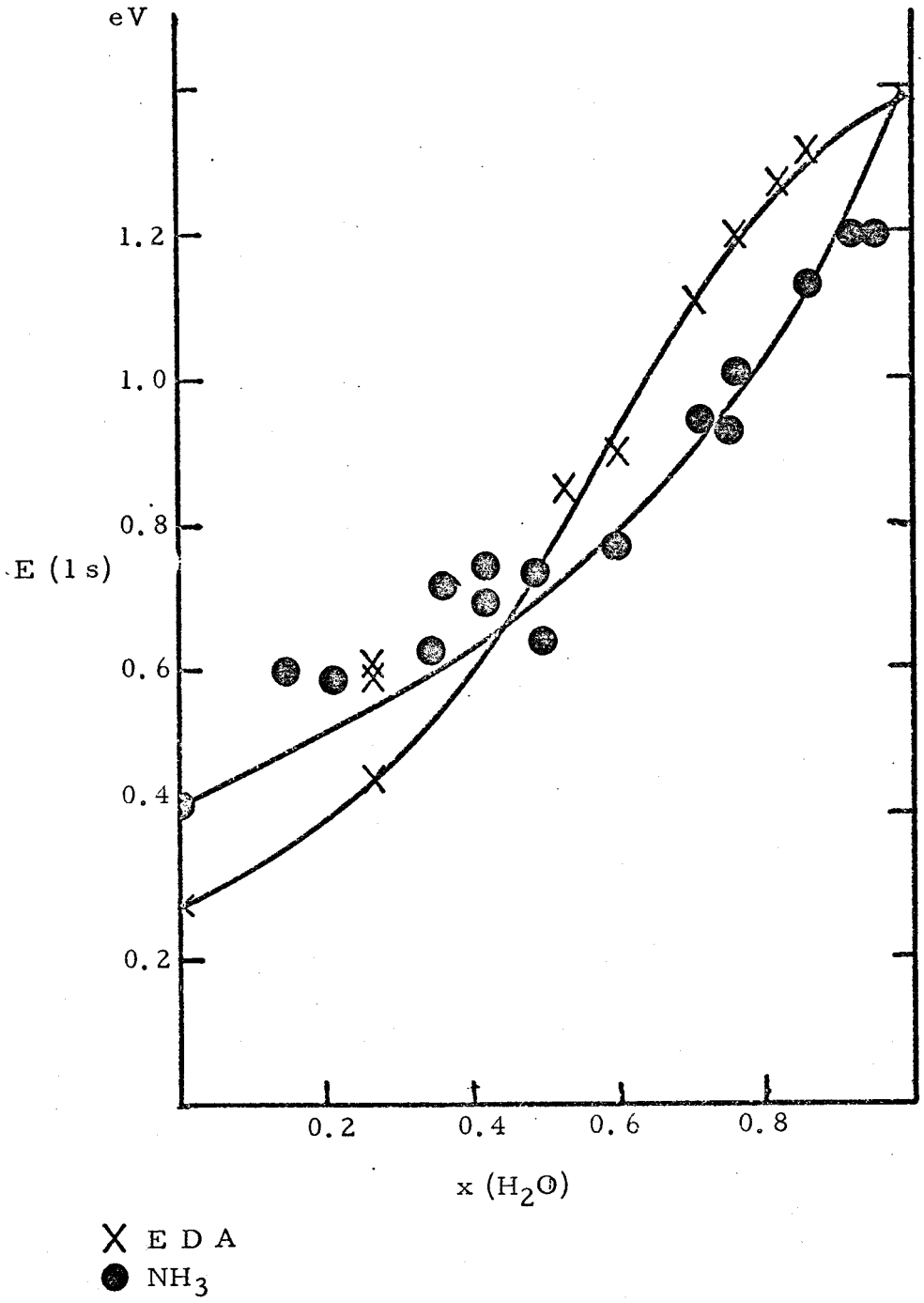

Fig. 3. Energie du seuil calculée en fonction de la composition du mélange.

Nous avons tracé la courbe E_{Max} en fonction de la profondeur du puits (figure 4). Nous y avons placé tous les points dont nous disposons. La relation que nous obtenons est linéaire ce qui indique que la connaissance de la position du maximum peut servir à définir la profondeur du puits. Ce résultat peut nous servir pour confirmer qu'un seul processus d'absorption est mis en oeuvre pour toutes les solutions.

c) Variation de la largeur à mi-hauteur.

Dans le cas des mélanges eau-ammoniac, la largeur à mi-hauteur de la courbe d'absorption est multipliée par un facteur deux en passant de l'ammoniac à l'eau. Cette variation ne peut s'expliquer par des corrélations simples. Dans le cas des mélanges eau - éthylènediamine la largeur du pic reste constante quelque soit la concentration du mélange. Dans ce dernier cas, nous avons aussi noté que le rayon du puits de potentiel ne varie pas en fonction de la concentration du mélange.

Nous avons essayé de relier la valeur de la largeur à mi-hauteur à une fonction du rayon du puits. La largeur à mi-hauteur semble être une fonction linéaire du volume du puits. (Figure 5)

d) Interprétation de la variation des paramètres du puits de potentiel.

Dans notre calcul nous ne faisons aucune supposition sur les raisons physiques qui permettent d'obtenir un potentiel de la forme que nous utilisons. De même l'existence d'un seul état lié est une conséquence des calculs.

Plusieurs travaux récents utilisent un modèle similaire.

Copeland, Kestner et Jortner (6) obtiennent un puits de potentiel carré à l'intérieur de la cavité en considérant que la première couche de solvatation intervient de façon discrète dans l'expression du potentiel

$$V(r) = -\frac{N\ \mu}{r_d^2} - \frac{\beta}{r_c} \qquad r < R$$

$$V(r) = -\frac{\beta}{r} + V_o \qquad r > R$$

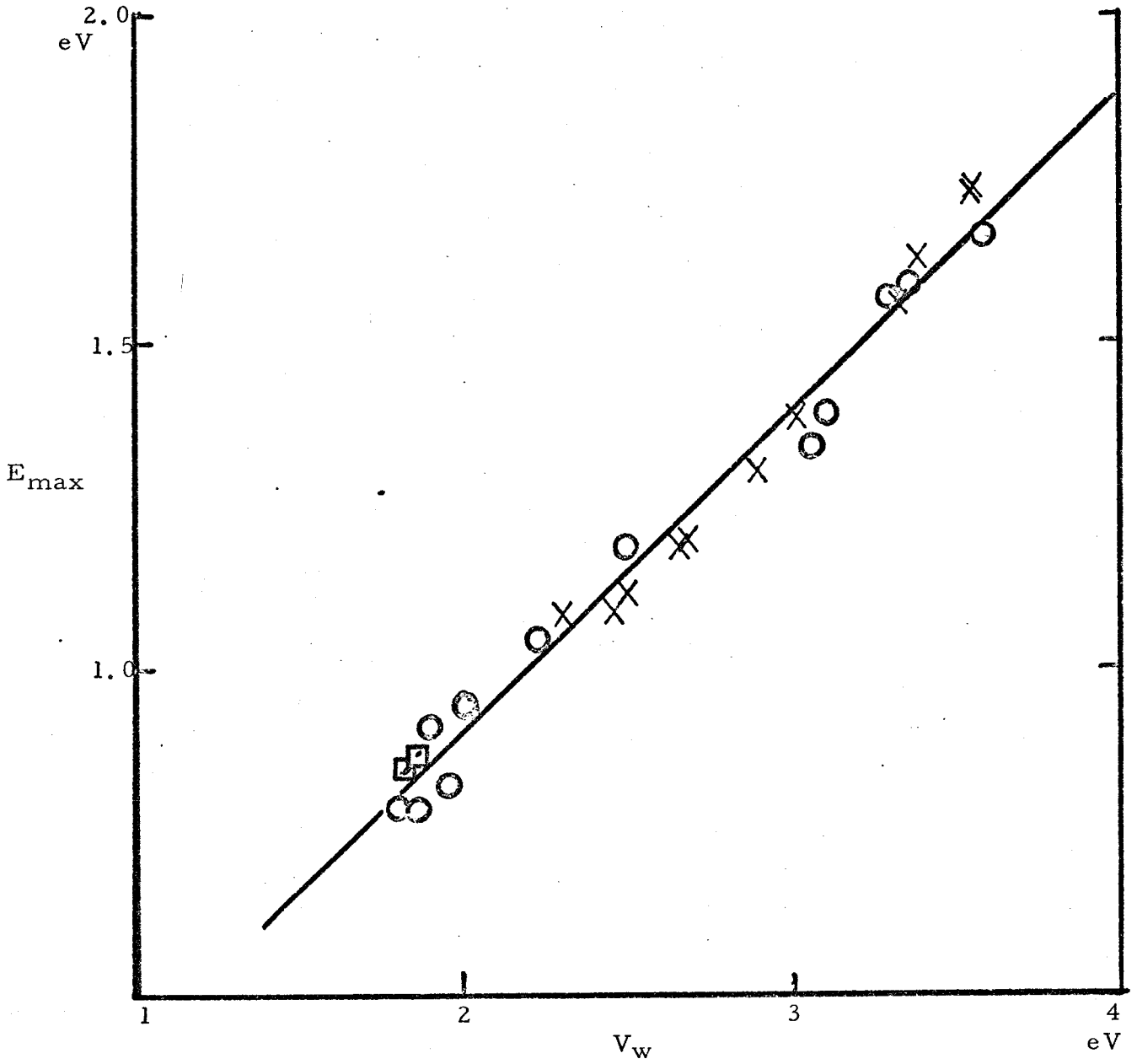

X E D A O NH_3 ⊡ NH_3 pur à basse température

$E_{max} = 0.486\ V_w - 0.072\ (\pm 0.05)$

Fig. 4 . Relation entre la position du maximum et la profondeur du puits.

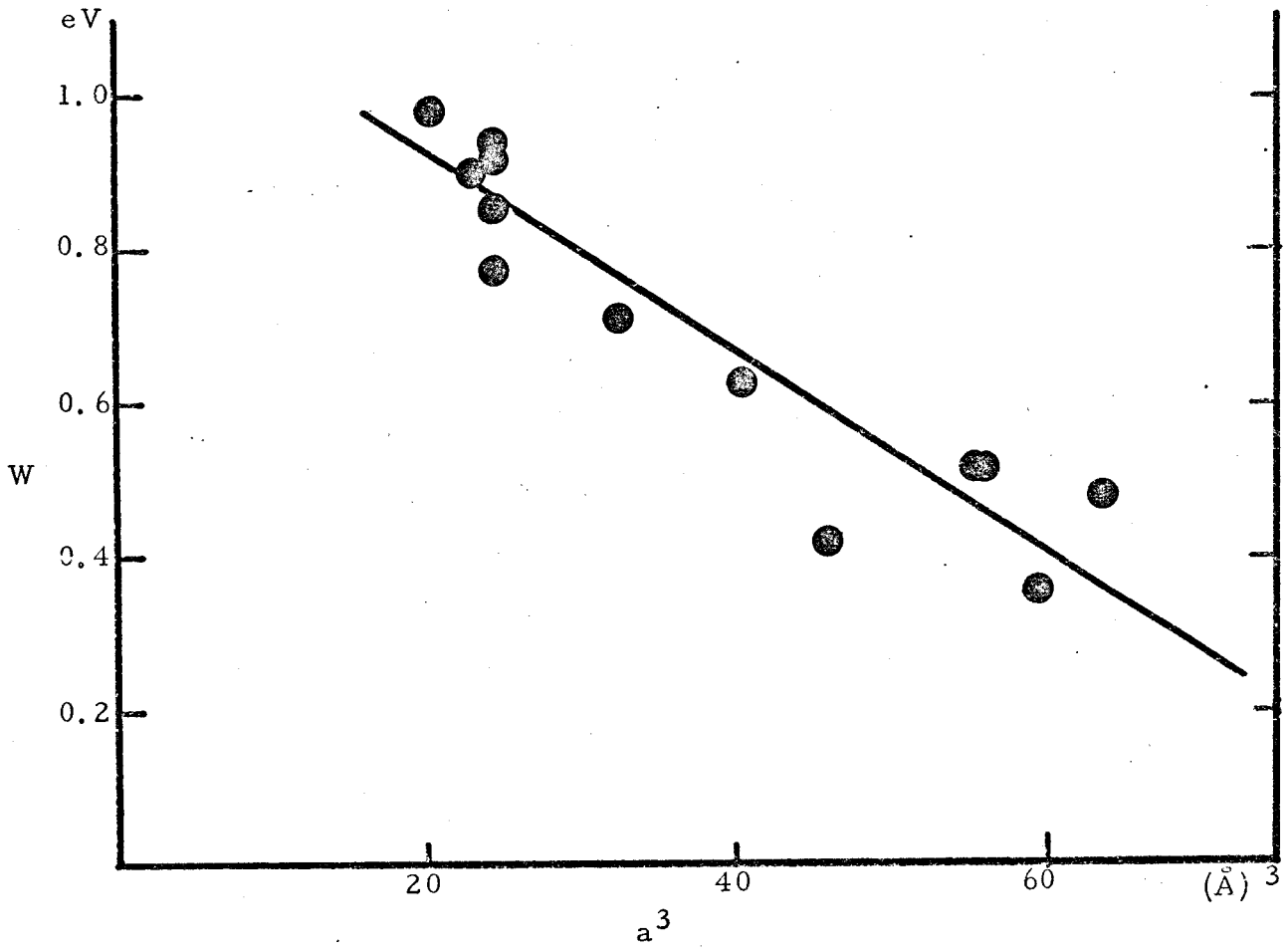

Fig. 5 . Relation entre la largeur à mi-hauteur et le volume de la cavité.

Il faut noter que le potentiel est constant à l'intérieur de la cavité. (voir figure 6b).

Dans l'expression précédente μ est le moment dipolaire effectif, r_d est la distance du centre de la cavité au centre du dipole de la molécule, r_c est la distance du centre de la cavité au continuum situé après la première couche de solvatation et N est le nombre de molécules constituant cette couche de solvatation.

L'utilisation d'un tel calcul est compliquée par la nécessité de calculer le moment dipolaire effectif . En particulier un tel calcul est beaucoup trop difficile pour des solvants contenant des molécules de nature différente.

Kajiwara, Funabashi et Naleway (7) ont démontré que le spectre de l'électron solvaté pouvait être décrit en considérant un potentiel sphérique. En particulier c'est le premier travail permettant de reproduire l'asymétrie de la bande d'absorption. Dans leur modèle, l'approximation du puits sphérique est obtenue à partir du potentiel continu en considérant les fluctuations de potentiel produites par les molécules constituant les couches de solvatation (fig. 6 c)

Nous pouvons à l'aide de ces derniers résultats essayer de relier la profondeur du puits aux valeurs du potentiel prévues par la théorie du milieu continu

$$V = \frac{\beta}{a} \quad \text{où } \beta = \frac{1}{\varepsilon_\infty} - \frac{1}{\varepsilon_0}$$

a est le rayon du puits de potentiel, ε_∞ est la constante diélectrique optique, et ε_0 la constante diélectrique statique.

Nous avons tout d'abord réalisé ce calcul dans le cas de l'ammoniac pur. Pour ce solvant les indices de refraction sont connus en fonction de la température.

Nous pouvons comparer les valeurs expérimentales mises sous la forme du produit $V_w \cdot a$ aux valeurs de β .

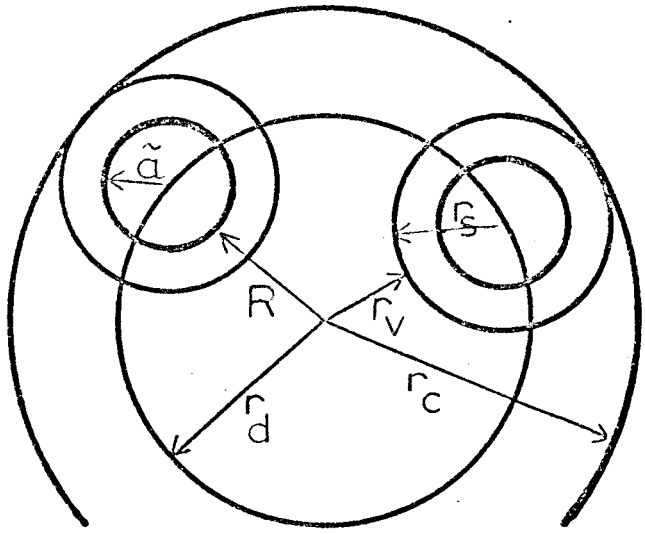

Fig. 6. a . Description d'un modèle de cavité.

$\tilde{a}$: rayon de sphère dure effectif des molécules situées à une distance r_d du centre de la cavité.

r_v : rayon de la cavité "vide".

r_s : rayon effectif des molécules de solvant.

r_c : distance à laquelle commence le continuum.

(b)

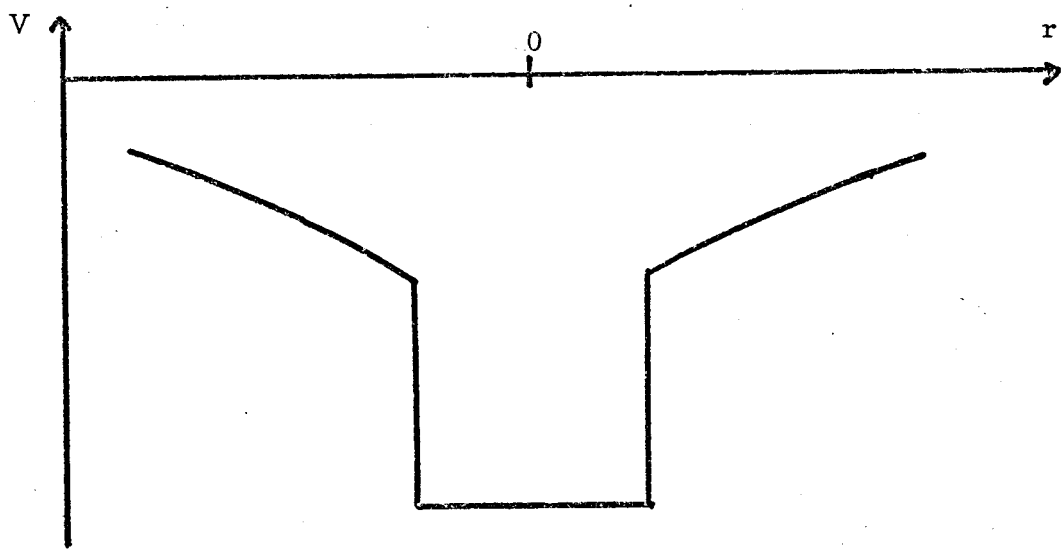

(c)

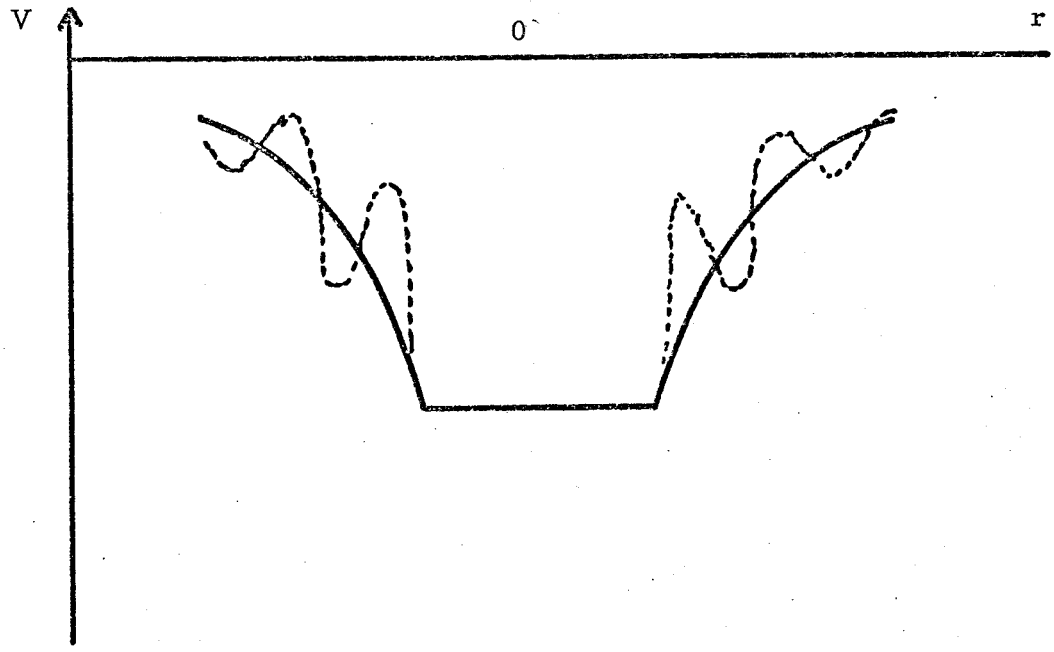

Fig. 6 . b, c . Formes de puits de potentiel.

Ce calcul est reporté dans la table 5 pour l'ammoniac pur aux trois températures étudiées. Nous notons que les valeurs du produit $V_w \cdot a$ sont systématiquement plus élevées que celles obtenues pour β bien que cette différence ne soit jamais supérieure à 10%.

Ceci provient en partie de l'imprécision des mesures expérimentales, le domaine de température étudié étant trop restreint. Il faut aussi noter que les valeurs de l'indice de réfraction de l'ammoniac pur ont été extrapolées assez loin de l'endroit ou des points expérimentaux étaient disponibles.

Compte tenu de la simplicité du modèle utilisé cet accord est très satisfaisant.

Nous avons ensuite appliqué le même calcul aux mélanges eau - ammoniac et eau - éthylènediamine. Les constantes diélectriques de ces mélanges ne sont pas connues et des approximations ont dû être faites. La constante diélectrique optique des mélanges est considérée comme une fonction linéaire des fractions molaires de chacun des constituants. Nous avons calculé la constante diélectrique statique des mélanges en supposant l'additivité des polarisabilités molaires et en utilisant la formule de Kirkwood

$$p = \frac{(\varepsilon_0 - 1)\ (2\varepsilon_0 + 1)}{9\ \varepsilon_0}\ V$$

où V est le volume molaire.

A l'aide de ces constantes nous avons calculé les valeurs de et nous les avons comparées aux valeurs de $V_w \cdot a$. Nous notons immédiatement que pour les mélanges riches en eau nous avons un écart très important entre les valeurs de β calculées et expérimentales :

$x\ (H_2O)$	β	$V_w \cdot a$	
0.949	0.556	0.687	(eau - NH_3)
0.863	0.536	0.714	(eau - EDA)

TABLE 5

EFFET DE TEMPERATURE DANS L'AMMONIAC PUR

T °C	ε_∞	ε_0	β	$V_w \cdot a$
-55	1.893	25.0	0.49	0.50
-65	1.908	26.2	0.49	0.52
-75	1.924	27.8	0.48	0.53

Les valeurs de ε_∞ sont extrapolées des mesures d'indices de refraction de l'ammoniac pur (8).

Pour les mélanges riches en amine ou ammoniac, les écarts ne sont plus dans le même sens pour l'ammoniac et l'éthylènediamine

$x\ (H_2O)$	β	$V_w . a$	
0.144	0.520	0.488	(NH_3)
0.263	0.448	0.510	(EDA)

Comme nous le montrons figure 7 l'écart entre les valeurs calculées et expérimentales est systématique et s'accroit lorsque l'on s'approche de l'eau pure. Pour expliquer cette déviation, nous postulons que l'erreur introduite provient de l'utilisation des constantes diélectriques optiques du milieu continu et qu'il serait sans doute plus approprié d'utiliser des constantes diélectriques effectives au voisinage de la cavité. Pour évaluer ces constantes effectives, nous avons évalué une valeur effective en utilisant une méthode de moindres carrés pour résoudre l'équation

$$V_w . a = \frac{1}{x(H_2O) \cdot \varepsilon_\infty(H_2O) + (1 - x(H_2O)) . \varepsilon_\infty (NH_3)} - \frac{1}{\varepsilon_0}$$

Nous obtenons de cette façon les valeurs suivantes à partir des mélanges eau - ammoniac

$$\varepsilon_\infty (H_2O) = 1.38 \pm 0.02$$
$$\varepsilon_\infty (NH_3) = 2.10 \pm 0.04$$

à partir des mélanges eau - éthylènediamine

$$\varepsilon_\infty (H_2O) = 1.23 \pm 0.03$$
$$\varepsilon_\infty (EDA) = 2.05 \pm 0.04$$

Les valeurs expérimentales déduites des indices de réfraction étaient :

$$\varepsilon_\infty (H_2O) = 1.69$$
$$\varepsilon_\infty (NH_3) = 1.77$$
$$\varepsilon_\infty (EDA) = 2.12$$

A l'aide de ces valeurs nous avons établi la comparaison entre β et la valeur calculée $V_w . a$. Nous avons tracé ces courbes en fonction de la concentration en eau sur la figure 7. On peut voir ainsi qu'en ayant ajusté les constantes diélectriques des constituants purs on peut décrire la variation du produit $V_w . a$ en fonction des propriétés macroscopiques du solvant.

Il est à noter que la valeur de l'indice de réfraction de l'ammoniac est assez sujette à caution. La valeur de n pour des solutions à 30% en poids d'ammoniac dans l'eau est déjà de 1.35 (9) ce qui donne une constante diélectrique de 1.87. En supposant la loi d'additivité des constantes diélectriques cela nous donne $\varepsilon_\infty (NH_3) = 1.92$, valeur beaucoup plus proche de 2.10 que ne l'était la valeur 1.77 citée ci-dessus.

Nous sommes donc amenés à supposer que l'on peut utiliser les constantes diélectriques optiques des solvants purs dans le cas de l'ammoniac et des amines mais que cette approximation n'est plus valable dans le cas de l'eau.

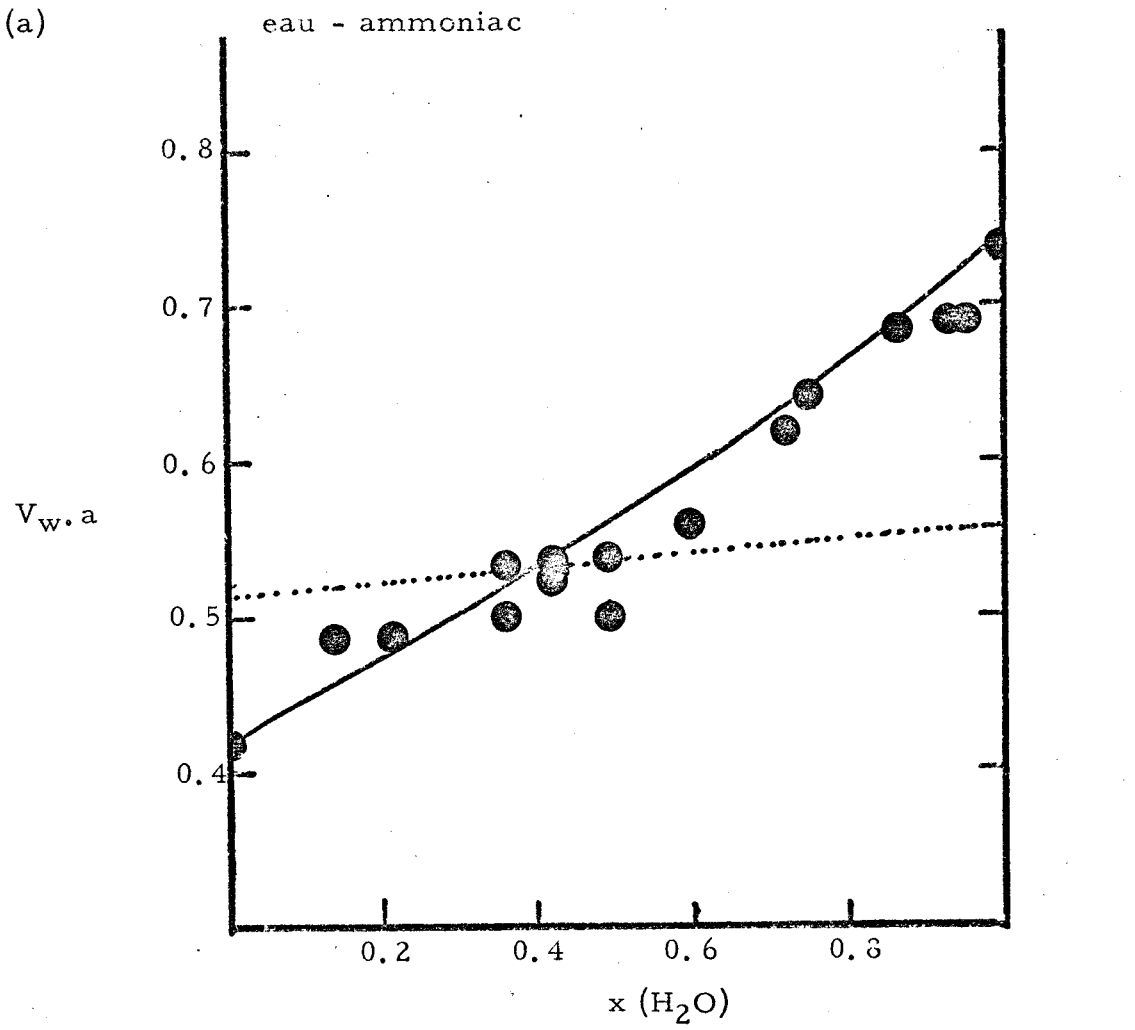

——— β corrigé ..... β non corrigé

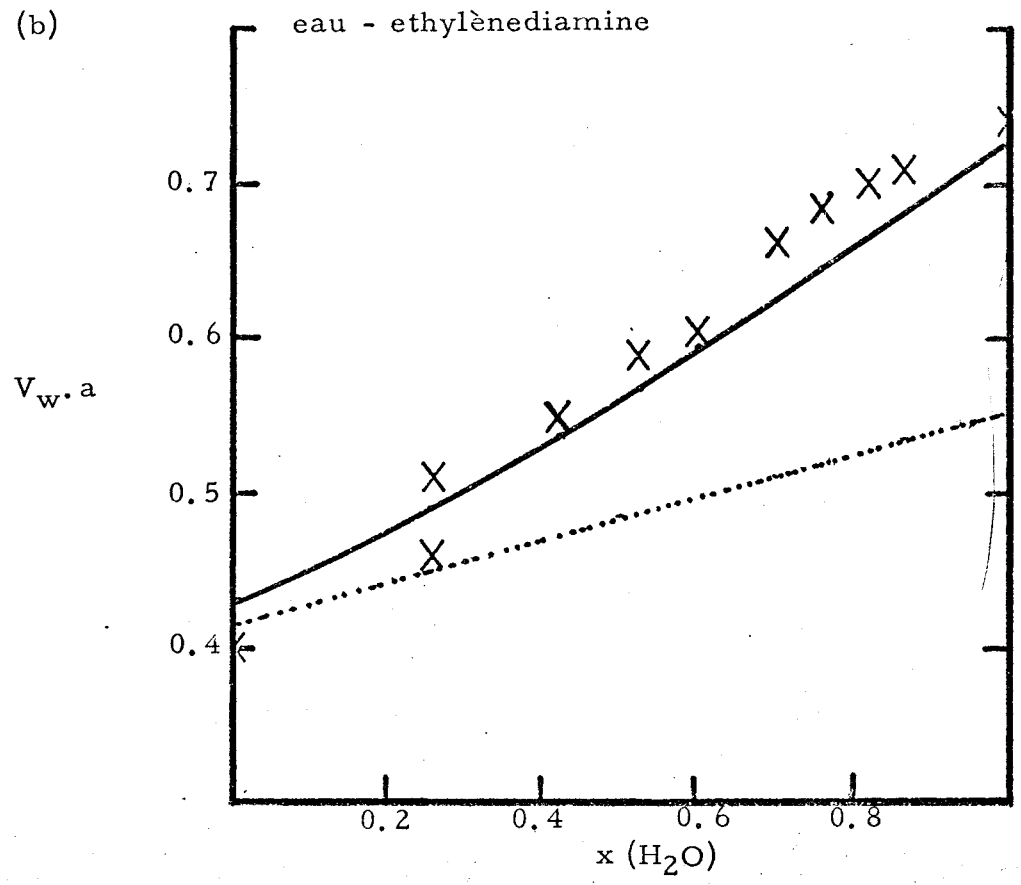

Fig. 7 . Comparaison entre β et V_w. a.

II. 3. Comparaison avec d'autres méthodes.

II. 3. 1. Transfert de charge au solvant (ctts).

Depuis longtemps ont été cherchées des corrélations entre les positions des maximum des spectres de l'électron solvaté et de l'iodure en solution dans les mêmes solvants (10).

Récemment Fox et Hayon (11) ont publié une remarquable relation linéaire entre la position des spectres de l'iodure et de l'électron solvaté dans 43 solvants dont les constantes diélectriques statiques vont de 2 à 80 .

Le mécanisme de l'absorption de l'iodure en solution est interprété en termes de transfert de charge au solvant (ctts). Les principaux critères pour qu'un tel mécanisme soit présent sont les suivants :

a - dépendance de la position du maximum sur la nature du solvant

b - variation linéaire de la position du maximum en fonction de la température

c - relation linéaire entre les positions des maxima de deux chromophores absorbant par ctts dans divers solvants

Ces critères sont vérifiés pour l'électron solvaté. Il semble donc intéressant de comparer nos résultats avec ceux que l'on peut calculer par la théorie ctts. Le calcul théorique de la position du maximum d'absorption a été réalisé par plusieurs auteurs. La formulation la plus acceptée est celle de Stein et Treinin. La position du maximum n'est pas calculée par la mécanique quantique. On utilise un cycle de Born - Haber mettant en jeu des quantités connues.

Le cycle proposé dans le mécanisme de Stein et Treinin est le suivant (II)

$$\begin{array}{ccc} X^-(solv) & \xrightarrow{h\nu} & X(solv)^- \\ \downarrow E_1 & & \uparrow E_2 \\ X^-_g + (solv) & \xrightarrow[E_x]{} & X_g + e^-_g + (solv) \end{array}$$

La charge est portée par l'ion placé au centre de la cavité formée par les molécules de solvant. L'action de la lumière consiste à répartir cette charge sur ces molécules de solvant.

Décrivons maintenant les diverses étapes du cycle.

On considère que l'énergie mise en jeu pour la transition optique est égale à l'énergie du maximum d'absorption de cette transition. Ceci n'est bien entendu qu'une approximation.

Dans la première étape, l'ion est retiré de la cavité en laissant celle-ci intacte donc sans changer la polarisation du milieu. E_1 est donc la somme de l'énergie d'interaction de l'ion avec la polarisation permanente du milieu et de la polarisation électronique induite par l'ion. La seconde étape (E_x) correspond à l'ionisation de $X_{(g)}$. Dans la dernière étape (E_2) l'électron est réintroduit dans l'état excité du milieu et l'atome est remis dans la cavité.

Un tel cycle peut être aisément modifié pour décrire l'électron solvaté

$$\begin{array}{ccc} e^- \text{(solv)} & \xrightarrow{h\nu} & \text{(solv)}^- \\ E_1 \searrow & & \nearrow E_2 \\ & e^-_g + \text{(solv)} & \end{array}$$

Les termes E_1 et E_2 ont la même signification que précédemment. Afin de dériver une formule reliant les valeurs spectroscopiques aux diverses propriétés du solvant, nous allons expliciter les deux termes E_1 et E_2 . E_1 est la somme de l'énergie due à la polarisation permanente du diélectrique β/r_o et de l'énergie due à la polarisation électronique $\frac{1}{2\,r_o}\left(1 - \frac{1}{\varepsilon_\infty}\right)$ où r_o est le rayon de la cavité. Le terme E_2 met en jeu l'état excité. Dans le modèle c t t s, le puits de potentiel est de forme coulombique ce qui produit un nombre infini d'états liés dont l'énergie apparait explicitement dans la formulation du modèle. L'expression obtenue par Stein et Treinin s'écrit :

$$E_{max} = \frac{1}{r_o}\left(\frac{1}{2} + \frac{1}{2\varepsilon_\infty} - \frac{1}{\varepsilon_0}\right) - \frac{1}{2R_e}\left(1 - \frac{1}{\varepsilon_\infty}\right) - \frac{1}{8}\,\beta^2$$

(en unités atomiques)

Les deux derniers termes correspondent à l'état excité.

De nombreux auteurs ont utilisé cette formule pour définir des rayons de "cavité" dans le cas des spectres de l'électron solvaté (13). Cette procédure n'est pas correcte.

Dans la discussion suivante nous allons détailler les hypothèses supplémentaires introduites dans le modèle c t t s appliqué à l'électron et effectuer des comparaisons avec le modèle du puits carré. Voir les figures 8 a, et 8 b pour la signification des termes.

- Dans le modèle c t t s classique (avec un ion au centre de la cavité), on considère qu'à l'état fondamental, l'électron est fortement lié à l'atome et qu'il se trouve au fond du puits. La profondeur du puits est β/r_0 où r_0 est le rayon crystallographique. Il est bien connu que l'énergie d'un électron placé seul dans un puits de potentiel n'est pas au fond du puits.

Dans le modèle du puits carré l'énergie du niveau fondamental E (1 s) correspond au seuil d'excitation spectroscopique.

- L'approximation, faite dans le cycle c t t s, de prendre $h\nu_{max}$ comme énergie moyenne de la transition optique n'est valable que si le spectre est symétrique par rapport à ν_{max}. C'est donc une très mauvaise approximation dans le cas de l'électron solvaté.

- La théorie c t t s permet d'identifier l'énergie séparant le niveau correspondant à l'électron au repos dans le solvant et le niveau correspondant au vide. On retrouve cette valeur dans le cas du puits carré de potentiel. Nous posons dans ce cas

$$V_e = S_e = \frac{1}{2a}\left(1 - \frac{1}{\varepsilon_\infty}\right) \quad \text{(en unités atomiques)}$$

La comparaison entre les deux formes de puits de potentiel est valide si dans le cas du puits coulombique, le niveau 2 p est placé suffisamment près du haut du puits pour que cet état soit déjà très délocalisé. Dans le cas du puits carré de potentiel l'état 2p n'existe pas, et l'état excité est délocalisé. Ainsi que nous l'avons cité plus haut (II. 2. 3, d) le puits carré de potentiel peut être pris comme approximation d'un potentiel coulombique si les fluctuations du solvant sont prises en considération.

Nous avons montré en II 2. 3. b qu'une relation empirique de type $E_{max}(e^-) = A.\ V_w + B$ existait. D'après la figure 8a on peut voir qu'à condition que l'état 2 p soit suffisamment délocalisé on peut écrire E_{max} (I) = $V_w + C$ C étant une valeur représentant la différence entre l'énergie du niveau 2p et celle de l'électron libre au repos. On note que l'existence d'une telle relation donne une explication qualitative aux corrélations de Fox et Hayon (11)

La valeur de $E(1s) + V_e$ a un sens physique; elle correspond à l'énergie qu'il faut fournir à un électron solvaté pour l'éjecter dans le vide. Cette valeur devrait donc correspondre au seul de photoéjection mesuré par Delahay (14) : 1.8 - 1.9 eV pour des solutions métal-ammoniac à -60°C .

D'après le cycle thermodynamique, on peut voir aussi que cette quantité correspond à la chaleur de solvatation de l'électron. Cette valeur a été évaluée par Jortner (15), elle est de 1.7 ± 0.7 eV. Pour l'ammoniac pur à -65°C, nous obtenons une valeur de 1.54 eV en prenant pour E (1s) sa valeur calculée dans la publication 2. Cette valeur se compare assez bien aux valeurs obtenues par d'autres méthodes. Elle est inférieure à celle obtenue par Delahay.

Ceci peut s'expliquer en notant que de nombreuses approximations ont été faites dans notre calcul; en particulier l'énergie nécessaire pour franchir l'interface vide - solution a été négligée. Pour les mélanges eau - ammoniac et eau - éthylenediamine, nous avons reporté les valeurs de V_e et de V_e + E (1 s) dans la table 6. Ces valeurs sont tracées en fonction de la composition du mélange figure 9 et 10. La variation de ces valeurs ne présente pas de singularité entre les limites des solvants purs.

Il est à noter que la valeur de V_e est du même ordre de grandeur que celle que Jortner (6) utilise dans son modèle.

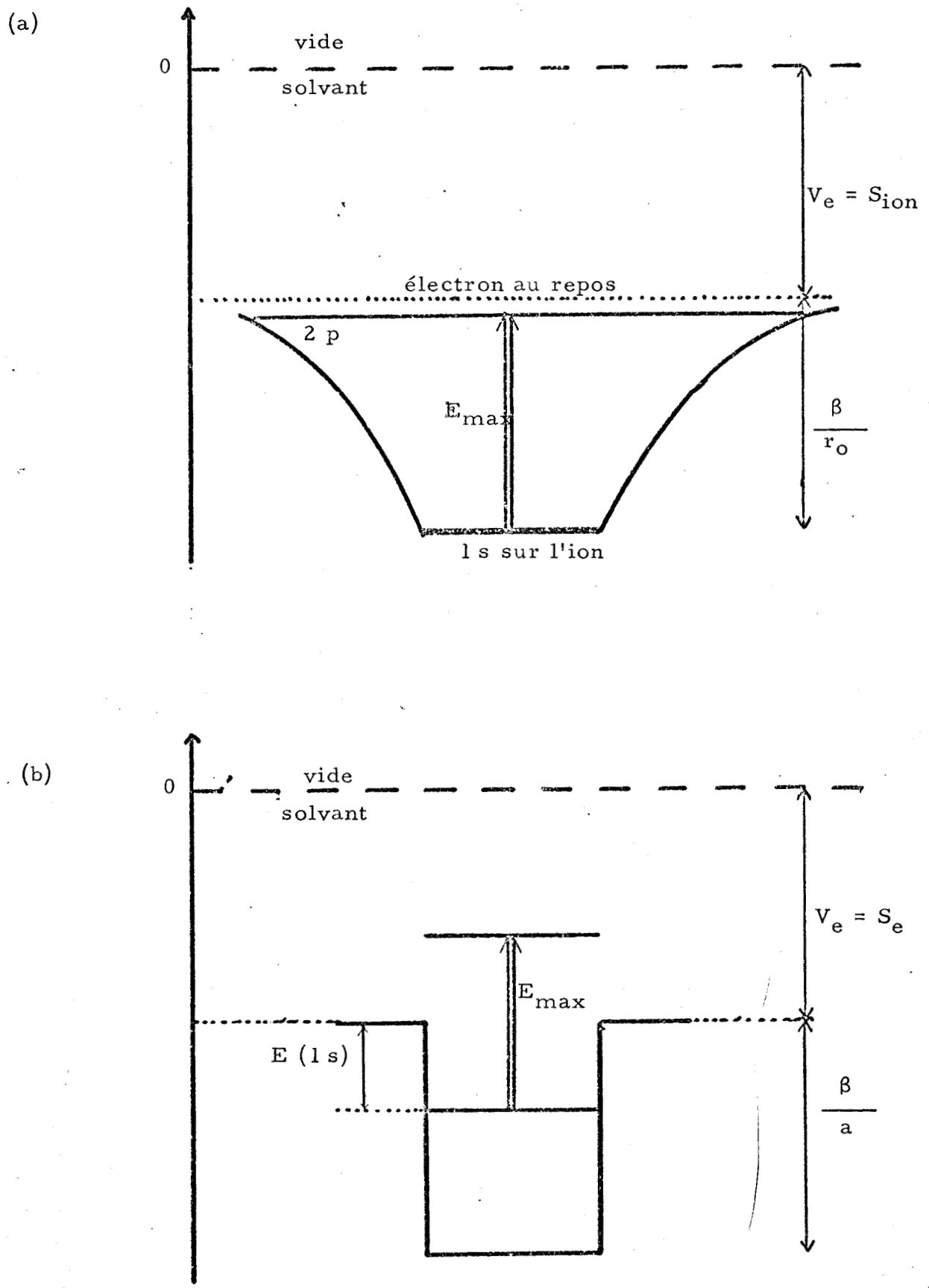

Fig. 8 . Comparaison des grandeurs introduites dans la théorie c tts et celles du puits carré de potentiel.

TABLE 6

CALCUL DE V_e

MELANGES EAU AMMONIAC

	x (H_2O)	E (1s) eV	a A	ε_{opt}	V_e eV	V_e + E (1s) eV
*	0.00	0.41	4.00	2.101	0.94	1.35
	0.144	0.60	3.90	1.998	0.92	1.52
	0.213	0.59	3.59	1.934	0.97	1.56
	0.358	0.63	3.83	1.821	0.85	1.48
	0.367	0.72	4.00	1.814	0.81	1.53
	0.421	0.74	3.64	1.772	0.86	1.60
	0.421	0.70	3.82	1.772	0.82	1.52
	0.489	0.73	3.45	1.719	0.87	1.60
	0.496	0.64	3.50	1.713	0.86	1.50
	0.594	0.77	3.20	1.637	0.87	1.64
	0.717	0.94	2.90	1.541	0.87	1.81
	0.752	0.93	2.85	1.514	0.86	1.79
	0.862	1.13	2.90	1.428	0.74	1.87
	0.930	1.20	2.76	1.375	0.71	1.91
	0.949	1.20	2.75	1.360	0.69	1.89
*	1.00	1.39	2.90	1.320	0.60	1.99

* Valeurs extrapolées

TABLE 6 (suite)

CALCUL DE V_e

MELANGE EAU ETHYLENEDIAMINE

	$x(H_2O)$	E (1s) eV	a Å	ε_{opt}	V_e eV	V_e + E (1s) eV
*	0.0	0.28	2.90	2.051	1.27	1.55
	0.263	0.59	2.92	1.859	1.14	1.73
	0.263	0.45	2.92	1.859	1.14	1.59
	0.263	0.61	3.00	1.859	1.10	1.71
	0.424	0.72	2.88	1.741	1.06	1.78
	0.424	0.72	2.85	1.741	1.07	1.79
	0.524	0.85	2.93	1.668	0.98	1.83
	0.603	0.90	2.88	1.610	0.95	1.85
	0.702	1.11	2.86	1.538	0.88	1.99
	0.757	1.19	2.91	1.498	0.81	2.00
	0.820	1.27	2.86	1.452	0.78	2.05
	0.863	1.31	2.85	1.420	0.75	2.06
*	1.00	1.39	2.90	1.320	0.60	1.99

* Valeurs extrapolées

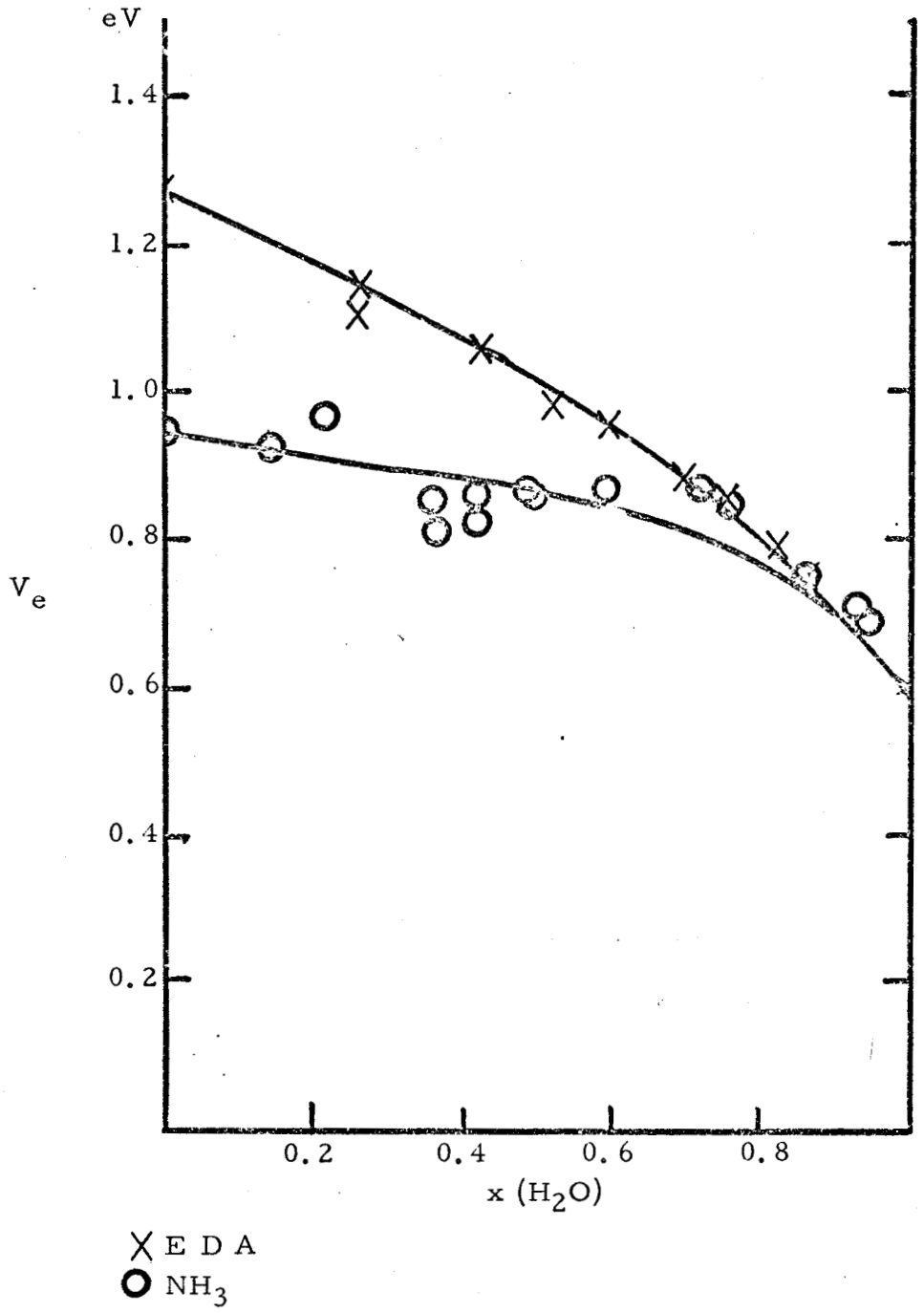

Fig. 9 . Variation de V_e en fonction de la composition du mélange.

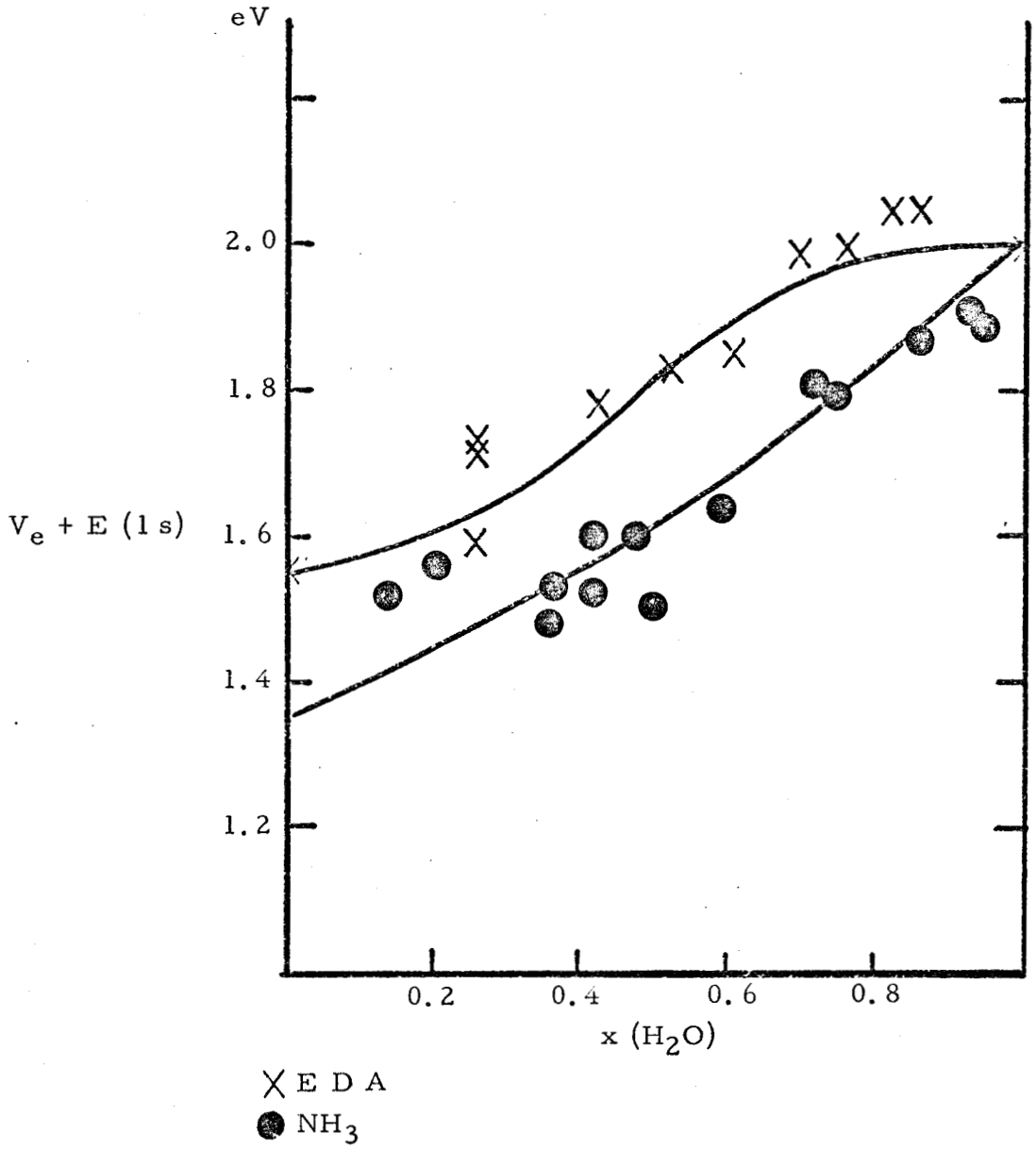

Fig. 10 . Variation de V_e + E (1 s) en fonction de la composition du mélange.

II. 3. 2. Modèles moléculaires.

Webster (15) a utilisé un modèle constitué de quatre molécules placées au sommet d'un tétraèdre entourant la cavité. Dans ce calcul assez proche des méthodes ab initio, les fonctions d'onde des molécules de solvant sont prises en considération pour définir le potentiel subi par l'électron. Webster a appliqué son modèle aux mélanges eau - ammoniac en substituant successivement les molécules d'eau par des molécules d'ammoniac. De cette façon il a pu obtenir les valeurs de l'énergie de la transition optique pour cinq valeurs. La comparaison de ses résultats avec les valeurs expérimentales est montrée ci-dessous

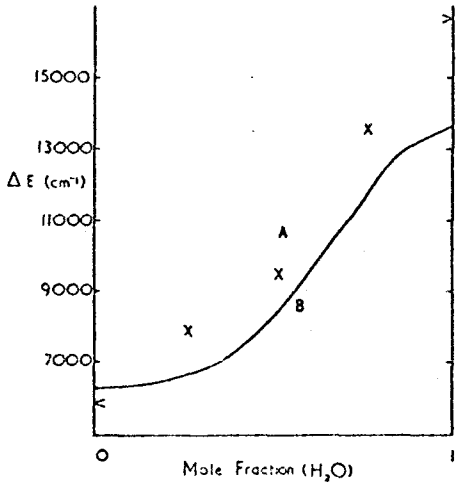

Cependant pour résoudre le problème d'une façon plus fine une structure plus complexe qu'un tétraèdre est nécessaire.

II. 3. 3. Vérification du modèle de Jortner. (Publication 3)

Dans leur article, Copeland, Kestner et Jortner (6) décrivent le spectre de l'électron solvaté en termes de configuration du solvant. (section II. 2. 3)

La coordonnée choisie est une mesure du déplacement radial de N molécules de solvant par rapport au centre de la densité électronique. Ces calculs donnent des courbes d'énergie indiquant la stabilité de l'état fondamental et de l'état excité. D'après la courbe donnant l'énergie totale de l'état fondamental, il est possible de calculer les niveaux d'énergie de vibration de la cavité. Les hypothèses introduites dans ce calcul sont les suivantes :

- Les molécules sont traitées comme des sphères dures
- Les N molécules formant la cavité se comportent comme des oscillateurs harmoniques de telle sorte que la forme de la courbe d'énergie potentielle dans la région du minimum d'énergie peut être représentée par une parabole.

Les fréquences calculées se trouvent dans la région 25-75 cm^{-1} pour l'électron dans l'ammoniac liquide, et ces auteurs ont suggéré que cette vibration serait observable en spectroscopie Raman. Par analogie avec des calculs similaires sur les centres colorés, cette vibration est appelée un "mode symétrique".

Nous avons entrepris une étude des spectres Raman de solutions de métaux alcalins dans l'ammoniac en nous intéressant de plus près à la région des basses fréquences. Cette étude présente un certain nombre de problèmes. Comme nous l'avons vu précédemment, le maximum d'absorption se trouve aux environs de 7000 cm^{-1} (1,43 μ) dans le proche IR. Il est donc impossible d'avoir une longueur d'onde excitatrice située à une énergie plus faible que celle de la première transition électronique.

Bien qu'absorbant dans le proche infrarouge, ces solutions sont intensément colorées. Il faut donc faire un compromis entre la concentration en électrons solvatés que l'on veut aussi haute que possible et la nécessité d'avoir de la lumière diffusée par l'échantillon. La concentration des solutions étudiées était de 10^{-3} à 10^{-5} M.

Nous n'avons pas observé de raies Raman supplémentaires dans le domaine des basses fréquences. Nous avons essayé ensuite de voir si un effet pouvait être observé sur les fréquences de vibration du solvant lui-même. A part une légère variation de l'intensité des raies dues probablement à l'absorbance de la solution, aucune variation n'a pu être détectée. L'absence d'effet de l'électron solvaté sur le spectre Raman peut s'expliquer en partie pour les raisons exprimées ci-dessus. Ce résultat ne permet pas de confirmer ou d'infirmer le modèle de Copeland, Kestner et Jortner.

PUBLICATION 3

RAMAN SPECTRA OF DILUTE METAL-AMMONIA SOLUTIONS

Raman Spectra of Dilute Metal–Ammonia Solutions

M.G. DeBacker, P.F. Rusch, B. DeBettignies, and G. Lepoutre

Abstract

Studies of the Raman spectrum of dilute potassium-ammonia solutions are reported. No new bands appeared, and no difference between the spectrum of pure ammonia and that of the solution could be detected. Possible reasons for the failure to observe any new bands are discussed.

The most striking feature of the optical absorption spectrum of dilute and moderately concentrated metal–ammonia solutions is the presence of a single absorption band in the near-infrared region with a maximum at about 0.8 eV. This band is very intense ($\varepsilon = 4.5 \times 10^4$ liter mole^{-1} cm^{-1}), broad (half-width = 0.4 eV) and noticeably asymmetric towards higher energy. It is generally accepted [1, 2] that this band results from an optical transition of the solvated electron. The cavity model [3] is able to explain the absorption band in terms of a transition of the solvated electron from a 1s (ground) to a 2p (excited) state.

In a recent paper [4], Copeland, Kestner, and Jortner provide a theoretical description of the solvated electron in terms of a configuration coordinate (cc) model. The coordinate chosen is a measure of the radial displacement of n solvent molecules about the center of the solvated electron density. These calculations yield total energy curves characteristic of stable systems for both the ground and excited states. From the total energy curve for the 1s state it is possible to calculate the vibrational energy levels of the cavity by making the following assumptions. First, the ammonia molecules forming the cavity are essentially hard spheres, and second, the n cavity molecules act as a harmonic oscillator such that the potential energy curve in the region of the minimum can be approximated by a parabola. Thus from the second derivative of the curve evaluated at the minimum, the frequency of vibration can be calculated as a function of n and of the potential energy V_0 which represents the energy of a quasi-free electron in the medium. The calculated frequencies are in the range 25—75 cm^{-1}, and Copeland, Kestner, and Jortner suggest that this vibration can be observed by Raman scattering. By analogy with similar calculations on electron impurity centers in the solid state, this vibration is called a "symmetric breathing mode".

In the solid state cc calculations for the F-center [5], the symmetric breathing mode is found to be of rather low energy and can be used to explain quantitatively the observed broadening of the electron absorption band. On the basis of these calculations it was predicted [6] that this mode of vibration of the cc (i.e. the lattice surrounding the F-center) should be observable by Raman scattering. Although there was a Raman spectrum observed with F-centers in NaCl and KCl, the results showed "no evidence for a strong sharp localized mode of vibration" [7].

The absorption spectrum of the solvated electron has been investigated by many researchers [8, 9] but the spectrum of the solvent has, until recently [10], not received much attention. The infrared (IR) spectrum of the solvent has been observed [11] for solutions of potassium and lithium in ammonia. In this investigation it was observed that the presence of the solvated electron perturbed the spectrum in the 3 μ region much more strongly than ordinary salts in ammonia. A study of the Raman spectrum of dilute potassium-ammonia solutions was initiated in order to look for new bands or for the perturbation of the ammonia vibration bands. It is the purpose of this paper to present some of the preliminary results.

Experimental

Potassium solutions with metal concentrations ranging from 10^{-3}—10^{-5} M were prepared in cylindrical 6 mm OD Pyrex tubing. These cells could withstand the pressure of ammonia at room temperature. The stability of the solutions at room temperature was excellent; no decomposition problems occurred during the runs.

The Raman spectrometer used was a CODERG PH 1. This instrument has a double monochromator equipped with gratings ruled at 1800 lines/mm. Entrance and exit slits were adjustable and could give resolutions from 0.1—10 cm^{-1}. The detector was a photomultiplier of the S 20 type with a spectral range from 3000—8000 Å, and a maximum sensitivity at 4200 Å. The light source was a tunable Krypton laser (CRL model 52). The total power output of this laser is of the order of 1 watt. The light beam was focused on the cell containing the solution and passed through it twice. The scattered light was received in a direction perpendicular to the incident light. The cell holder was equipped with a cryostat cooled by the controlled evaporation of liquid nitrogen. The temperature could be regulated with an accuracy of $\pm 2°$ C.

All of our study was done by comparing the spectra of pure ammonia and of a metal solution taken under exactly the same conditions. It is good to keep in mind that liquid ammonia is a poor scatterer of light. The laser exciting line has to be chosen carefully in order to use the photomultiplier where its sensitivity is good. To detect the weakest of the bands of pure ammonia, slit-widths of the order of 10 cm^{-1} were needed. The concentration of the solutions had to be adjusted in order to have enough light reaching the detector.

Results

The spectral region from 0—4000 cm^{-1} was carefully investigated. The region between 0 and 100 cm^{-1} was studied with special attention since it was where Jortner *et al.* predicted the appearance of a new band. A careful alignment of the optical system and the selection of narrow slits allowed us to work as close as 10 cm^{-1} from the Rayleigh line. This region was studied with seven exciting lines from the Krypton laser (from 4619—6764 Å). No new bands appeared, and we could not detect any difference between the spectrum of pure NH_3 and that of the K-NH_3 solution. The region of the vibration bands of NH_3 was studied with

the 4762 Å line and settings such the vibration bands of ammonia were well defined. It was impossible to detect any new band.

As shown in Fig. 1, the use of the 4762 Å (2.605 eV) exciting line places the Raman spectrum of the fundamental solvent vibrations outside of the region of intense solvated electron absorption. This should allow the use of solutions of high concentration. The first feature noted was a marked decrease of the intensity of the solvent spectrum; much of this is expected on the basis of absorption of scattered light by the blue band.

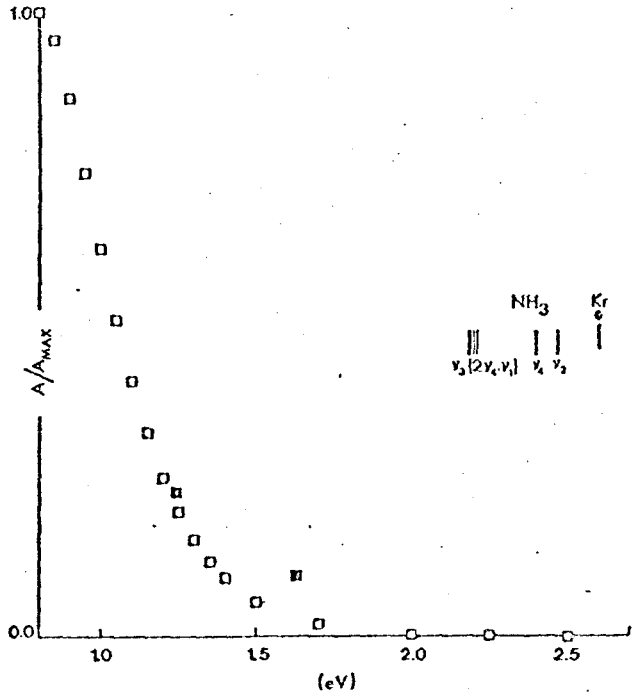

Fig. 1. Position of the Kr exciting line (4762 Å) and the solvent fundamental vibrations relative to the solvated electron absorption peak (data from Ref. [9])

In the region of 1000 cm^{-1} we found the ν_2 and ν_4 fundamental vibrations of ammonia. These bands were weak even in pure NH_3 and the signal-to-noise ratio was of the order of 10. In one experiment we detected a slight shift of the ν_2 band to lower energies but this feature could not be reproduced. Within experimental error, the normalized bands of the pure ammonia and of the metal-ammonia solutions were identical. The lowering of the ν_2 and ν_4 bands was the same for both bands when going from pure solvent to the metal solution.

In the region of 3000 cm^{-1}, three peaks were observed. Typical spectra of pure NH_3 and a 10^{-3} M K–NH_3 solution at +23° C are shown in Fig. 2. The least intense peak of this group (3384 cm^{-1}) has been assigned the asymmetric N–H stretching vibration ν_3 [12, 13]. The two remaining peaks (3305 and 3215 cm^{-1}) are attributed to the asymmetric H–N–H bending overtone ($2\nu_4$) and to the sym-

metric N–H stretching vibration (ν_1). The overtone occurs with enhanced intensity because of Fermi resonance with the fundamental vibration ν_1. An unambiguous assignment of these two, more intense peaks is not possible for several reasons. First, both peaks show a depolarization ratio approaching zero, which indicates that the vibrations each have a common symmetry element. Secondly, the large number of combination and overtone peaks observed in the near-infrared region of the spectrum of liquid NH_3 and M–NH_3 solutions is not observed in the Raman spectrum. Thus it is impossible to deduce the assignments by forming sums (and differences) of the fundamental frequencies. An assignment of the pure solvent

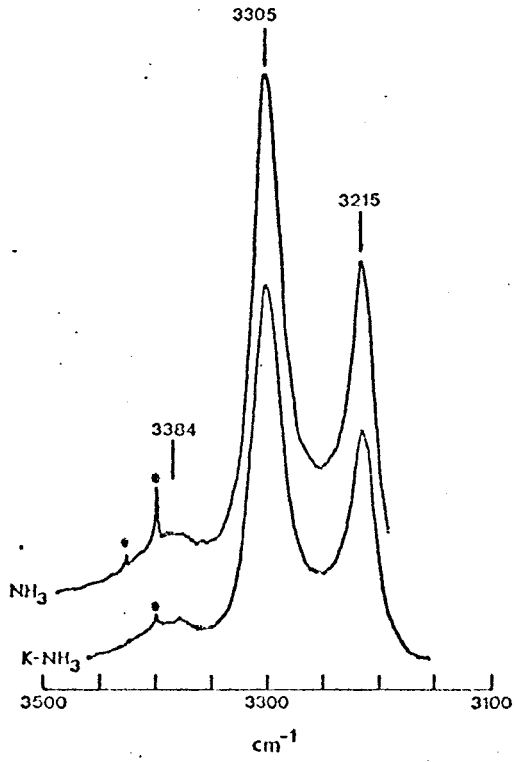

Fig. 2. Raman spectra of the solvent fundamental vibrations in the 3 μ region for pure NH_3 and 10^{-3} M K–NH_3 at +20° C. Starred peaks are laser emission lines

Table I. Observed laser Raman frequencies of pure liquid ammonia

t(°C)	ν_2	ν_4	$2\nu_4$	ν_1	ν_3	Ref.
−63	1060	1634	3296	3206	3375	[14]
−55	1070	1641	3296	3206	3363	[15]
+25	1066	1638	3301	3215	3379	[15]
+23	1056	1634	3305[a]	3215[a]	3384	This work
+20	1055	1645	3218[a]	3303[a]	3386	[16]
+25			3215[a]	3301[a]	3384	[17]

[a] Doublet assigned to ν_1 and $2\nu_4$ in Fermi resonance.

bands is given in Table I where the data from this investigation are compared to other laser Raman data.

Three features of the 3000 cm^{-1} region spectrum merit special attention. First, there appear to be no new peaks. Secondly, within the resolution of the observation there is no shift of the peaks in the K–NH_3 solution relative to pure solvent at the same temperature. Thirdly, the intensity of the peaks is decreased in the K–NH_3 solution as compared to pure solvent. All three features are in apparent contradiction to the observed infrared spectrum [11] in the same region. The lack of new peaks or shift of the solvent peaks can be shown by normalizing both spectra of Fig. 2; both spectra can be completely superimposed.

Discussion

In spite of the fact that no new bands were observed, our results cannot exclude the existence of a Raman active symmetric breathing mode of the solvated electron cavity. There are several reasons for this: 1. The exciting line used should have an energy lower than the first electronic transition. At present, there are no Raman spectrometers capable of operating in the near-infrared region. 2. The concentration of scattering centers may be too low to observe the transitions. In most Raman experiments, the concentration of the solution must be at least 10^{-2} M to give rise to a signal. Raman spectra of F-centers have been reported [7] at much lower concentrations than those used in this study, but the sample was cooled to liquid nitrogen temperature to narrow the electron absorption band. 3. The use of a single cc may not be a valid description of the cavity. It has been stated [5] that even though the single cc may be a useful device, it may not correspond to a real coordinate of the system. Such a statement is particularly important when discussing the liquid state (i.e. solvated electrons). The cc description of an electron impurity center in the solid state makes use of the fact that the nearest neighbors of the excess electron are ions in positions which are more or less fixed in space. In the case of a solvated electron the neighbors are the solvent molecules which have normal modes of vibration of their own. Furthermore, neither the positions of the neighbors nor the orientation of the cavity is fixed in space.

Both the Raman and the IR data on metal–ammonia solutions suggest that there is an interaction between the solvated electron and the solvent. The fact that the solvent vibrational peak occurs at the same position in both pure solvent and in metal solutions is somewhat surprising. From the infrared absorption data, one would expect that the totally symmetric vibration (ν_1 and ν_3) would shift with increasing metal concentration. It might even be succesfully argued that either the positions or half-widths or both would change because of the effects of site symmetry of the solvent molecule in the absorption of the cavity.

The decrease in intensity is probably due to the absorption of the scattered radiation by the high-energy tail of the solvated electron absorption peak. A quantitative comparison of the intensities in this preliminary investigation is not possible. There is also a lack of data for the extinction coefficient of the solvated electron at these energies and temperature.

References

1. Metal-ammonia solutions. Lepoutre, G., Sienko, M. J., (Eds.). New York: Benjamin 1964.
2. Metal-ammonia solutions. Lagowski, J. J., Sienko, M. J. (Eds.). London: Butterworths 1970.
3. Jortner, J.: J. Chem. Phys. 30, 839 (1959).
4. Copeland, D. A., Kestner, N. R., Jortner, J.: J. Chem. Phys. 53, 1189 (1970).
5. Lax, M.: J. Chem. Phys. 20, 1752 (1952).
6. Kleinman, D. A.: Phys. Rev. 134, A423 (1964).
7. Worlock, J. M., Porto, S. P. S.: Phys. Rev. Letters 15, 697 (1965).
8. Lepoutre, G., Corset, J.: In Ref. [1], pp. 186.
9. Gold, M., Jolly, W. L.: Inorg. Chem. 1, 818 (1962).
10. Rusch, P. F.: Ph. D. Thesis. The University of Texas at Austin, 1971.
11. Rusch, P. F., Lagowski, J. J.: These proceedings, p. 168.
12. Herzberg, G.: Molecular spectra and molecular structure. Vol. II. Infrared and Raman spectra of polyatomic molecules. New York: Van Nostrand 1945.
13. De Bettignies, B., Wallart, F.: Compt. Rend. 271, 640 (1970).
14. Smith, B. L., Koehler, W. H.: J. Phys. Chem. (to be published).
15. Birchall, T., Drummond, I.: J. Chem. Soc. A, 1970, 1859.
16. De Bettignies, B.: These de 3e Cycle. Université des Sciences et Techniques, Lille, 1971.
17. Ceccaldi, M., Leickman, J. P.: CEA-R-3586 (1968). Commissariat à l'énergie Atomique, France.

III. Solutions de métaux alcalins dans les amines.

Lorsque l'on dissout un métal alcalin dans les amines aliphatiques, plusieurs espèces sont en présence. On peut les mettre en évidence par l'étude du spectre d'absorption optique de ces solutions ou par R P E. L'existence d'équilibres entre ces espèces se manifeste dans les mesures de conductances.

III. 1. Coefficient d'extinction et équilibres. (publication 4)

Le spectre des solutions de métaux dans les amines et éthers a déjà été très étudié. Aucune de ces études n'a donné les valeurs des coefficients d'extinction. Ceci est du au fait que ces solutions sont instables, la décomposition étant catalysée par les parois des cellules. Une autre source d'ennuis provient du fait que le sodium contenu dans le verre s'échange avec d'autres ions alcalins et provoque des perturbations dans le spectre.

On observe en général deux bandes d'absorption pour les solutions de métaux dans les amines. On attribue la bande observée dans l'infrarouge à l'électron solvaté et celle apparaissant dans le visible à une espèce dépendant du métal probablement de structure M^-.

La position de la bande de l'électron solvaté est indépendante du métal mis en solution, sa forme est identique à celle que l'on obtient par radiolyse pulsée. La bande dépendant du métal apparait à 660, 850, 900 et 1020 nm pour Na, K, Rb et Cs. Dans l'éthylènediamine qui est le solvant que nous avons utilisé, la bande à 1020 nm du césium n'est observée que pour des concentrations très fortes en métal. En règle générale on observe un équilibre du type :

$$M^- \rightleftharpoons e^-$$

Cet équilibre est totalement déplacé vers la droite dans le cas de solutions diluées de césium et vers la gauche dans le cas du sodium.

a) Coefficient d'extinction

Nous avons mis à profit ces observations pour mettre au point une méthode de mesure du coefficient d'extinction de Na^-. Nous avons

utilisé la réaction $Na^+ + 2\,e^- \longrightarrow Na^-$. Cette réaction est complète. Nous l'avons réalisée en mélangeant rapidement (1 ms) une solution de bromure de sodium à une solution diluée de césium. Pour éviter les problèmes de décomposition, la concentration de la solution de césium était toujours supérieure à celle de sodium c'est à dire qu'il y avait toujours une absorption résiduelle dans l'infrarouge.

Nous avons obtenu l'absorbance réelle de Na^- en utilisant une méthode de déconvolution. En traçant l'absorbance de Na^- en fonction de la concentration en Na^+ ajoutée, nous avons obtenu une droite dont la pente est le coefficient d'extinction de Na^-. Nous avons trouvé un coefficient d'extinction de $8.2 \times 10^4 M^{-1} cm^{-1}$ en admettant qu'il y ait un atome de sodium par espèce absorbante. La force d'oscillateur de cette transition est égale à 2 ce qui est conforme avec la stoechiométrie Na^- .

b) Etudes des équilibres.

En utilisant la même technique de mélange rapide que précédemment, nous avons mélangé des solutions d'ion potassium à une solution de césium métal. Le mélange se faisant dans une cellule en quartz, il n'y avait pas de contamination par le sodium.

Nous avons observé l'apparition de la bande à 850 nm caractéristique des solutions de potassium. Aux très fortes concentrations en K^+, les deux bandes correspondant à K^- et à l'électron étaient toujours observées.

Les résultats obtenus indiquent clairement l'existence d'équilibres.

PUBLICATION 4

METAL-ETHYLENEDIAMINE SOLUTIONS.

EXTINCTION COEFFICIENTS AND EQUILIBRIA.

Metal-Ethylenediamine Solutions. Extinction Coefficients and Equilibria[1]

by Marc G. DeBacker and James L. Dye*

Department of Chemistry, Michigan State University, East Lansing, Michigan 48823 *(Received March 15, 1971)*

Publication costs assisted by the U. S. Atomic Energy Commission

The V band, characteristic of the optical absorbance of solutions of sodium metal in ethylenediamine, was produced by the reaction of cesium metal solutions with solutions of sodium salts. By keeping the cesium concentration in excess and using flow techniques, problems caused by decomposition were minimized. The absorbance of the V band was a linear function of the initial concentration of the sodium salt and yielded an oscillator strength of 1.9 ± 0.2 and an extinction coefficient of 8.2 ± 0.3 × 10^4 M^{-1} cm^{-1} based upon the stoichiometry Na^-. Combination of these results with pulse-radiolysis studies yielded an oscillator strength of 0.88 ± 0.12 and an extinction coefficient of 2.0 ± 0.3 × 10^4 M^{-1} cm^{-1} for the solvated electron in ethylenediamine. Other equilibria involving M^+ and e^- were examined.

Introduction

The spectra of metal solutions in amines and ethers have been studied extensively[2-11] but these studies have failed to provide quantitative values of the molar extinction coefficients. The major obstacle has been the instability of solutions, especially in spectral cells of large surface-to-volume ratio. Catalysis of the decomposition by the container walls seems to be a major limiting factor.[10] Another source of difficulty has been the confusion over band assignments which was ultimately traced to the ease of contamination by sodium from the Pyrex container.[6]

There has been general agreement that the broad absorption band in the infrared is characteristic of the

(1) This work was supported by the U. S. Atomic Energy Commission.

(2) R. R. Dewald and J. L. Dye, *J. Phys. Chem.*, 68, 121 (1964). (See this paper for earlier references.)

(3) M. Ottolenghi, K. Bar-Eli, H. Linschitz, and T. R. Tuttle, Jr., *J. Chem. Phys.*, 40, 3729 (1964).

(4) M. Ottolenghi, K. Bar-Eli, and H. Linschitz, *ibid.*, 43, 206 (1965).

(5) L. R. Dalton, J. D. Rynbrandt, E. M. Hansen, and J. L. Dye, *ibid.*, 44, 3969 (1966).

(6) I. Hurley, T. R. Tuttle, Jr., and S. Golden, *ibid.*, 48, 2918 (1968).

solvated electron, either alone or in ion pairs or higher aggregates.[12] Recent pulse-radiolysis studies have confirmed the similarity in band shape between the infrared band of metals in ethylenediamine and that of the solvated electron at high dilution in the same solvent.[13] After the realization that the V band at 650–700 nm requires that sodium be present[6] it became apparent that this band is the sodium analog of the R bands at about 850, 900, and 1020 nm for K, Rb, and Cs respectively.[2] Matalon, Golden, and Ottolenghi,[7] by analogy with the spectrum of iodide ion in amine solvents, assigned the metal-dependent band to a charge-to-transfer-solvent (ctts) transition of the alkali anion, M^-. This assignment was also used in several photochemical studies[14,15] of the bleaching and reformation of the sodium V band.

With the observation that sodium ions react rapidly and quantitatively with the solvated electron in ethylenediamine,[16] we decided to take advantage of this property to measure the extinction coefficient of the sodium V band at 650 nm. Several other properties of these solutions were measured as well.

Experimental Section

Ethylenediamine was first dried *in vacuo* over calcium hydride or barium oxide. It was then subjected to a freeze-purification procedure[17] involving at least five cycles. Solvent prepared in this way could be distilled onto a potassium film to form stable blue solutions. However, it could not be mixed with a very dilute metal solution without causing decomposition. Therefore, the freeze purification was followed by a degassing and distillation procedure. The ethylenediamine was distilled from a blue solution of potassium and/or sodium immediately prior to use. The salts used were AR grade. They were dried under vacuum and washed with anhydrous ammonia prior to use. The metals (Na and K; J. T. Baker Co., 99.99%; Cs; a gift from the Dow Chemical Co.) were distilled under high vacuum through several constrictions. Solutions of cesium in ethylenediamine of *ca.* 2×10^{-4} *M* concentration, when prepared in this way and stored in 1-l. vessels, usually had half-lives of 12 hr or more at room temperature. Sodium solutions were much more stable.

Analyses for sodium and potassium were made by both emission and absorption flame photometry by using a Beckman DB flame photometer and/or a Jarrel-Ash atomic absorption flame photometer. These metals were introduced into dilute aqueous HCl and analyzed by comparison with standard solutions.

Optical spectra were measured in a flow system (path length 1.0 mm) which has been described elsewhere.[18] This utilizes a Perkin-Elmer Model 108 rapid-scan monochromator. The signal and a reference signal were detected by two RCA 7102 multiplier phototubes, (which limited the spectral range covered to 600–1000 nm) converted to absorbance by a logarithmic operational amplifier, and recorded on an Ampex SP-300 FM tape recorder. Absorbance calibrations were made by using neutral density filters (Oriel Optical Corp.) which were checked with a Cary Model 14 spectrophotometer. Wavelength calibration was done by using neodymium glass filters. The data were transferred to punched cards *via* a Varian C-1024 computer of average transients and a C-1001 CAT-to-Card coupler. All corrections were made and all spectra were fitted to equations by using a CDC-6500 digital computer and the appropriate least-squares programs.[19]

Results

Contamination by Sodium from Pyrex. We verified the observations of Hurley, Tuttle, and Golden[6] which indicated that Pyrex can easily be a source of sodium contamination. Distillation of potassium through Pyrex with an oxy–gas flame always resulted in sodium contamination of the distillate. However, distillation with a "cool flame" did not give detectable contamination. Potassium solutions, when prepared in Pyrex vessels, always showed a V band. Analysis showed that these solutions contained enough sodium to have been responsible for the absorption. Solutions prepared in a quartz apparatus did not show a V band and contained no detectable sodium contamination. However, contact of such solutions with Pyrex for as little as 10 sec resulted in the formation of a V band, and sodium could be detected by analysis. These observations are in complete agreement with the earlier work.[6] It should be noted, however, that fresh solutions of rubidium and cesium in ethylenediamine do not show a V band, even in a Pyrex cell.

Extinction Coefficients. In order to minimize the effects of decomposition, the V band (maximum absorbance at 650 nm) was produced by the reaction of dilute cesium solutions with sodium bromide or sodium

(7) S. Matalon, S. Golden, and M. Ottolenghi, *J. Phys. Chem.*, **73**, 3098 (1969).

(8) J. L. Dye, M. G. DeBacker, and V. A. Nicely, *J. Amer. Chem. Soc.*, **92**, 5226 (1970).

(9) I. Hurley, T. R. Tuttle, Jr., and S. Golden, *Pure Appl. Chem.*, 449 (1970).

(10) G. Gabor and K. Bar-Eli, *J. Phys. Chem.*, **75**, 286 (1971).

(11) V. A. Nicely and J. L. Dye, *J. Chem. Phys.*, **53**, 119 (1970).

(12) J. L. Dye and R. R. Dewald, *J. Phys. Chem.*, **68**, 135 (1964).

(13) J. L. Dye, M. G. DeBacker, and L. M. Dorfman, *J. Chem. Phys.*, **52**, 6251 (1970).

(14) D. Huppert and K. Bar-Eli, *J. Phys. Chem.*, **74**, 3285 (1970).

(15) S. H. Glarum and J. H. Marshall, *J. Chem. Phys.*, **52**, 5555 (1970).

(16) J. L. Dye, ref 9, p 483.

(17) L. H. Feldman, R. R. Dewald, and J. L. Dye, *Advan. Chem. Ser.*, **No. 50**, 163 (1964).

(18) J. L. Dye and L. H. Feldman, *Rev. Sci. Instrum.*, **37**, 154 (1966).

(19) V. A. Nicely and J. L. Dye, *J. Chem. Educ.*, **48**, 443 (1971).

iodide in the stopped-flow system. The cesium solutions showed only the ir band (maximum absorbance at 1280 nm) of the solvated electron.[2,13] Growth of the V band was complete within the mixing time (*ca.* 1 msec) and the spectra did not change with time after mixing over a period of at least several minutes. When the sodium ion concentration was even in slight excess, no infrared absorbance (detection limit 1050 nm) was detected, in agreement with the results for pure sodium solutions.[2] When the ratio $[Cs]/[Na^+]$ was high enough to give a residual infrared absorption, the absorbance of the V band was a linear function of the concentration of Na^+ as shown in Figure 1. Either NaBr or NaI could be used with identical results. In order to subtract the contribution of the infrared band to the total absorbance, the spectrum was fitted by least-squares to a linear combination of the spectra of pure cesium solutions and of pure sodium solutions in ethylenediamine.[2] A typical fit is shown in Figure 2. The results and a statistical estimate of the standard deviation for each fit are given in Table I. The variation of absorbance of the V band with concentration shown in Figure 1 yields a least-squares value of the molar extinction coefficient of $8.2 \pm 0.3 \times 10^4\ M^{-1}\ cm^{-1}$ based upon 1 mol of sodium ions per mole of absorbing species. (All of the uncertainties given in this paper represent statistical estimates of the standard deviation). If two sodium ions were required, the molar extinction coefficient would be $1.64 \pm 0.06 \times 10^5\ M^{-1}\ cm^{-1}$.

Table I: Absorbance of the V Band at 15,200 cm^{-1} Produced by the Addition of Sodium Ions to a Cesium Solution (Path Length: 1.0 mm. Individual Entries Represent the Average of Three to Five Replications)

$[Na^+]$, $M \times 10^5$	A	Standard deviation
2.15	0.23	0.02
2.50	0.195	0.02
3.15	0.22	0.02
4.30	0.41	0.04
6.30	0.356	0.07
9.45	0.85	0.07
10.75	0.94	0.07
12.60	0.89	0.03
14.60	1.25	0.08
18.90	1.82	0.10
18.90	2.11	0.05
22.00	1.79	0.12
37.85	2.65	0.15
44.00	3.86	0.40

Pulse-radiolysis studies of the reaction between Na^+ and e_{solv}^- in ethylenediamine[16,20] show that the growth of the V band and the decay of the ir band occur simultaneously and are both second order in $[e^-]$. Either NaBr or NaI could be used with identical results. The

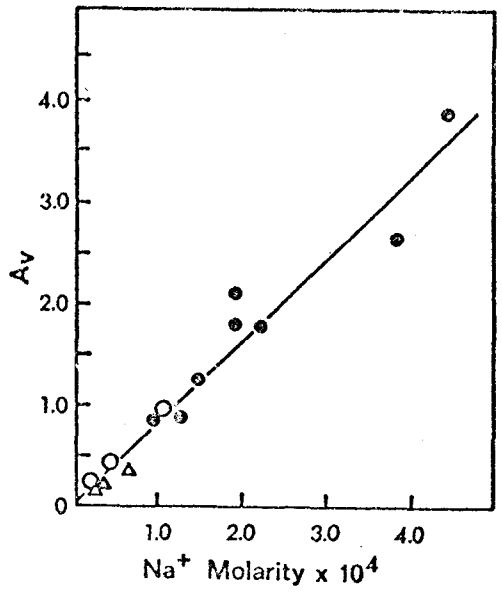

Figure 1. Contribution of the V band to the absorbance of solutions formed by mixing a solution of cesium in ethylenediamine with a solution of either sodium bromide or sodium iodide in ethylenediamine. The different symbols refer to different runs.

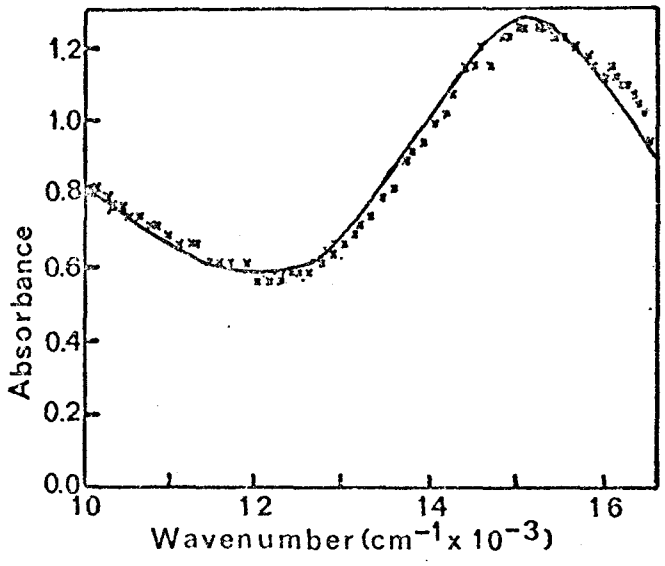

Figure 2. A typical spectrum of a solution formed by mixing a solution of cesium metal in ethylenediamine with a $1.26 \times 10^{-4}\ M$ solution of sodium iodide in ethylenediamine. The solid line was obtained by the least-squares fit of a linear combination of the spectra of pure Cs (ir band) and pure Na(V band).

spectrum at "infinite time" is that of the V band only and shows little or no ir band. By comparing the absorbance of the V band at the end of the reaction with the absorbance of the solvated electron at the beginning of the reaction, the ratio of extinction coefficients of the two species per mole of electrons could

(20) J. L. Dye, M. G. DeBacker, J. Eyre, and L. M. Dorfman, unpublished work.

be obtained. This ratio was independent of the concentration of sodium bromide (or sodium iodide) over the range of concentration 10^{-2} M < [Na^+] < 0.5 M. These experiments yield $A_V^\infty/A_{ir}^0 = 2.1 \pm 0.3$. The ratio given refers to absorbances at the wavelengths of maximum absorbance of the V band and the ir band respectively. Other details of these pulse radiolysis studies will be reported elsewhere.[20]

Equilibrium Studies. The addition of potassium salts ($C = 4 \times 10^{-4}$ to 6×10^{-3} M) to a solution of cesium in ethylenediamine resulted in the appearance of the potassium R band at 850 nm. Since even pure potassium solutions contain both the R band and the ir band,[2] complete conversion of the ir band to the R band was not expected, nor was it found. The contribution of each band was determined by using the spectra of the separate bands[2] and a least-squares fit of the absorbance over the entire wavelength region studied (600–1050 nm). The results are displayed in Figure 3. The absorbances of the two bands are the computed values at the respective maxima.

Solutions containing KI at relatively high concentrations were mixed with solutions of sodium in ethylenediamine in the expectation that the V band of sodium might be converted into the R band of potassium. Surprisingly, the change in absorption corresponded to a contribution from the ir band rather than the R band. To verify the presence of a common-ion effect, solutions which contained both KI and NaI were mixed with sodium solutions. No change in the spectrum occurred in these cases. The results of these experiments are given in Table II and the spectra are shown in Figure 4. Once again, Table II gives the computed absorbances at the respective maxima of the ir, R, and V bands which would be required to fit the observed spectra. The values given for A_R should be considered as upper limits only.

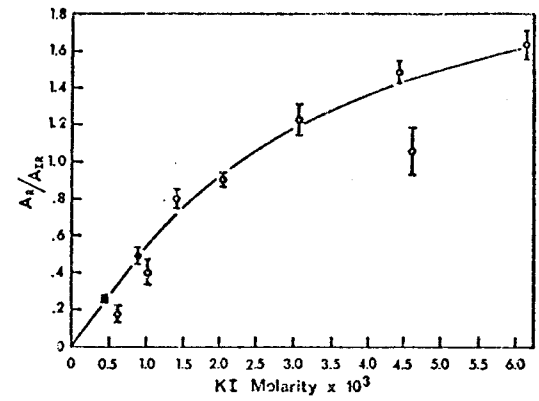

Figure 3. The ratio of the absorbance contribution of the R band of K to the ir band of Cs in solutions formed by mixing a solution of cesium metal in ethylenediamine with a solution of potassium iodide in ethylenediamine. The uncertainties represent statistical estimates of the standard deviation for repeated determinations (normally three replications). The estimated initial absorbance of Cs is 4.0 for points represented by open circles and 0.6 for points represented by solid circles.

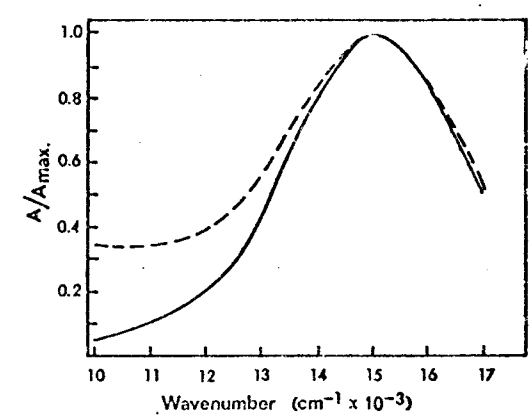

Figure 4. Comparison of the spectra of a solution of sodium in ethylenediamine in the presence (dashed line) and absence (solid line) of added potassium iodide.

Table II: Equilibrium Studies: K^+ + V Band (Contributions to the Total Absorbance by Three Species.[a] Path Length: 1.0 mm)

Run number	[K^+], M	A_{ir}	A_R	A_V
3.3	0.125	0.108	0.036	0.253
3.4		0.143	0.030	0.379
3.5		0.129	0.031	0.292
3.6		0.136	0.030	0.373
3.7		0.146	0.019	0.348
5.2	0.125	0.0	0.020	0.297
5.3	[Na^+] added	0.0	0.013	0.334
5.4		0.012	0.010	0.324
6.3	0.1875	0.044	0.00	0.610
6.4		0.042		0.641
6.5		0.042		0.646
7.3	0.375	0.139	0.00	0.431
7.4		0.165	0.00	0.554
7.5		0.149	0.01	0.374
8.7	0.375 [Na^+] added	0.026	0.00	0.481

[a] See text for a description of the method of data treatment and the meaning of the A values.

The addition of KI to a solution of sodium in ethylenediamine was repeated with a cell which permitted the ir region to be scanned. The ir band which formed upon addition had the same shape and peak position (7800 cm^{-1}) as the solvated electron.

Discussion

In order to determine the stoichiometry of the species responsible for the V band, oscillator strengths were calculated from the data on the basis of one and two sodium nuclei per units. Because of the characteristic asymmetry of the absorption bands it seems inappropriate to attempt to fit the bands with symmetrical functions or to calculate the oscillator strengths from half-widths. As shown by Dye, DeBacker, and Dorf-

man,[13] the absorption band shapes of solvated electrons in water–ammonia and water–ethylenediamine mixtures are conveniently and accurately described by a combination of gaussian and lorentzian functions. Such a procedure fits the entire band, including the high-energy "tail." When the oscillator strengths are computed from these functions, the values are appreciably higher for the solvated electron in water and in ammonia than had been previously assumed. Instead of the value of 0.71 for the hydrated electron[21] we obtain an oscillator strength of 0.81 while the value of 0.64 for the ammoniated electron[22] becomes 0.92 ± 0.10.

When the spectra obtained by the addition of Na^+ to cesium solutions are treated in this way, an oscillator strength of 1.9 ± 0.2 is obtained for the V band, based upon one sodium nucleus per absorbing unit. This would become 3.8 ± 0.4 if two sodium nuclei were required. According to the f sum rule[23,24] we would expect that an oscillator strength of about 2 would require at least two equivalent electrons involved in the transition. The species Na^- fulfills this requirement. As an added comparison, it should be noted that the oscillator strength for the $3^1P \leftarrow 3^1S$ transition of the gaseous magnesium atom is 1.745.[25] This gives strong evidence that the species responsible for the V band contains two electrons per sodium nucleus. It should be noted that because of the requirements of charge balance, studies on pure sodium solutions would be expected to yield an extinction coefficient and oscillator strength per sodium nucleus which is only $^1/_2$ that found in these studies.

A further verification of the stoichiometry is obtained from the pulse-radiolysis studies.[20] The assumed stoichiometry

$$2e^- + Na^+ \longrightarrow Na^-$$

and the ratio $A_V^\infty/A_{ir}^0 = 2.1 \pm 0.3$ yield an extinction coefficient for the solvated electron in ethylenediamine of $2.0 \pm 0.3 \times 10^4$ and an oscillator strength of 0.88 ± 0.12. The agreement of this value with those for the hydrated and ammoniated electron adds further strength to the assigned stoichiometry.

Similarity of the V and R bands strongly suggests that the latter also result from absorption by M^-. Since the peak positions are strongly dependent upon the metal used, it seems likely that the alkali metal interaction with the pair of electrons is not the result of weak interactions such as would be expected for the ion pair $M^+e_2^{2-}$. Indeed, the simultaneous existence in solution of bands attributable to Na^- and K^- and the complete absence of peaks at intermediate wavelengths[26] suggests that the species might well be the spherically symmetrical alkali anion with both electrons in s orbitals. The existence of such a species in metal–ammonia solutions has been suggested.[27] However, in this case, no metal-dependent absorption bands have been observed.

The results obtained by mixing KI with cesium solutions indicate the presence of the equilibrium

$$K^+ + 2e^- \rightleftarrows K^-$$

At the salt concentrations used, we would expect most of the ions to be paired so that the equilibrium might better be written as

$$K^+\cdot I^- + 2M^+\cdot e^- \rightleftarrows M^+\cdot K^- + M^+\cdot I^-$$

in which M^+ represents either Cs^+ or K^+. This would be further complicated by the tendency for solvated electrons to form spin-paired species.[28] Therefore, correct analysis of the equilibrium data is virtually impossible. We can note from Figure 3, however, that the intensity of the R band relative to the ir band increases with increasing concentration of KI.

We expected that the addition of KI to a sodium solution would yield the R band of K^- according to

$$Na^- + K^+\cdot I^- \rightleftarrows K^- + Na^+\cdot I$$

However, this was not the case. Instead, the addition of KI caused the growth of an infrared absorption, presumably caused by the solvated electron. This effect has also recently been observed in pulse-radiolysis studies.[20] It seems that the presence of KI shifts the equilibrium

$$2e^- + Na^+ \rightleftarrows Na^-$$

to the left. We have no explanation for this phenomenon.

Acknowledgments. We wish to acknowledge support of this research by the U. S. Atomic Energy Commission under Contract AT-11-1-853. We thank Drs. V. A. Nicely and E. R. Minnich, who provided valuable assistance with the experiments and with the data analysis and also Mssrs. M. T. Lok and F. J. Tehan, who checked some of the results. We are also grateful to Professor Leon Dorfman of the Ohio State University for many helpful discussions and for the opportunity to use the OSU LINAC.

(21) E. J. Hart and M. Anbar, in "The Hydrated Electron," Wiley-Interscience, New York, N. Y., 1970, p 40.

(22) R. K. Quinn and J. J. Lagowski, *J. Phys. Chem.*, 73, 2326 (1969).

(23) W. Kuhn, *Z. Phys.*, 33, 408 (1925).

(24) W. Thomas, *Naturwissenschaften*, 13, 627 (1925).

(25) L. Bierman and E. Trefftz, *Z. Astrophys.*, 26, 213 (1949).

(26) See, however, ref 10 for evidence of additional bands in solutions which contain a high concentration of a single metal.

(27) S. Golden, C. Guttman, and T. R. Tuttle, Jr., *J. Chem. Phys.*, 44, 3791 (1966).

(28) J. L. Dye, ref 10, p 1.

III. 2. Etude cinétique de la réaction $Na^+ + 2e^- \longrightarrow Na^-$. (publication 5)

La technique de mélange rapide de solutions ne permet pas l'étude de réactions dont le temps de demi réaction est inférieur à 10 ms . Nous avons étudié cette réaction par radiolyse pulsée de solutions d'ions sodium dans l'éthylènediamine. En l'absence d'ions sodium, le temps de vie de l'électron solvaté était de plusieurs secondes.

Nous avons suivi la réaction en mesurant simultanément la disparition de l'électron solvaté et l'apparition de la bande de Na^-.

Nous avons vérifié que les formes des spectres d'absorption des deux espèces ne changeaient pas au cours de la réaction.

En l'absence d'autres ions que Na^+ ou Cs^+, la réaction est strictement du second ordre par rapport à la concentration en électrons solvatés. Les mêmes constantes peuvent être utilisées pour décrire la disparition de e^- et l'apparition de Na^- . L'addition d'ions K^+ au milieu réactionnel ne provoque pas l'apparition de la bande de K^- à 850 nm mais provoque l'apparition d'une absorbance résiduelle à la fin de la réaction. Ce phénomène avait déjà été observé dans l'étude des mélanges de solutions Na^-, K^+ (publication 4).

Nous avons étudié l'influence de la concentration en ions sodium sur les constantes cinétiques. Aux concentrations élevées, la constante de vitesse semble indépendante de la concentration en sodium aux erreurs de mesure près.

Pour interpréter ces divers phénomènes, nous proposons le mécanisme suivant

$$e^-_s + e^-_s \rightleftharpoons e_2^{2-}$$

$$e_2^{2-} + Na^+ \longrightarrow Na^-$$

Nous obtenons un accord raisonnable avec les valeurs expérimentales.

PUBLICATION 5

PULSE RADIOLYSIS STUDY OF THE KINETICS OF FORMATION OF Na^- in ETHYLENEDIAMINE BY THE REACTION OF SOLVATED ELECTRONS WITH SODIUM IONS.

Pulse Radiolysis Study of the Kinetics of Formation of Na^- in Ethylenediamine by the Reaction of Solvated Electrons with Sodium Ions[1]

by James L. Dye, Marc G. DeBacker,

Department of Chemistry, Michigan State University, East Lansing, Michigan 48823

John A. Eyre, and Leon M. Dorfman*

Department of Chemistry, The Ohio State University, Columbus, Ohio 43210 *(Received October 12, 1971)*

Publication costs assisted by the U. S. Atomic Energy Commission

Fast reaction studies of the formation of Na^- in ethylenediamine from e_{sol}^- and sodium ion were carried out by the pulse radiolysis method. The decay of the absorbance of e_{sol}^- and the growth of that of Na^- were both second order with similar rate constants which were independent of the concentration of sodium ion above about 10^{-2} *M* but decreased with a decrease in the concentration of Na^+ below this value. The presence of Cs^+ had no effect upon the rate. At low concentrations of Na^+, excess K^+ caused the reaction to reach equilibrium rather than to proceed to completion. The results show that the formation of species containing two electrons (which may be coupled with metal cation) precedes the reaction in which Na^- is formed. Quantitative kinetic tests of the mechanism are presented.

Introduction

Bimolecular reactions of the solvated electron with another single-electron species have now been observed by a variety of methods in a number of solvents. The reaction in water

$$e_{sol}^- + e_{sol}^- \xrightarrow{H_2O} H_2 + 2OH^- \qquad (1)$$

has been established by isotopic[2] and by kinetic studies.[2,3] Reaction of the solvated electron with a metal atom (or monomer or ion pair) according to

$$e_{sol}^- + Na\cdot \longrightarrow Na^- \qquad (2)$$

(1) This work was supported by the U. S. Atomic Energy Commission and was initiated while J. L. D. was a visiting scientist on sabbatical leave at The Ohio State University in 1969.

(2) L. M. Dorfman and I. A. Taub, *J. Amer. Chem. Soc.*, 85, 2370 (1963).

(3) M. S. Matheson and J. Rabani, *J. Phys. Chem.*, 69, 1324 (1965).

has been proposed to explain the flash[4] or laser[5] photolysis of alkali metal–amine solutions. The reactions

$$e_{sol}^- + M^+ \rightleftarrows M\cdot \quad (\text{or } M^+,e^-) \qquad (3)$$

and

$$e_{sol}^- + M\cdot \rightleftarrows M^- \quad (\text{or } 2M^+,e^- \longrightarrow M^-) \qquad (4)$$

where M· is the alkali metal atom or monomer and M^+,e^- is the ion pair, have been invoked in esr kinetic studies[6] and optical studies[7] of flash photolyzed metal–ether solutions. Recently, reaction 3 has been proposed to explain some of the absorbance changes which follow the photolysis of dilute solutions of pyrenide ion in tetrahydrofuran.[8] The detailed role of the alkali metal species in the kinetics remains somewhat obscure, and the identity of individual elementary reactions uncertain. The present pulse radiolysis study of the solvated electron in ethylenediamine solutions in the presence of sodium ions, with and without potassium or cesium ions, was undertaken in an attempt to sort out the roles of the various metal ions and to further relate the decay of the electron absorbance to the growth of the V band, attributed to Na^-.[9,10]

Solutions of alkali metals in ammonia and in amines have been studied for a number of years. However, in spite of these efforts, even the stoichiometry of the species present in solution has not been unequivocally determined. Electrochemical, thermodynamic, and magnetic resonance studies of metal–ammonia solutions give evidence for the existence of species with the stoichiometry M, M^-, and possibly M_2.[11–14] The absence of definitive changes in the spectroscopic properties of metal–ammonia solutions with concentration has led to the proposal that the metal-containing species and also the spin-paired species are formed by relatively weak interaction among solvated electrons and alkali metal cations.[14,15]

In contrast to the behavior of metal–ammonia solutions, metal solutions in some amines and ethers show new optical bands[16] and esr absorptions[17] which are characteristic of metal-containing species. The esr results show unequivocally that at least one species of stoichiometry M is present as a minor constituent. However, the stoichiometry of the species responsible for the metal-dependent optical absorption has been the subject of speculation for some time. With the demonstration by Hurley, Tuttle, and Golden[18] that metal–amine solutions could release significant amounts of sodium from Pyrex, some of the confusion in the field was removed. The similarity of the solvent and temperature dependence of the position of the optical band with these properties of the charge-transfer-to-solvent band of iodide ion, led Matalon, Golden, and Ottolenghi[9] to propose the stoichiometry M^-. This stoichiometry was also used to explain the kinetics of recombination of species produced by flash photolysis of metal–amine[4,5] and metal–ether[6,7] solutions.

It has recently been shown[10] that the major absorption in solutions of sodium in ethylenediamine (maximum at 650 nm) originates from a species of stoichiometry Na^-. The absorption of e_{sol}^- is small even in dilute solutions.[16] At the other extreme, dilute cesium solutions in this solvent show only the infrared absorption of the solvated electron.[19,20] Solutions of potassium and rubidium and concentrated solutions of cesium in ethylenediamine show both the solvated electron absorption and a metal-dependent band, presumably from M^-. In less strongly solvating media such as in ethylamine and the higher monoamines and in ethers the solvated electron absorption becomes less pronounced and the spectrum is dominated by the absorption of M^-. The equilibrium

$$Na^+ + 2e_{sol}^- \rightleftarrows Na^- \qquad (5)$$

lies so far to the right in ethylenediamine that the addition of a sodium salt to a solution of cesium in this solvent yields only the band of Na^- when stoichiometric amounts of salt are used.[10]

Several investigators have shown[4–7,21,22] that metal solutions in amines and in ethers yield the solvated electron upon photolysis. The rate of formation of Na^- [4,5] and of intermediates[7] after a dissociating flash have been studied. Huppert and Bar-Eli[5] studied this process as a function of temperature and ionic strength in 1,2-propanediamine and in ethylenediamine. They found the growth of the Na^- absorption to be a second-order process with a rate which was independent of

(4) A. Gaathon and M. Ottolenghi, *Israel J. Chem.*, 8, 165 (1970).

(5) D. Huppert and K. H. Bar-Eli, *J. Phys. Chem.*, 74, 3285 (1970).

(6) S. H. Glarum and J. H. Marshall, *J. Chem. Phys.*, 52, 6251 (1970).

(7) J. G. Kloosterboer, L. J. Giling, R. P. H. Rettschnick, and J. D. W. VanVoorst, *Chem. Phys. Lett.*, 8, 462 (1971).

(8) M. Fisher, G. Ramme, S. Claesson, and M. Szwarc, *ibid.*, 9, 309 (1971).

(9) S. Matalon, S. Golden, and M. Ottolenghi, *J. Phys. Chem.*, 73, 3098 (1969).

(10) M. G. DeBacker and J. L. Dye, *ibid.*, 75, 3092 (1971).

(11) E. Becker, R. H. Lindquist, and B. J. Alder, *J. Chem. Phys.*, 25, 971 (1956).

(12) E. Arnold and A. Patterson, Jr., *ibid.*, 41, 3089, 3093 (1964).

(13) S. Golden, C. Guttman, and T. R. Tuttle, Jr., *ibid.*, 44, 3791 (1966).

(14) For a review of models and additional references see J. L. Dye, *Pure Appl. Chem.*, 1 (1970).

(15) M. Gold, W. L. Jolly, and K. S. Pitzer, *J. Amer. Chem. Soc.*, 84, 2264 (1962).

(16) For references to optical properties of metal solutions see I. Hurley, T. R. Tuttle, Jr., and S. Golden in ref 14, p 449.

(17) For references to esr studies of metal solutions see R. Catterall, ref 14, p 105.

(18) I. Hurley, T. R. Tuttle, Jr., and S. Golden, *J. Chem. Phys.*, 48, 2818 (1968).

(19) R. R. Dewald and J. L. Dye, *J. Phys. Chem.*, 68, 121 (1964).

(20) J. L. Dye, M. G. DeBacker, and L. M. Dorfman, *J. Chem. Phys.*, 52, 6251 (1970).

(21) J. Eloranta and H. Linschitz, *ibid.*, 39, 2214 (1963).

(22) M. Ottolenghi, K. Bar-Eli, and H. Linschitz, *ibid.*, 43, 206 (1965).

added Na^+. Several years ago it was reported[23] that reaction 5 could be studied in ethylenediamine by using pulse radiolysis to produce the solvated electron. Both the decay of the absorption of e^- and the growth of the absorption of Na^- followed second-order kinetics. The present paper describes the kinetics of this reaction including the effect of concentration of sodium ion and of other salts.

Experimental Section

The techniques of pulse radiolysis[24-26] used in this laboratory[27] have been described in detail. A Varian V-7715A electron linear accelerator was used as a pulse source of 3–4-MeV electrons, generally at a pulse current of about 350 mA. The pulse width was varied from 100 to 500 nsec. A 100-nsec pulse delivers a dose of about 6×10^{16} eV/g to water.

The transient optical absorption was simultaneously observed with two separate photodetectors. Either an RCA 7102 or 7200 photomultiplier was used below about 1000 nm and for all kinetic studies. To study absorption spectra into the infrared, a liquid nitrogen cooled indium antimonide detector, Model A10X, obtained from Barnes Engineering, Inc., was used. This detector, which has been used[28] out to 2250 nm, has a rise-time (10 to 90%) of about 80 nsec with the circuitry which has been described.[28] The linearity of the detector was tested with a chopped light signal superimposed on a steady signal. No deviation from linearity could be detected within a sensitivity of 1%. A flashed 500-W Osram xenon lamp, Type X BO 450 W, was used as light source. Bausch and Lomb grating monochromators, Type 33-86-25, $f/3.5$, were used with appropriate cutoff filters.

Reaction cells with high purity silica optical windows, of a geometry previously described,[20] were used. With runs containing sodium and potassium, the procedures previously described[20] were used with the modification that ethylenediamine was either poured or distilled from a storage bulb under vacuum into the reaction cell. For runs with cesium, a waste storage bulb was added to the cell configuration to permit prior rinsing of the cell with ethylenediamine. A side arm permitted cesium-containing capillaries to be broken under vacuum. Alkali metal salts were added in small, thin-walled bulbs which were broken *in situ* as required.

Ethylenediamine, obtained as a gift from Dow Chemical Co., had a stated purity of 99%. It was freeze-purified as recommended,[10,29] and then was distilled onto a potassium mirror to form a stable blue solution. After a 24-hr storage over potassium, the solvent was distilled into an evacuated storage bulb. Sodium and potassium, with nominal purities of 99.99%, were obtained from J. T. Baker Co. Cesium was obtained as a gift from Dow Chemical Co. The metals were triply distilled by using a cool flame and stored in short lengths of 2-mm i.d. capillary tubing.

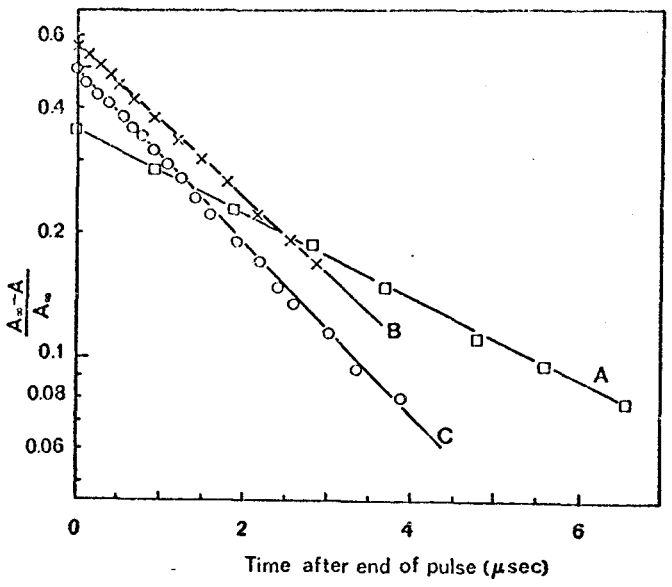

Figure 1. First-order growth of e_{sol}^- in basic ethylenediamine after the end of the pulse. Absorbance measured at 1000 nm. A, Dilute KNHR ($\approx 10^{-2}$ *M*) with $\approx 10^{-2}$ *M* KI present; B, 4×10^{-3} *M* KNHR; C, 4×10^{-3} *M* KNHR + 3×10^{-3} *M* NaBr.

Results and Discussion

The formation of solvated electrons in pure ethylenediamine and in basic ethylenediamine (containing $\approx 5 \times 10^{-3}$ *M* potassium ethylenediamide, KNHR) has been described previously.[20] The lifetime of e_{sol}^- in the irradiated pure solvent is only a few microseconds, being limited by reaction with the counterion. However, in basic ethylenediamine, the solvated electron is stable for at least several seconds after the pulse. By contrast, in basic ammonia, the lifetime is only about a microsecond unless a radical scavenger such as ethanol is present.[20] There is another significant difference between the behavior with ammonia and that with ethylenediamine. In basic ammonia which contains ethanol ($\gtrsim 10^{-2}$ *M*) the absorbance of the electron grows only during the pulse, while in basic ethylenediamine (made basic with decomposed sodium, potassium, or cesium solutions) there is an additional substantial growth of the absorbance after the pulse. The growth of absorbance is first order in all cases. As shown in Figure 1, the final value of the absorbance can be nearly three times that at the end of the pulse. Within a given run

(23) J. L. Dye, ref 14, p 483.

(24) M. S. Matheson and L. M. Dorfman, *J. Chem. Phys.*, 32, 1870 (1960).

(25) L. M. Dorfman and M. S. Matheson, *Progr. React. Kinet.*, 3, 237 (1965).

(26) M. S. Matheson and L. M. Dorfman, "Pulse Radiolysis," M.I.T. Press, Cambridge, Mass., 1969.

(27) W. D. Felix, B. L. Gall, and L. M. Dorfman, *J. Phys. Chem.*, 71, 384 (1967).

(28) L. M. Dorfman, F. Y. Jou, and R. Wageman, *Ber. Bunsenges. Phys. Chem.*, 75, 681 (1971).

(29) L. H. Feldman, R. R. Dewald, and J. L. Dye, *Advan. Chem. Ser.*, No. 50, 163 (1964).

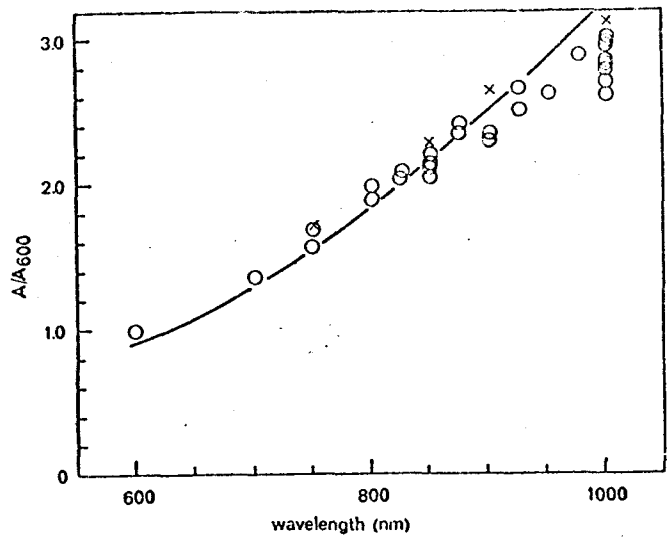

Figure 2. Absorbance after growth of e_{sol}^- in basic ethylenediamine in the presence of K^+. The pulse radiolysis results have been normalized to 600 nm: O, run of 4/2/69; ×, run of 6/7/69; —, spectrum of Cs and e_{sol}^- in ethylenediamine.[19,20]

(fixed basicity) both the rate constant for this formation and the relative increase in absorbance were independent of total radiation dose, salt concentration, and (above 700 nm) wavelength For example, 22 growth curves in a solution which was 4×10^{-3} M in KNHR (and for some of the pulses also 3×10^{-3} M in NaBr) were examined over the wavelength range from 700 to 1000 nm. Analysis of these data yielded $A_\infty/A_0 = 2.62 \pm 0.28$ and $k = 5.22 \pm 0.89 \times 10^5$ sec^{-1}. [All uncertainties given in this paper represent statistical estimates of the standard deviation obtained by a least-squares analysis of the data.] At shorter wavelengths (650–375 nm) the value of A_∞/A_0 remained constant, but the first-order rate constant for the growth of absorbance increased progressively by a factor of 2–3. The spectrum is unchanged during the growth (checked over the complete wavelength range of 600 to 1600 nm only with solutions made basic with potassium). Even when the concentration of KI was as high as 0.27 M there was not more than 10% contribution from the R band of K^-. This is illustrated by Figure 2 in which the wavelength dependence of the absorbance (relative to that at the reference wavelength of 600 nm) is compared with that of the solvated electron in ethylenediamine.

The independence of the growth rate with metal, salt, and pulse length suggests the decomposition of an intermediate species to produce the solvated electron. One possible reaction scheme consists of the scavenging reaction

$$NH_2CH_2CH_2NH\cdot + NH_2CH_2CH_2NH^- \longrightarrow NH_2CH_2CH_2NH_2 + NH_2CH_2\dot{C}HNH^- \quad (6)$$

followed by a rearrangement and electron detachment

$$NH_2CH_2\dot{C}HNH^- \longrightarrow NH_2CH_2CH = NH + e_{sol}^- \quad (7)$$

Reaction 6 represents the abstraction of an α-hydrogen in basic solutions. The first-order formation of the solvated electron could then presumably result from reactions 6 and 7.

Whenever sodium ions were present in the solution, the growth of absorbance of e_{sol}^- was followed by its decay and the simultaneous growth of the absorbance of Na^-. The spectrum at times long enough to reach equilibrium is compared in Figure 3 with that of a solution of sodium in ethylenediamine.[19] If the stoichiometry of the conversion is given by eq 5, then we may relate the absorbances A_1 and A_2 at two different wavelengths to the corresponding extinction coefficients by

$$A_1 - A_1^\circ = \frac{{}^1\epsilon_{Na^-} - 2{}^1\epsilon_{e^-}}{{}^2\epsilon_{Na^-} - 2{}^2\epsilon_{e^-}}(A_2 - A_2^\circ) \quad (8)$$

in which A_1° and A_2° represent the absorbance at the time of maximum e_{sol}^- absorbance. The absorbance at 600 nm proved to be a linear function of that at 1000 nm during the entire reaction. The slope was independent of the nature and concentration of the cation and of pulse duration. Data obtained from 19 sets of traces yielded

$$\frac{\epsilon_{Na^-}{}^{600} - 2\epsilon_{e^-}{}^{600}}{2\epsilon_{e^-}{}^{1000} - \epsilon_{Na^-}{}^{1000}} = 1.77 \pm 0.19$$

The band shapes are known from studies of metal solutions.[19] These can be used with the present result to determine the ratio of the extinction coefficients at the respective band maxima. By using the known extinction coefficient of Na^-, $\epsilon_{Na^-} = 8.2 \times 10^4$ M^{-1} cm^{-1} [10] at 650 nm, we obtain $\epsilon_{e^-} = 2.0 \pm 0.3 \times 10^4$ M^{-1} cm^{-1} for the solvated electron at 1280 nm at 25°. This gives an oscillator strength of 0.88 ± 0.12.[10]

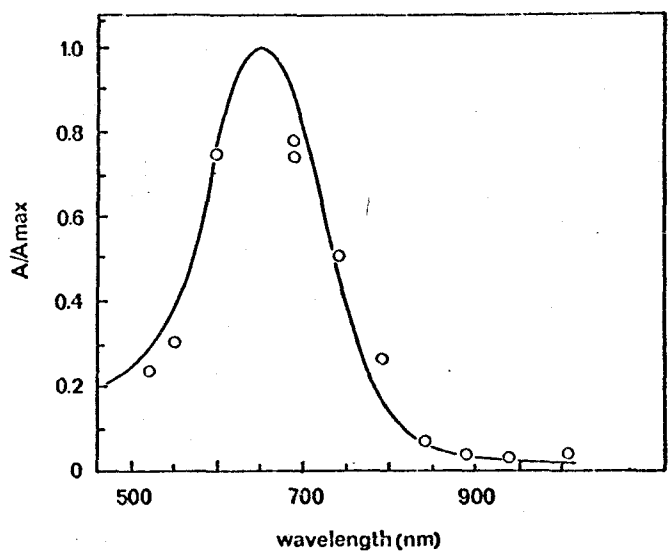

Figure 3. Absorbance (normalized to 650 nm) at long times after the reaction $2e^- + Na^+ \rightarrow Na^-$: O, pulse radiolysis results; ——, spectrum of Na in ethylenediamine.[19]

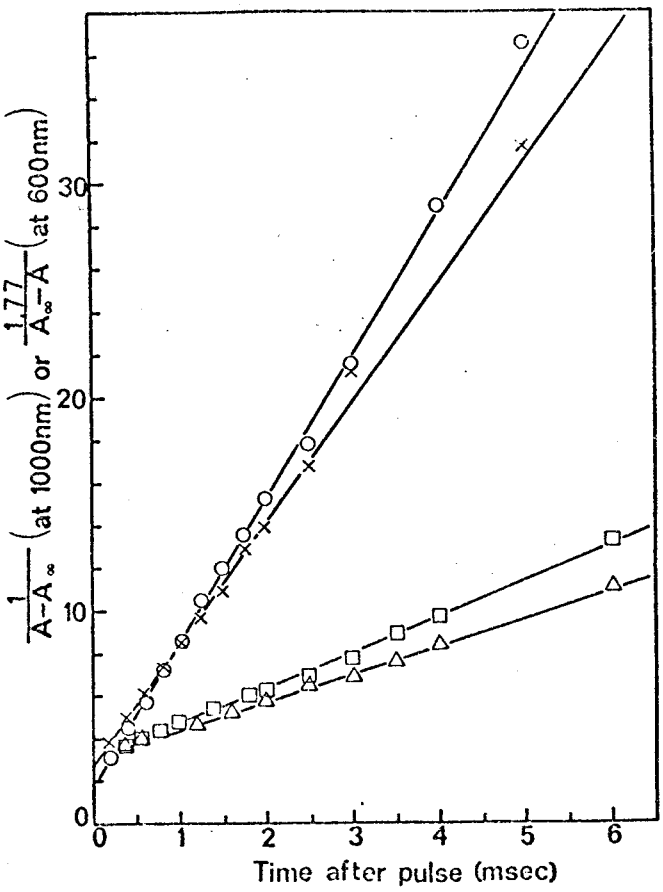

Figure 4. Representative second-order decay of the absorbance of e_{sol}^- and growth of that of Na^- in ethylenediamine. The conversion factor of 1.77 is obtained from the extinction coefficients. The slopes for decay and growth are equal within the uncertainty of the conversion factor: □, decay; △, growth for 1.6×10^{-3} *M* NaBr and 9×10^{-3} *M* CsNHR; ○, decay; ×, growth for 0.038 *M* NaBr and $\approx 3 \times 10^{-3}$ *M* NaNHR.

Reaction 5 is essentially complete at the concentrations of e_{sol}^- and Na^+ used in these experiments (with or without added Cs^+; however, see later for the effect of K^+). From the extinction coefficients and the equilibrium absorbances at 600 and 1000 nm, we obtain $K_5 \geq 10^{10}\ M^{-2}$ at ambient temperatures.

Both the decay of absorbance of e_{sol}^- and the growth of that of Na^- followed second-order kinetics. Figure 4 shows second-order plots of the decay of absorbance at 1000 nm and growth at 600 nm for two different sets of conditions. About half of the data were treated by a simultaneous fit of second-order kinetics to both growth and decay with a nonlinear least-squares program.[30] For the rest of the data, the growth and the decay were separately fit to second-order expressions. The results are summarized in Table I. A plot of the average second-order rate constant *vs.* the total concentration of added sodium (metal plus salt) is given in Figure 5. The rate constant refers to the rate law

$$-d[e^-]/dt = 2d[Na^-]/dt = 2k[e^-]^2$$

Most of the individual points in this figure represent the average value of from 4 to 15 determinations of the rate constant. Some of the data were obtained with low concentrations of sodium ions and higher concentrations of potassium ions. As will be shown later, under these conditions reaction 5 is not complete. For such cases, the rate constants shown in Figure 5 refer to the forward reaction.

Table I: Summary of Pseudo-Second-Order Rate Constants for the Reaction of e_{sol}^- with Na^+ in Ethylenediamine

$10^3[Na^+]$ (total molarity)	No. of replications	$k \times 10^{-9}$, M^{-1} sec^{-1}	Stand. dev $\times 10^{-9}$	Comments
0.7	3	0.132	0.015	*a, b*
0.9	2	0.10	0.03	*d, f*
1.6	3	0.38	0.06	*a, b*
1.8	3	0.21	0.04	*d, f*
2.6	3	0.70	0.11	*d, f, h*
2.7	3	0.64	0.06	*d, f*
2.8	5	1.61	0.15	*d, e*
3	5	0.63	0.13	*a, c*
3.3	8	1.18	0.08	*d, e*
3.5	3	1.04	0.19	*a, b*
5.6	1	0.82	0.17	*d, f, h*
6.3	3	1.20	0.17	*a, b*
7.5	7	1.51	0.26	*a, d*
7.5	7	1.78	0.28	*d, f, g*
10	3	1.33	0.15	*a, c*
18	8	1.79	0.33	*d, e*
22	4	1.58	0.12	*d, e*
40	4	1.54	0.20	*a, c*
65	4	1.74	0.31	*d, e*
86	5	1.76	0.25	*d, e*
121	5	1.27	0.10	*d, e*
160	3	1.42	0.27	*a, c*
542	15	1.48	0.15	*d, e*

[a] Average rate constant obtained by fitting growth and decay separately. [b] Solution made basic by decomposition of 9×10^{-3} *M* Cs. [c] Solution made basic by decomposition of saturated solution of Na ($\approx 3 \times 10^{-3}$ *M*). No K^+ or Cs^+ added. Na^+ added as NaBr. [d] Solution made basic by decomposition of K. Values from 2 to 6×10^{-3} *M* depending on the run. [e] Simultaneous fit of decay and growth of absorbance. [f] $[K^+] > [Na^+]$; reaction goes to equilibrium. Decay and growth of absorbance fitted simultaneously to obtain both forward and backward rate constant. [g] KI added in amounts from 2.7×10^{-3} to 0.17 *M*. [h] For this run, the coefficient in eq 8 was too small by about 20%. The origin of this discrepancy is not known.

It can be seen from Figure 5 that the second-order rate constant is essentially independent of sodium ion concentration above 0.01 *M*. However, between 0.01 and 0.001 *M*, the rate constant decreases by an order of magnitude. These results provide a basis for discussion of several possible mechanisms. It should be noted at the outset that the results of conductance

(30) J. L. Dye and V. A. Nicely, *J. Chem. Educ.*, 48, 443 (1971).

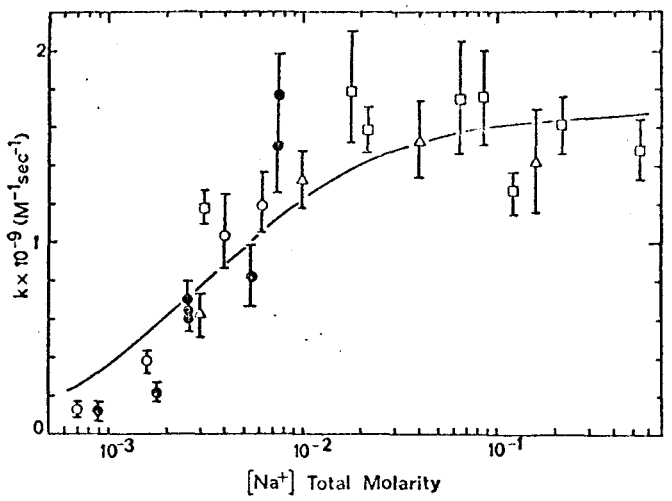

Figure 5. Pseudo-second-order rate constant for the reaction of e_{sol}^- with Na^+ in ethylenediamine. The solid line was obtained by least-squares fit of eq 15. Na^+ was added as NaBr: ○, CsNHR = 9×10^{-3} M; △, no Cs or K^+, NaNHR $\approx 3 \times 10^{-3}$ M; □, KNHR varied from ≈ 2 to 5×10^{-3} M; ●, forward rate constant; KNHR varied from ≈ 2 to 6×10^{-3} M; for some cases KI was also added. Reaction proceeds to equilibrium.

studies of metal solutions[31] in ethylenediamine seem to demand that solvated electrons form ion pairs with added cations in ethylenediamine just as do ordinary salts and that the formation constants are not strongly dependent on the cation. Even for the most dilute solutions used in this study, the reaction

$$M^+ + e_{sol}^- \rightleftarrows M^+,e_{sol}^- \qquad (9)$$

is more than 90% complete at equilibrium. Furthermore, we would expect "loose" ion-pair formation to occur by diffusion control. Therefore, on the time scale used for the study of the kinetics of formation of Na^-, reaction 9 should be at equilibrium. The invariance of the spectral shape of dilute cesium–ethylenediamine solutions with concentration[19] and the similarity with the spectrum of e_{sol}^- in this solvent[20] indicate that the optical properties of the solvated electron are not altered significantly by such ion-pair formation. This is also the case for metal–ammonia solutions.[14]

A plausible reaction mechanism for the formation of Na^- seemed, on the basis of the results for solutions containing only sodium ions, to be that previously proposed[6] as a result of esr studies

$$e_{sol}^- + Na^+ \longrightarrow Na^+,e_{sol}^- \text{ (or Na·)} \qquad (10)$$

$$Na^+,e_{sol}^- + e_{sol}^- \longrightarrow Na^- \qquad (11)$$

with the modification that reaction 12 be written as equivalent to reaction 11

$$Na^+,e_{sol}^- + Na^+,e_{sol}^- \longrightarrow Na^- + Na^+ \qquad (12)$$

This would simply require that the equilibrium for reaction 10 lie far to the right and be reached within a few microseconds at the appropriate concentration of sodium ion. The rate need then not depend on the concentration of sodium ions when other cations are not present at appreciable concentrations. If, however, another cation is present in excess, the pseudo-second-order rate constant would decrease by the factor

$$\frac{K_5^{Na}[Na^+]}{K_5^{M}[M^+]}$$

in which K_5^{Na} and K_5^{M} are the appropriate equilibrium constants for reaction 5. The data, however, show that the rate is independent of the presence of other cations, even when they are in excess concentration. This mechanism (reactions 10 and 12) appears, therefore, to be ruled out. Only if the equilibrium constant for the formation of a species of stoichiometry Na were much greater than the corresponding reaction to form Cs or K and if the spectrum of Na were nearly the same as that of e_{sol}^- could the data be compatible with this mechanism.

Since the results with mixed metal cations rule out the foregoing mechanism, we are forced to conclude that the formation of a species containing *two* electrons occurs prior to the step in which Na^- is formed. One such mechanism is

$$e_{sol}^- + e_{sol}^- \rightleftarrows e_2^{2-} \qquad (13)$$

$$e_2^{2-} + Na^+ \longrightarrow Na^- \qquad (14)$$

It should be noted that the following two reactions, in which the solvated electron and the dielectron species might be associated with metal cations, are considered equivalent forms of reactions 13 and 14, respectively.

$$M^+,e_{sol}^- + M^+,e_{sol}^- \rightleftarrows (M^+,e_{sol}^-)_2 \qquad (13a)$$

$$(M^+,e_{sol}^-)_2 + Na^+ \longrightarrow Na^- + 2M^+ \qquad (14a)$$

By using the steady-state approximation for the concentration of the dielectron species the rate law gives

$$k = \frac{k_{13f}}{1 + k_{13r}/(k_{14}[Na^+])} \qquad (15)$$

in which k is the pseudo-second-order rate constant. The solid line in Figure 5 was obtained by an appropriately weighted least-squares fit of all of the data to eq 15. This yields $k_{13f} = 1.66 \pm 0.12 \times 10^9$ M^{-1} sec^{-1} and $k_{13r}/k_{14} = 3.5 \pm 0.8 \times 10^{-3}$ M. Although the fit to this mechanism is not very good, complications caused by ion-pair dissociation at low concentrations and by ionic strength effects at high concentrations would be expected and are not included in the data treatment. The approximate value of k_{13f} may be compared with the value[2,3] $k_1 = 5 \times 10^9$ M^{-1} sec^{-1} for the analogous reaction in water.

It has recently been noted[10] that potassium salts can apparently reverse reaction 5. To study this effect,

(31) R. R. Dewald and J. L. Dye, *J. Phys. Chem.*, 68, 128 (1964).

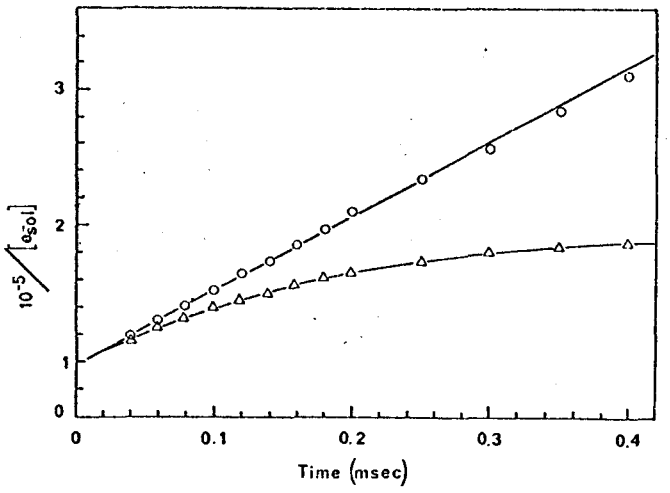

Figure 6. Effect of K^+ on reaction of e_{sol}^- with Na^+ in ethylenediamine: O, [NaBr] = 1.6×10^{-3} M; [CsNHR] = 9×10^{-3} M; △, [NaBr] = 1.8×10^{-3} M, [KNHR] = 5×10^{-3} M.

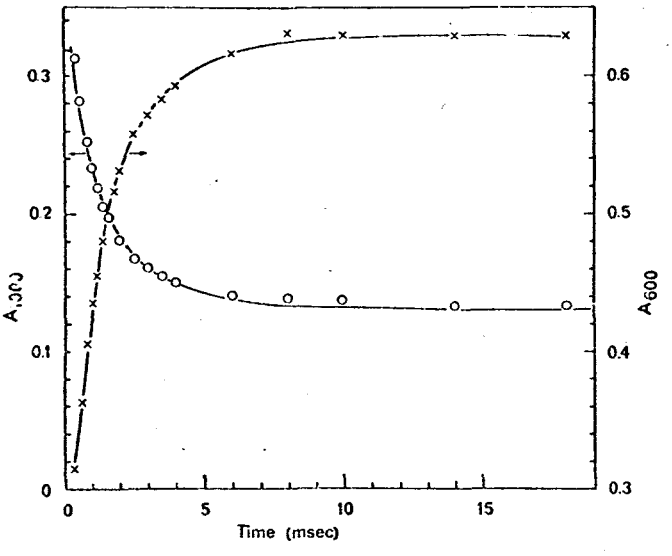

Figure 7. Decay of e_{sol}^- and growth of Na^- in ethylenediamine fit by approach to equilibrium $e^- + e^- \underset{k'}{\overset{k}{\rightleftharpoons}} Na^-$ (Na^+). Solid lines give the best least-squares fit to both growth and decay simultaneously with adjustment of initial absorbances and k. Reverse rate constant calculated from final absorbances and k: O, decay at 1000 nm; ×, growth at 600 nm.

solutions containing both Na^+ and K^+ with the latter in excess were studied by pulse radiolysis. In these cases, the reaction proceeded to an equilibrium in which appreciable absorbance remained at 1000 nm. Figure 6 compares the rate of decay of the absorbance at 1000 nm for a solution which contains Cs^+ and one which contains about the same concentration of K^+. Both solutions have about the same concentration of Na^+. For reactions which did not go to completion, the decay of absorbance at 1000 nm and the growth at 600 nm were fit simultaneously by the rate law

$$\frac{d[Na^-]}{dt} = -\frac{1}{2}\frac{d[e_{sol}^-]}{dt} = k[e_{sol}^-]^2 - k'[Na^-] \quad (16)$$

The concentrations of e_{sol}^- and of Na^- were calculated from the absorbance values at the two wavelengths by using the extinction coefficients previously obtained. A typical fit of the data is shown in Figure 7 which gives the calculated and observed absorbances at the two wavelengths as a function of time. As shown in Figure 8, the values of the equilibrium "constant" K_5 calculated from the rate data as k'/k and also from the absorbances at equilibrium are nearly the same. The data are summarized in Table II.

Table II: Kinetic and Equilibrium Data for the Reaction of e_{sol}^- with Na^+ in Ethylenediamine in the Presence of an Excess of K^+ [a]

10^3-[Na^+],[b] M	10^3[K^+],[b] M	$10^{-3}k'$,[c] sec^{-1}	$10^{-6}k/k'$, M^{-1}	10^3-[Na^-]$^\infty$, M	10^5[e^-]$^\infty$, M	$10^{-6}K_5$,[d] M^{-1}
0.9	2	3.8	0.30	0.25	0.81	0.38
0.9	2	5.0	0.18	0.43	1.12	0.34
1.8	5	2.1	0.91	0.26	0.50	1.02
1.8	5	1.6	1.75	0.19	0.39	1.23
1.8	5	3.1	0.51	0.21	0.56	0.68
2.7	5	0.77	7.1	0.25	0.18	8.0
2.7	5	0.74	6.3	0.37	0.23	7.2
2.7	5	0.68	12.1	0.21	0.21	4.7
7.5	11	e	...	0.50	0.11	39
7.5	81	e	...	0.50	0.15	23
7.5	81	2.4	6.6	0.42	0.22	8.8
7.5	81	1.6	10.6	0.41	0.18	12.7
7.5	170	0.64	2.8	0.46	0.28	5.9
7.5	170	1.67	11.5	0.25	0.21	5.9
7.5	170	1.86	6.8	0.35	0.29	4.2

[a] The run described in footnote h of Table I is not included. [b] Total molarity. The solution was made basic by decomposition of K metal solution. K^+ added as KI, Na^+ added as NaBr. [c] See eq 16. k and k' obtained by simultaneous least-squares fit of decay of absorbance at 1000 nm and growth at 600 nm. [d] Calculated as $10^{-5}[Na^-]^\infty/([e^-]^\infty)^2$. [e] $k' = 0$ within uncertainty.

Figure 5 shows that the forward rate constant, k, has about the same dependence on the total sodium ion concentration as in the absence of potassium ions. The data are not extensive enough to permit a quantitative determination of the dependence of the rate constants and the equilibrium constant on the concentration of potassium and sodium ions. The value of K_5 decreases with decreasing [Na^+] and with increasing [K^+] as expected for the formation of a species such as K^+,e^- from Na^- and K^+. (These spectra and those obtained when KI was added to solutions of sodium in ethylenediamine[10] show no evidence of the formation of the band of K^- at 850 nm.) However, attempts to fit the data with several simple equilibrium schemes failed, largely because they predicted a much larger effect at high concentrations of K^+ than was observed. Both these data

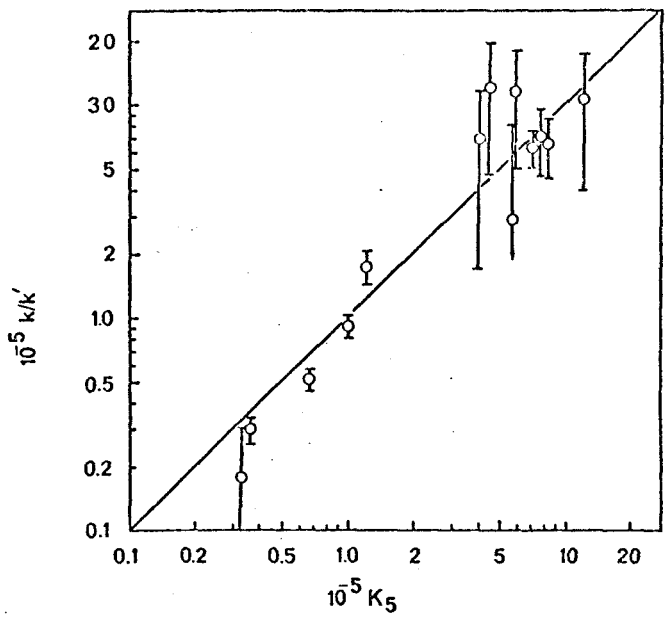

Figure 8. k/k' obtained from least-squares fit of kinetic data compared with the equilibrium constant, K_5, obtained from absorbances at the end of reaction. Error bars calculated from ± 1 standard deviation on k'.

and those obtained previously[10] show that the potassium ion has a significantly greater affinity for the electron than does cesium ion.

Conclusions

Recent kinetic studies of the formation of M^- [4–7] in amines and ethers have been interpreted in terms of an intermediate of stoichiometry M to which a second electron adds in a subsequent step. Indeed, consideration of coulombic interactions leads us to expect the diffusion-controlled formation of ion pairs. However, the present studies indicate that the formation of Na^- in ethylenediamine occurs by reaction of Na^+ with a species which already contains two electrons.

The conclusions from this work may be compared with other recent studies[4–7] in which different experimental methods have been used. The experimental results from the photochemical studies of Gaathon and Ottolenghi[4] and of Huppert and Bar-Eli[5] are similar to ours. The absence of an ionic strength effect would be expected if most of the electrons formed ion pairs. The equation used by Glarum and Marshall[6] to fit their data (their eq 4a) has the same dependence on the cation concentration as that given by eq 15, derived from our proposed mechanism. The high value of the preexponential noted by Glarum and Marshall[6] does not rule out the present mechanism because the observed second-order rate constant is a combination of rate constants and concentrations. The results of Kloosterboer, *et al.*,[7] indicate that in the ethers which they used (diglyme, DME, tetraglyme), a new species of stoichiometry Na is formed. Its absorption at 830 nm is so far removed from that of their stated absorption maximum for the solvated electron (≈ 1500 nm) that it cannot be merely a "loose" ion pair Na^+,e^-. Since no similar transient was observed in the present work in ethylenediamine, no direct comparison with the kinetics in these ethers can be made.

III. 3. Utilisation de composés couronnés et de cryptates.
(Publications 6 et 7)

Une nouvelle voie d'étude des équilibres existant dans les solutions de métaux alcalins a été introduite par l'utilisation d'éthers macrocycliques capables de complexer les ions alcalins.

L'utilisation de ces composés permet de dissoudre des métaux alcalins dans des solvants où ils sont habituellement insolubles.

Il est ainsi possible d'obtenir des solutions de sodium dans l'éther éthylique ou dans le tetrahydrofurane (THF).

La constante d'association de l'ion alcalin avec le complexant joue un rôle important sur la nature des espèces en solution. Ainsi, pour le sodium mis en solution dans le THF par le dicyclohexyl 18 - crown - 6, l'espèce la plus stable est l'espèce Na^- et l'électron solvaté ne peut être observé que par RPE alors qu'avec le cryptate 2, 2, 2, l'électron solvaté est l'espèce prépondérante.

PUBLICATION 6

SOLUBILIZATION OF ALKALI METALS IN TETRAHYDROFURAN AND DIETHYL ETHER BY USE OF A CYCLIC POLYETHER.

[Reprinted from the Journal of the American Chemical Society, 92, 5226 (1970).]

Solubilization of Alkali Metals in Tetrahydrofuran and Diethyl Ether by Use of a Cyclic Polyether

Sir:

We wish to report a new technique for dissolving alkali metals in solvents in which they are ordinarily either insoluble or only slightly soluble. This method may extend the range of solvents in which the properties of relatively stable solutions of solvated electrons and other species common to metal–amine solutions[1,2] can be studied. Of particular interest would be the ability to make extended comparisons with the properties of solvated electrons produced by pulse radiolysis.

The basis for this increased solubility is the ability of certain cyclic polyethers to complex alkali metal cations.[3,4] Noting that stabilization of the cations

(1) R. R. Dewald and J. L. Dye, *J. Phys. Chem.*, 68, 121 (1964).
(2) M. Ottolenghi, K. Bar-Eli, and H. Linschitz, *J. Chem. Phys.*, **43**, 206 (1965).
(3) C. J. Pedersen, *J. Amer. Chem. Soc.*, **89**, 7017 (1967).
(4) C. J. Pedersen, *ibid.*, **92**, 386 (1970).

should increase the solubility of the metals, we studied the effect of adding cyclohexyl-18-crown-6,[5] **1**, to tetrahydrofuran (THF) and diethyl ether (Et_2O) in the presence of a mirror of potassium. With both solvents,

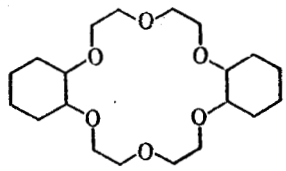

1

deep blue solutions were formed. Solutions of both potassium and cesium in THF formed readily at room temperatures and were stable for several hours even in the absence of excess metal. Metal concentrations of about 1×10^{-4} *M* were obtained by using 5×10^{-3} *M* solutions of **1**. Solutions stored at −78° for several days showed no visible signs of decomposition. In order to form solutions of potassium in Et_2O it was necessary to first cool the system to −78°. Once formed, however, the blue solutions in this solvent were stable at room temperatures for 5–10 min and for hours at −78°. At this writing only the three metal–solvent pairs described above have been examined. It is probable that many other systems will behave in a similar fashion.

It has been reported[6] that very dilute solutions of potassium in THF exhibit two epr signals, a four-line pattern characteristic of the potassium monomer and a single narrow line attributed to the solvated electron. In the presence of **1**, however, the much more concentrated potassium solutions in THF used in this work showed only a single epr line. In Et_2O at 25°, in addition to the single line ($C \simeq 10^{-7}$ *M*) a weak four-line pattern ($C \simeq 10^{-8}$ *M*, $A \simeq 11$ G) was observed, probably attributable to the potassium monomer. Both absorptions in Et_2O were absent at 0° and appeared upon warming to room temperature. The single line observed in THF solutions could be observed down to the freezing point of the solvent. In both solvents at low temperatures (−60° and below) a weak seven-line pattern was observed. The splitting value and relative intensities indicate that this absorption is probably from the benzenide anion.[7] This identification was strengthened by adding small amounts of benzene to a similar solution of potassium in THF containing **1**. The result was a marked increase in the intensity of the epr pattern but no change in the number of lines or the splitting value.

The epr results indicate that the relative concentration of monomer decreased when **1** is present. They also show, in comparison with the optical spectra, that only a small fraction of the total dissolved metal gives an epr pattern, a result which is consistent with the behavior of metal–amine solutions.[8]

The optical absorption spectra measured at room temperatures with a Beckman DK2 spectrophotometer are shown in Figure 1. These spectra have been cor-

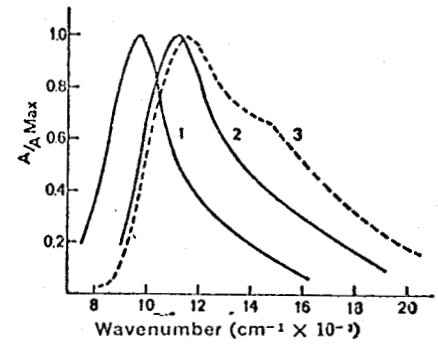

Figure 1. Absorption spectra in the presence of **1**: (1) cesium in THF, (2) potassium in THF, (3) potassium in Et_2O.

rected for decomposition by interpolating the results from successive scans. Potassium in THF in the presence of an excess of **1** showed only a single band with a maximum at 11,100 cm^{-1}, while the band maximum for cesium solutions occurred at 9700 cm^{-1}. With Et_2O the band maximum for potassium occurred at 11,400 cm^{-1} and a shoulder (probably caused by sodium from the Pyrex container[9]) was observed at ~14,000 cm^{-1}. These peaks can be identified with the corresponding metal-dependent "R-bands" in metal–amine solutions.[1,2] Even when the absorbance at the peak was ~3 in Et_2O (as judged by the positions of unit absorbance, 9500 and 16,000 cm^{-1}) there was no detectable absorption in the region from 8000 to 4000 cm^{-1}. A similar search was not possible for solutions in THF because of the strong solvent absorptions in this region. The absence of an optical band for the solvated electron is not necessarily at variance with the presence of an epr signal attributed to this species. The estimated spin concentration of 10^{-7} *M* is an order of magnitude below that which would have been detected optically.

Similar absorption bands in metal–amine solutions have been attributed to the alkali anion, M^-.[10] The absence of hyperfine splitting by the potassium nucleus in THF in the presence of **1** contrasts with the results in THF alone[6] and indicates that the equilibrium

$$M \rightleftharpoons M^+ + e^- \quad (1)$$

is shifted to the right by the complexation equilibrium

$$M^+ + 1 \rightleftharpoons \text{complex} \quad (2)$$

Presumably the solubility equilibrium

$$2M(s) \rightleftharpoons M^+ + M^- \quad (3)$$

is similarly shifted to the right. However, the absence of a solvated electron absorption band and the very low concentration of unpaired spin indicate that the equilibrium

$$M^- + 1 \rightleftharpoons \text{complex} + 2e^- \quad (4)$$

lies far to the left in these solvents.

Acknowledgment. Support of this research by the U. S. Atomic Energy Commission under Contract No. AT(11-1)-958 is gratefully acknowledged. We are indebted to Dr. H. K. Frensdorf of E. I. du Pont de

(5) See ref 3 for a discussion of the nomenclature of this class of compounds.
(6) R. Catterall, J. Slater, and M. C. R. Symons, *J. Chem. Phys.*, 52, 1003 (1970).
(7) T. R. Tuttle, Jr., and S. I. Weissman, *J. Amer. Chem. Soc.*, 80, 5342 (1958).
(8) L. R. Dalton, J. D. Rynbrandt, E. M. Hansen, and J. L. Dye, *J. Chem. Phys.*, 44, 3969 (1966).
(9) I. Hurley, T. R. Tuttle, Jr., and S. Golden, *ibid.*, 48, 2818 (1968).
(10) S. Matalon, S. Golden, and M. Ottolenghi, *J. Phys. Chem.*, 73, 3098 (1969).

Nemours Co. for providing us with a sample of the crown compound.

* Address correspondence to this author.

James L. Dye,* Marc G. DeBacker, Vincent A. Nicely
Department of Chemistry, Michigan State University
East Lansing, Michigan 48823
Received June 12, 1970

PUBLICATION 7

ALKALI METAL SOLUTIONS EFFECT OF TWO CYCLIC POLYETHERS ON SOLUBILITY AND SPECTRA.

Sonderdruck aus der Zeitschrift:

Berichte der Bunsen-Gesellschaft für physikalische Chemie (früher Zeitschrift für Elektrochemie)

Verlag Chemie GmbH, Weinheim/Bergstr. Band 75, Heft 7, 1971

Alkali Metal Solutions
Effect of Two Cyclic Polyethers on Solubility and Spectra

By James L. Dye, Mei Tak Lok, Frederick J. Tehan, Richard B. Coolen, Nicholas Papadakis, Joseph M. Ceraso, and Marc G. DeBacker*)

Department of Chemistry, Michigan State University, East Lansing, Michigan 48823, USA

Alkali metals can be made to dissolve in solvents in which they are normally insoluble or only slightly soluble, by using cyclic polyethers to complex the cations. Although the use of the cyclic polyether, dicyclohexyl-18-crown-6 results mainly in the formation of M^- as the reducing species, the bicyclic polyether, "cryptate" yields in addition, substantial concentrations of solvated electrons. It also increases the solubility compared with the "crown" compound.

Durch zyklische Polyäther, die Kationkomplexe zu binden vermögen, können Alkalimetalle auch in solchen Lösungsmitteln gelöst werden, in denen sie sonst nicht oder nur wenig löslich sind. Während Dicyklohexyl-18-crown-6 bevorzugt zur Bildung von M^- (M Metallatom) führt, ergibt der bicyklische Polyäther "Cryptat" bei erhöhter Metall-Löslichkeit zusätzlich beträchtliche Konzentrationen an solvatisierten Elektronen.

Introduction

Although metal-ammonia solutions are complicated by ion-pairing and spin-pairing processes, there is no direct spectroscopic evidence for the existence of reducing species other than the solvated electron, e^-_{solv}. Indeed, in one model of metal-ammonia solutions the properties of dilute solutions have been interpreted in terms of ion-pairing processes [1, 2] and other relatively long-range interactions among solvated electrons and solvated cations [3]. By contrast, certain metal-amine and metal-ether solutions have ESR and optical spectra which can only be interpreted in terms of additional species of stoichiometry M [4–6] and M^- [7–10], with the former a relatively minor component. The assignment of the "V-band" in sodium-amine solutions to a species of stoichiometry Na^-, as suggested by several investigators, has recently been confirmed in our laboratory by measuring its extinction coefficient and oscillator strength [11]. Another characteristic of these solutions is the generally low solubility of the alkali metals. The equilibria involved may be represented by the following scheme:

$$2M(s) \overset{K_1}{\rightleftarrows} M^+ + M^- ; \quad (1)$$

$$M^- \overset{K_2}{\rightleftarrows} M^+ + 2e^- ; \quad (2)$$

$$M \overset{K_3}{\rightleftarrows} M^+ + e^- . \quad (3)$$

Although the equilibrium constants are unknown, we can expect them to increase with an increase in the solvating power and dielectric constant of the solvent. Metal solutions in aliphatic mono-amines (except methylamine) and in polyethers can be described mainly by the first equilibrium. In these solvents M and e^- appear to be minor species compared with M^-.

The properties of metal solutions in ethylenediamine, methylamine and hexamethyl phosphoric triamide are intermediate between those in the monamines and ethers and those in ammonia. For example, sodium solutions in ethylenediamine show very little, if any, infrared absorption from the solvated electron [12] while cesium solutions have optical spectra [12] and conductances [13] which are characteristic of solvated electrons and their "ammonia-like" aggregates. The discovery that certain cyclic polyethers behave as complexing agents for the alkali cations [14, 15] led us to study the effect of compound I, dicyclohexyl-18-crown-6, or simply, "crown", on the solubility of alkali metals in simple ethers [16]. Similar studies have recently been reported in which straight-chain polyethers were used as complexing agents [17].

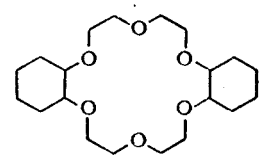

I

Solutions of potassium and cesium in diethyl ether and in tetrahydrofuran (THF) exhibited optical and ESR behavior which indicated that complexation of the cation had increased K_1 and K_3. However, although the ESR spectra indicated the presence of solvated electrons, the concentration of e^-_{solv} was several orders of magnitude below that of M^-.

The demonstration that the hexaoxa-diamine macrobicyclic molecule II, a member of a class of compounds referred to as "cryptates", is an even stronger complexing agent for the alkali ions than are the "crown" compounds [18–20] prompted us

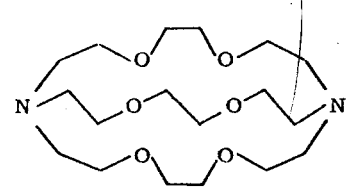

II

to begin an investigation of the ability of II to enhance metal solubility in ethers and other solvents. It was hoped that the

*) Present address: Ecole des Hautes Etudes Industrielles, 13 rue de Toul, 59 Lille, France.

complexing ability would be great enough to drive reaction (2) to the right. In this way the properties of solvated electrons in a variety of pure and mixed solvents might be studied. This paper reports some preliminary results of these studies.

Experimental

Solvents were dried over barium oxide then distilled onto a mixture of benzophenone and an excess of potassium. If the blue solutions of the ketyl so formed were not stable, the distillation was repeated. In some cases the solvent was stored over Na – K alloy prior to its final distillation into the cell. All glassware was cleaned first with an HF cleaner (33% HNO_3, 5% HF, 2% acid-soluble detergent, 60% water) followed by a thorough rinsing with conductance water. The cells were then cleaned with boiling *aqua regia* and rinsed at least ten times with boiling conductance water. The "cryptate", II, was introduced into the cell as received without further purification [21]. Potassium was distilled into the cell through a side-arm under vacuum ($< 10^{-5}$ Torr). The appropriate solvent was then vacuum-distilled into the cell. Each cell consisted of a 2.4 mm i.d. ESR tube sealed to an inverted U-tube such that the metal could be distilled into one arm of the U-tube and "cryptate" could be placed in the other arm. In this way, solutions containing the complexing agent could be kept away from the metal as long as desired. For some of the studies, Aminco cylindrical absorption cells of 0.3 or 1.0 mm path length were used.

ESR spectra were measured with an *X*-band Varian E-4 Spectrometer. Optical spectra were measured with either a Beckman DK-2 Spectrophotometer or with a scanning system which had been designed for stopped-flow measurements [22]. The latter system was modified to permit the use of lead-sulfide detectors as well as photomultipliers. The cell compartment was designed to permit measurement at various temperatures down to −100°C by using a Varian V-4540 variable-temperature control unit. Lack of stability of some of the solutions at room temperature made it imperative to work at low temperatures. A variable-temperature cell-holder was constructed for the DK-2 instrument which permitted measurements to be made over the range −100°C to +30°C.

Results

Although potassium does not dissolve in diethyl ether and although the polyether, II, is not visibly soluble, a suspension of II in diethyl ether, when brought into contact with a mirror of potassium, produces a very dark blue solution immediately. The solution is stable for many hours at −80°C but remains blue in the absence of metal for only 10 to 30 minutes at room temperature. In contrast to potassium solutions in diethyl ether in the presence of "crown", I, which show only a weak ESR singlet (ca. 10^{-6} to 10^{-7} M) and only the optical band of K^- [16], solutions containing II show a very strong singlet in the ESR spectrum (ca. 10^{-4} M) and a broad featureless absorption band in the infrared in addition to the K^- band. A typical room temperature spectrum (path length 0.3 mm) is shown in Fig. 1. In Fig. 2 the infrared band is compared with the solvated electron bands in ammonia and in ethylenediamine. When short-path length Pyrex cells were used, the V-band, characteristic of Na^-, was formed in addition to the K^- band. This is reminiscent of the behavior of solutions of potassium in ethylenediamine [13] and may be attributed to contamination by sodium from the Pyrex. The shape of the V-band is shown in Fig. 3 together with the spectrum of a solution of sodium in ethylenediamine.

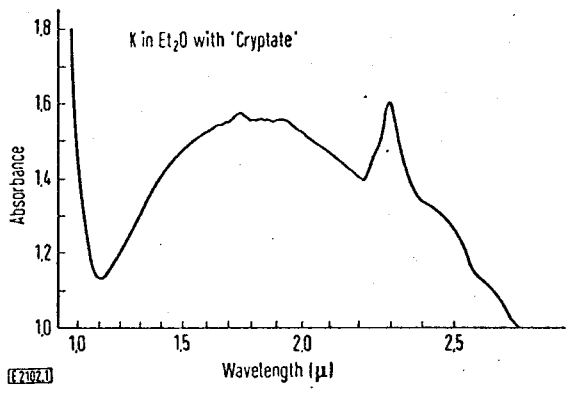

Fig. 1
Near-infrared spectrum of potassium in diethyl ether in the presence of "cryptate", II, at 25°C; path length 0.3 mm. Both the partially uncompensated band of the solvent at 2.2 – 2.3 μ and the band of K^- at 0.8 – 1.0 μ are evident

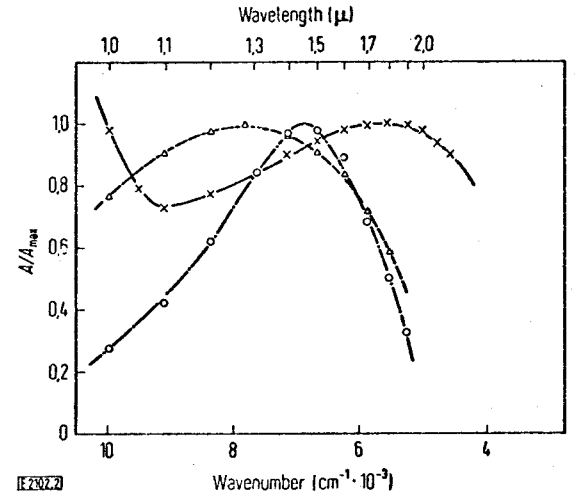

Fig. 2
Solvated electron spectra in —×—, diethyl ether, -.-O-.- ammonia, and --△-- ethyldiamine

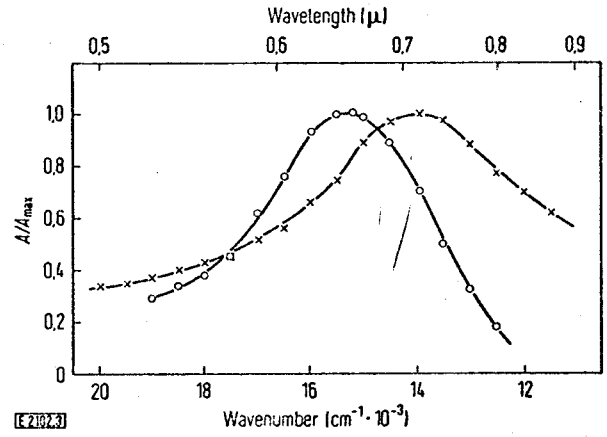

Fig. 3
Comparison of the band attributed to Na^- in ethylenediamine, —O— with that in diethyl ether —×—

All of the optical bands shift towards the blue with decreasing temperature as shown in Fig. 4. The temperature coefficients are −15.9, −13.5, and −12.6 cm^{-1} deg^{-1} for Na^-, K^-, and

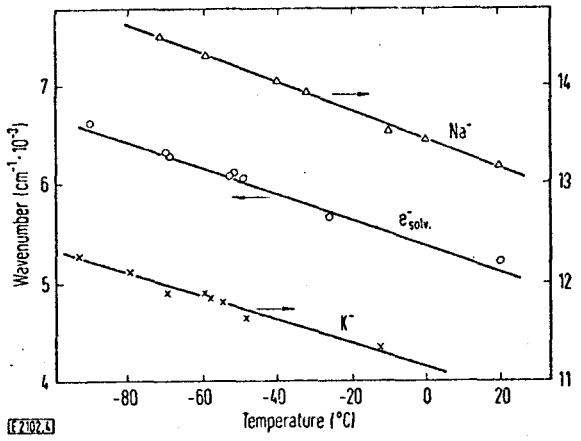

Fig. 4
Temperature dependence of the position of the band maximum for Na^-, e^- and K^- in diethyl ether

e^- respectively ($\sigma = 0.9$). These values are similar to those found for metal-ammonia solutions [1].

Three attempts to dissolve potassium in triethylamine were unsuccessful, perhaps because of the low dielectric constant of this solvent (2.42). Blue solutions of potassium in the presence of II which gave a singlet ESR signal were also obtained with di-i-propyl ether ($\varepsilon = 3.88$) and with di-n-propyl ether ($\varepsilon = 3.4$). Blue solutions were also obtained in this way with diethylamine. We have, in the past, attempted without success to dissolve the alkaline earth metals in amines. In the presence of II, deep blue solutions of barium in ethylenediamine were formed. However, lack of stability and the relatively high melting point of ethylenediamine have so far prevented the determination of spectra.

In order to test the supposition that reaction (2) is shifted to the right in the presence of "cryptate" a solution of sodium in ethylenediamine was studied in the absence and in the presence of II. A dark blue solution (absorbance of the V-band too high to measure in a 2.4 mm tube) in the absence of the complexing ether gave a relatively weak ESR singlet (10^{-5} to 10^{-6} M). The addition of II increased the strength of the ESR signal by at least two orders of magnitude. In addition to the usual V-band of Na^- a strong absorption band at 1.3 μ, characteristic of the solvated electron in ethylenediamine [13, 24], was observed. Contact with metal resulted first in an increase in the absorption of both Na^- and e^-, and ultimately in the disappearance of the band of e^-. The final solution showed only an off-scale absorbance in the region of the Na^- maximum and no absorbance in the infrared.

The previous study [16] showed that solutions of potassium in tetrahydrofuran in the presence of "crown", I, gave no ESR absorption from the monomer in contrast to the results in THF alone [24]. This phenomenon was further tested by observing the effect of the addition of the "crown" compound, I, to a solution of potassium in ethylamine. The original solution showed both the four-line ESR pattern of the potassium monomer and the singlet of the solvated electron. Addition of I caused the four-line pattern to disappear and the singlet to grow markedly. These results are shown in Fig. 5.

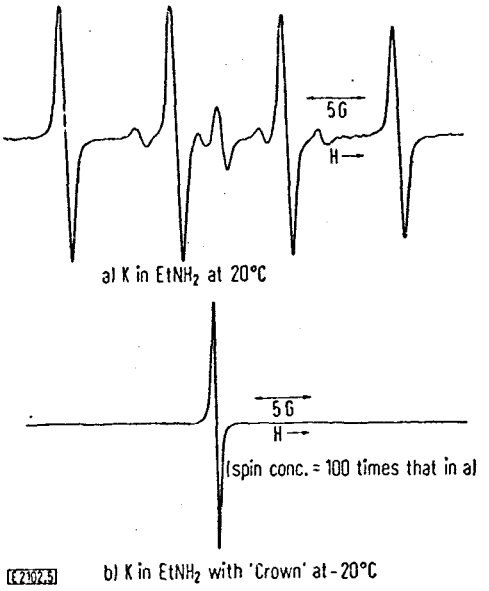

Fig. 5
ESR spectra of solutions of K in ethylamine. Spectrum (a): no added complexing agent. Spectrum (b): with "crown" added. Note the change in scale

The pronounced effect of these complexing agents can be demonstrated in another way. The ESR spectra of alkali salts of many aromatic radical anions show hyperfine splitting by the alkali cation, presumably because of contact pair formation. Complexation of the cation should be able to prevent such contact pair formation. To demonstrate this effect, the ESR spectrum of sodium anthracenide in diethyl ether at −70 °C was measured (Fig. 6a) and showed hyperfine splitting

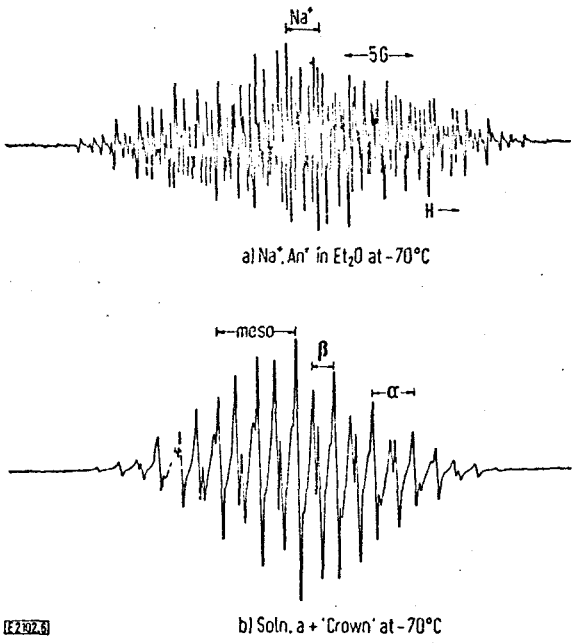

Fig. 6
ESR spectra of anthracenide radical anion in diethyl ether at −70 °C. (a) Spectrum of ion-paired species, (b) spectrum obtained after adding "crown" to the solution in (a)

by Na^+ in agreement with the results of Hirota [25, 26]. The addition of "crown", I, to the solution caused the disappearance of the Na hyperfine splitting as shown in Fig. 6b, in complete accord with expectation. These results are similar to those obtained when alkali solvating agents such as "glymes" are added to similar solutions [27].

Discussion

All of the results obtained so far, although preliminary in nature, are consistent with the equilibrium system described by reactions 1–3. The addition of a complexing agent which can stabilize the cation shifts all three equilibria to the right. The use of a good complexing agent, such as "cryptate", II, seems to provide enough stabilization energy to yield solvated electrons in solvents in which the metals would otherwise be insoluble or in which the major reducing species would normally be M^-. If this proves to be a general phenomenon, it should permit comparison of solvated electron spectra obtained with metal solutions in various solvents with those obtained by pulse-radiolysis.

The behavior of solutions of sodium in ethylenediamine in the presence of "cryptate" II requires further comment. In the absence of complexing agents (and even in the presence of "crown", I) only the Na^- band forms, indicating that reaction 2 is shifted far to the left. The effect of II (C) may be represented by the following in addition to equilibria 1–3:

$$2Na(s) + C \rightleftarrows Na^+C + Na^- ; \quad (4)$$

$$Na^- + C \rightleftarrows Na^+C + 2e^- . \quad (5)$$

As long as C is present in excess, both Na^- and e^- are observed. However, when most of the free C is consumed by reaction (4), reaction (5) is reversed. The solubility limits represented by (4) and (5) have not yet been determined.

Acknowledgements

This work was supported by the United States Atomic Energy Commission under Contract No. AT(11-1)-958.

References

[1] R. C. Douthit and J. L. Dye, J. Amer. chem. Soc. *82*, 4472 (1960).
[2] M. Gold, W. L. Jolly, and K. S. Pitzer, J. Amer. chem. Soc. *84*, 2264 (1962).
[3] J. L. Dye, in "Metal-Ammonia Solutions", supplement to Pure appl. Chem., p. 1, Butterworths, London 1970.
[4] K. D. Vos and J. L. Dye, J. chem. Physics *38*, 2033 (1963).
[5] K. Bar-Eli and T. R. Tuttle, Jr., Bull. Amer. physic. Soc. *8*, 352 (1963).
[6] For additional references to studies of the M species, see R. Catterall, Ref. 3.
[7] S. Matalon, S. Golden, and M. Ottolenghi, J. physic. Chem. *73*, 3098 (1969).
[8] S. H. Glarum and J. H. Marshall, J. chem. Physics *52*, 5555 (1970).
[9] D. Huppert and K. H. Bar-Eli, J. physic. Chem. *74*, 3285 (1970).
[10] A. Gaathon and M. Ottolenghi, Israel J. Chem. *8*, 165 (1970).
[11] M. G. DeBacker, Ph. D. Thesis, Michigan State University (1970).
[12] R. R. Dewald and J. L. Dye, J. physic. Chem. *68*, 121 (1964).
[13] R. R. Dewald and J. L. Dye, J. physic. Chem. *68*, 128 (1964).
[14] C. J. Pedersen, J. Amer. chem. Soc. *89*, 7017 (1967).
[15] C. J. Pedersen, J. Amer. chem. Soc. *92*, 386 (1970).
[16] J. L. Dye, M. G. DeBacker, and V. A. Nicely, J. Amer. chem. Soc. *92*, 5226 (1970).
[17] I. M. Panayotov, Ch. B. Tsvetanov, I. V. Berlinova, and R. S. Velichkova, Makromolekulare Chem. *134*, 313 (1970).
[18] B. Dietrich, J. M. Lehn, and J. P. Sauvage, Tetrahedron Letters 2885 (1969).
[19] B. Dietrich, J. M. Lehn, and J. P. Sauvage, Tetrahedron Letters 2889 (1969).
[20] J. M. Lehn, J. P. Sauvage, and B. Dietrich, J. Amer. chem. Soc. *92*, 2916 (1970).
[21] We are grateful to Dr. C. H. Park of E. I. duPont de Nemours Co. and to Prof. J. M. Lehn of the Institut de Chemie, Strasbourg, for providing samples of II.
[22] J. L. Dye and L. H. Feldman, Rev. Sci. Instr. *37*, 154 (1966).
[23] J. L. Dye, M. G. DeBacker, and L. M. Dorfman, J. chem. Physics *52*, 6251 (1970).
[24] R. Catterall, J. Slater, and M. C. R. Symons, J. chem. Physics *52*, 1003 (1970).
[25] N. Hirota, J. physic. Chem. *71*, 127 (1967).
[26] N. Hirota, J. Amer. chem. Soc. *90*, 3603 (1968).
[27] M. Szwarc, Accounts chem. Research *2*, 87 (1969).

E 2102

IV. CONCLUSIONS.

Première partie.

Nous avons réalisé une étude de l'influence de la composition du solvant sur les spectres de l'électron solvaté.

Nous avons mesuré les spectres de l'électron dans les mélanges eau - éthylènediamine et eau - ammoniac en utilisant la technique de la radiolyse pulsée. Pour ces mélanges, la position du maximum et la largeur à mi-hauteur varient d'une façon continue mais non linéaire entre les valeurs obtenues pour les solvants purs. En aucun cas la forme de la courbe ne permet de détecter plusieurs espèces en présence.

Pour analyser ces résultats, nous avons développé une nouvelle méthode reliant le spectre d'absorption à des grandeurs théoriques telles que l'hamiltonien choisi pour décrire les états énergétiques du système. Nous calculons dans cette méthode les moments du spectre expérimental et nous les comparons aux moments théoriques correspondant.

Le modèle choisi pour calculer ces derniers est un puits de potentiel sphérique de profondeur V_w et de rayon a . L'égalité de deux moments expérimentaux et calculés permet d'obtenir deux équations d'où nous tirons V_w et a .

Nous avons calculé les valeurs V_w et a pour l'ammoniac pur et pour les mélanges eau - ammoniac et eau - éthylènediamine. Dans tous les cas, nous avons observé que la taille du puits ne permettait d'obtenir qu'un seul état lié. Nous en concluons que les transitions sont du type 1 s ——— continuum.

Nous avons obtenu une corrélation linéaire entre la valeur de la profondeur du puits et l'énergie du maximum du spectre pour tous les solvants étudiés. Cette relation ne peut pas être déduite des hypothèses introduites dans le modèle. Une relation similaire a été obtenue pour relier la largeur à mi-hauteur au rayon du puits de potentiel; la meilleure relation linéaire

est obtenue si l'on relie la largeur à mi-hauteur au volume du puits de potentiel. A l'aide de ces deux relations il est donc possible d'évaluer les paramètres du puits de potentiel directement d'après le spectre d'absorption.

La variation de la profondeur du puits de potentiel en fonction de la composition des mélanges a été interprétée en considérant que le solvant se comportait comme en milieu continu. La valeur de V_W se compare bien avec celle de β à condition de prendre une valeur "effective" de la constante diélectrique optique de l'eau.

Ayant trouvé que la transition se faisait vers un continuum, nous avons essayé de comparer nos résultats avec ceux que prédit la théorie du transfert de charge au solvant. Pour pouvoir appliquer cette théorie au cas de l'électron solvaté nous avons du la modifier. De cette façon nous avons pu calculer la différence d'énergie entre le bord du puits et le vide.

Nous avons ainsi calculé des énergies correspondant au seuil d'éjection de photoélectrons à partir d'une solution contenant des électrons solvatés. La comparaison avec les valeurs expérimentales est bonne. Ce calcul permet ainsi d'obtenir une estimation du potentiel créé par le solvant sur un électron quasi libre se trouvant dans le milieu. Cette valeur se compare assez bien avec les valeurs de V_0 introduites par Jortner dans ses calculs.

Nous avons essayé de vérifier une des conclusions du modèle de Jortner. Il avait supposé qu'un mode normal de vibration de la cavité entourant l'électron serait actif en Raman. Nos résultats n'ont pas permis d'infirmer ou de confirmer cette supposition.

Deuxième partie.

Les résultats obtenus confirment l'existence d'espèces de stoechiométrie M^- dans les solutions de métaux alcalins dans l'éthylènediamine.

Nous avons d'abord mesuré le coefficient d'extinction et la force d'oscillateur de Na^-. La valeur 2 trouvée pour la force d'oscillateur indique que deux électrons participent à la transition. La stoechiométrie de cette espèce est donc $Na^+(e^-)_2$.

Pour le potassium et le rubidium, la forme K^- ou Rb^- est en équilibre avec l'électron solvaté. Ces équilibres sont complexes et les données ne peuvent pas être correctement décrites avec des équations simples.

La réaction de $K^+ + Na^-$ a été tentée, au lieu de l'espèce K^- à laquelle on s'attendait nous avons obtenu apparition d'électrons solvatés. Ce résultat est très surprenant et nous n'avons aucune explication à proposer pour ce phénomène.

La cinétique de la réaction $Na^+ + e^-$ a été mesurée par radiolyse pulsée. La réaction est strictement du second ordre par rapport à l'électron solvaté. La dépendance de la constante de vitesse sur la concentration en ion sodium nous a amenés à postuler un mécanisme plus complexe pour cette réaction. La réaction $K^+ + e^-$ ne produit pas d'espèce K^-, mais la présence d'ions K^+ empêche la réaction $Na^+ + 2e^- \longrightarrow Na^-$ d'être complète.

Une explication complète de ces résultats nécessiterait la connaissance de la structure détaillée des espèces dont nous ne connaissons que la stoechiométrie. En effet dans les solvants de faible constante diélectrique les espèces sont associées et une étude complète des équilibres doit mettre en jeu leurs constantes d'association.

Nous avons montré qu'il était possible de modifier les équilibres existant en solution en utilisant des agents complexant les cations.

A l'aide de ces composés nous avons pu montrer qu'il était possible de dissoudre des métaux alcalins dans d'autres solvants que l'ammoniac et les amines. Selon la constante d'association du complexant et de l'ion alcalin, diverses espèces peuvent être mises en évidence.

BIBLIOGRAPHIE

1. P.F. RUSCH et J.P. LELIEUR, Anal. Chem., 45, 1541 (1973)

2. G. RUBENSTEIN, Ph.D. Thèse Brandeis University (1972)

3. M.G. DE BACKER, J.N. DECARPIGNY et M. LANNOO, J. Phys. Chem., 81, 159 (1977)

4. J.L. DYE, M.G. DE BACKER et L.M. DORFMAN J. Chem. Phys., 52, 6251 (1970)

5. V. MAZZACURATI et G. SIGNORELLI, Lett. Nuovo Cimento, 12, 347 (1975)

6. D.A. COPELAND, N.R. KESTNER et J. JORTNER, J. Chem. Phys., 53, 1189 (1970)

7. T. KAJIWARA, K. FUNABASHI et C. NALEWAY, Phys. Rev., 6, 808 (1972)

8. A.W. FRANCIS, J. Chem. Eng. Data, 5, 534 (1960)

9. Handbook of Chemistry and Physics, CRC Press, 53e édition p-D-184

10. M. ANBAR et E.J. HART, J. Phys. Chem. 69, 1244 (1966)

11. M. FOX et E. HAYON, J. Chem. Soc. Farad. Trans I, 72, 1990(1976)

12. G.STEIN et A. TREININ, Trans. Farad. Soc., 55, 1086 (1959)

13. PIKAEV dans The Solvated Electron in radiation chemistry Chapitre 7. Israel. Prog. Sci. Trans. (1971)

14. H. AULICH, B. BARON, P. DELAHAY et R. LUGO, J. Chem. Phys. 58, 4439 (1973)